

Process Chain Design for Post-Processing of Wire and Arc Additively Manufactured Ti-6Al-4V

Christina Theresia Fuchs

Vollständiger Abdruck der von der TUM School of Engineering and Design der Technischen Universität München zur Erlangung einer

Doktorin der Ingenieurwissenschaften (Dr.-Ing.)

genehmigten Dissertation.

Vorsitz: Prof. Dr. Tim C. Lüth

Prüfende der Dissertation:

1. Prof. Dr.-Ing. Michael F. Zäh
2. Prof. Dr.-Ing. Eberhard Abele

Die Dissertation wurde am 29.11.2023 bei der Technischen Universität München eingereicht und durch die TUM School of Engineering and Design am 07.03.2024 angenommen.

Acknowledgments

This dissertation was written during my work as a research assistant at the Institute for Machine Tools and Industrial Management (*iwb*) of the Technical University of Munich. I would like to express my special thanks for encouraging my work to Prof. Dr.-Ing. Michael F. Zäh, Prof. Dr.-Ing. Gunther Reinhart, and Prof. Dr.-Ing. Rüdiger Daub, the heads of this institute.

I was supported by several people during my dissertation thesis, whom I would like to thank in the following. To my colleagues at the *iwb*, thank you for always being there to discuss research challenges and to develop new ideas. To Daniel Baier, Christian Fritz, and Martina Sigl, thank you for taking the time to read and correct my dissertation. I highly value your input! To the number of students I had the opportunity to work with, thank you for your dedication and ideas. To Ignacio Rodríguez and Laura Kick, thank you for helping me during long hours of experiments at our machining center.

My father once commented that he didn't think he should be included in the acknowledgments, since I was the one who did the work on this dissertation thesis. While this is technically true, thank you for always taking my call and listening to me when I was in doubt about the research.

Last but not least, a special thank you goes to my partner. Thank you for trying to understand my research and for giving up a lot of time we could have spent together, so I could finish this thesis.

Leonberg, Mai 2024
Christina Fuchs

Contents

List of Abbreviations	ix
List of Latin Symbols	xi
List of Greek Symbols	xv
1 Introduction	1
1.1 Motivation	1
1.2 Objective and structure	2
2 Background and Literature Review	5
2.1 Wire and arc additive manufacturing	5
2.1.1 Principles of wire and arc additive manufacturing	6
2.1.2 Ti-6Al-4V component microstructure and mechanical properties	9
2.1.3 WAAM-part geometry	14
2.2 Machining	19
2.2.1 Principles of the milling process	19
2.2.2 Milling process challenges	22
2.2.3 Machinability of material manufactured with wire-based processes	25
2.3 Process chain design	27
2.3.1 Definition of terms and general considerations	27
2.3.2 Process chain design for additive-subtractive manufacturing	28
2.3.3 Process and operations planning for sequential additive-subtractive manufacturing	30
2.4 Summary and need for action	35
3 Objective and Research Approach	37
3.1 Objective and scope	37
3.2 Research approach	38
4 Integrated Process Planning for WAAM and Milling	43
4.1 Process planning and orientation – Publication ①	43

4.2	Feature-based sequence definition by performing a cost analysis – Publication ②	46
4.3	Determining the machining allowance – Publication ③	48
4.4	Summary of the integrated process planning	50
5	Considerations for the Milling Operations Planning	51
5.1	Connection between microstructure, mechanical properties and machinability – Publication ④	51
5.2	Impact of the WAAM-geometry on the milling process – Publication ⑤	54
5.3	Summary of the considerations for the milling operations planning	56
6	Potential Analysis and Discussion	57
6.1	Potential analysis	57
6.1.1	Part orientation	60
6.1.2	Cost analysis	62
6.1.3	Machining allowance	64
6.1.4	Milling operations planning	64
6.2	Discussion	67
7	Summary and Outlook	69
7.1	Summary	69
7.2	Outlook	70
	Bibliography	73
	Glossary	87
A	Appendix	89
A.1	Descriptions of process and planning steps	89
A.2	Test parts for the potential analysis	92
A.3	Data for the potential analysis	95
B	Supervised Student Theses	97
C	Publications and presentations	99

List of Abbreviations

Abbreviation	Description
ACARE	Advisory Council for Aviation Research and Innovation
AdDEDValue	Fully Automated Additive Manufacturing with DED Processes for the Automotive Series Production (German: Vollautomatisierte Additive Fertigung mit DED-Verfahren für die automobiler Serienproduktion)
AISI	American Iron and Steel Institute
Al	Aluminum
AM	Additive Manufacturing
ASTM	American Society for Testing and Materials
BMWK	Federal Ministry for Economic Affairs and Climate Action (German: Bundesministerium für Wirtschaft und Klimaschutz)
BTF	Buy-to-Fly
CAD	Computer-Aided Design
CAM	Computer-Aided Manufacturing
CAPP	Computer-Aided Process Planning
CFRP	Carbon Fiber Reinforced Polymer
CMT	Cold Metal Transfer
CNC	Computerized Numerical Control
CO ₂	Carbon Dioxide
DIN	German Institute for Standardisation Registered Association (German: Deutsches Institut für Normung e.V.)
FE	Finite Element
GMAW	Gas Metal Arc Welding
GTAW	Gas Tungsten Arc Welding
HSLA steel	High-strength low-alloy steel
<i>iwb</i>	Institute for Machine Tools and Industrial Management of TUM

Abbreviation	Description
ISO	International Organization for Standardization
MAT	Medial Axis Transformation
NC	Numerical Control
NO _x	Nitrogen Oxides, including nitric oxide (NO) and nitrogen oxide (NO ₂)
PAW	Plasma Arc Welding
PBF-EB/M	Powder-bed Fusion of Metals with an Electron Beam
PBF-LB/M	Powder-bed Fusion of Metals with a Laser Beam
POP	Process and Operations Planning
REGULUS	Resource-efficient production of large-volume aerospace structural components (German: Ressourceneffiziente Fertigung von großvolumigen Luftfahrt-Strukturkomponenten)
SMAW	Shielded Metal Arc Welding
Ti-6Al-4V	Titanium alloy with 6 wt.% aluminum and 4 wt.% vanadium
TUM	Technical University of Munich
UTS	Ultimate Tensile Strength
VDI	Association of German Engineers (German: Verein Deutscher Ingenieure)
Work Sequence X	premanufacturing features with WAAM and milling from a near-net shape
Work Sequence Y	filling features with material during the WAAM process and milling from a conventional shape
WAAM	Wire and Arc Additive Manufacturing
WAAM-geometry	Wire and Arc Additively Manufactured geometry
WAAM-material	Wire and Arc Additively Manufactured material
YS	Yield Strength

List of Latin Symbols

Symbol	Description	Unit
a	machining allowance	mm
a_e	radial depth of cut	mm
a_p	axial depth of cut	mm
A_0	initial specimen cross-section	mm ²
b	standoff distance between the torch and the substrate	mm
c	edge contact length	mm
$C_{LA,MI}$	milling labor hourly rate	€/h
$C_{LA,WA}$	WAAM labor hourly rate	€/h
C_M	material costs per volume	€/ m ³
$C_{ME,MI}$	milling machine hourly rate	€/h
$C_{ME,WA}$	WAAM machine hourly rate	€/h
c_p	specific heat capacity	J/(kg K)
$C_{W,MI,X}$	WAAM tool costs for work sequence X	€
$C_{W,MI,Y}$	WAAM tool costs for work sequence Y	€
$C_{W,WA}$	WAAM tool costs	€
D	tool diameter	mm
d	distance between weld beads	mm
DR_{mass}	deposition rate	kg/h
E	Modulus of elasticity (Young's modulus)	GPa
e	elongation	%
F	force	N
F_a	cutting force in the tool's axial direction	N
F_r	cutting force in the tool's radial direction	N
F_t	cutting force in the tool's tangential direction	N
F_x	cutting force in the X-direction	N

Symbol	Description	Unit
F_y	cutting force in the Y-direction	N
F_z	cutting force in the Z-direction	N
f_z	feed per tooth	mm/tooth
h	uncut chip thickness	mm
h_{layer}	height of the deposited layer	mm
$H(x)$	position dependent height of the deposited surface	mm
H	height of the deposited surface	mm
K	cutting force coefficient	mm
K_{ac}	axial shearing cutting force constant	N/mm ²
K_{ae}	axial edge constant	N/mm
K_{rc}	radial shearing cutting force constant	N/mm ²
K_{re}	radial edge constant	N/mm
K_{tc}	tangential shearing cutting force constant	N/mm ²
K_{te}	tangential edge constant	N/mm
L	current specimen length	mm
l	batch size	–
L_0	initial specimen length	mm
M_a	machining allowance mass	kg
M_b	bounding box mass	kg
M_d	deposited material mass	kg
M_f	material mass in the final part	kg
M_p	material mass for production	kg
MRR_{vol}	volumetric material removal rate	mm ³ /min
MRR_{mass}	material removal rate	kg/h
M_s	substrate material mass	kg
n	spindle speed	rev/min
ORi_j	orientation i of the test part j , example OR1 ₁	–
P_1	substrate usage parameter	–
P_2	deposited material parameter	–
P_3	build time parameter	–
P_4	build complexity parameter	–
Pz	maximum height of the primary profile	mm
Q_c	cost coefficient for determining the optimal manufacturing sequence	–

Symbol	Description	Unit
R_m	ultimate tensile strength	MPa
R_{p02}	yield strength	MPa
T	manufacturing time	h
T_d	deposition time	h
T_m	milling time	h
T_{MI}	milling tool life span	h
T_{WA}	WAAM tool life span	h
$t_{w,MI}$	milling tool change time	h
$t_{w,WA}$	WAAM tool change time	h
U	welding voltage	V
\dot{V}	shielding gas flow rate	m ³ /min
v_c	cutting speed	m/min
v_f	feed velocity	mm/min
v_T	torch speed	mm/min
v_W	wire feed speed	m/min
w_e	effective wall width	mm
Wz	maximum height of the waviness profile	mm
x_{MI}	number of milling machines one worker supervises	–
x_{WA}	number of WAAM machines one worker supervises	–
z	number of teeth	–

List of Greek Symbols

Symbol	Description	Unit
γ	helix angle	°
δ	travel angle	°
ε	strain	N/mm ²
ζ	tilt angle	°
η	inclination of a deposited surface	°
Θ	inclination of a deposited wall	°
λ	heat conductivity	W/(m K)
ρ	density	g/cm ³
σ	stress	N/mm ²
Φ_e	cutter's angle of entry	°
Φ	cutter angle	°

Chapter 1

Introduction

1.1 Motivation

The coronavirus pandemic that started in 2019 led to a decrease in the number of worldwide commercial flights by 45% between 2019 and 2021 (IATA 2022). Nonetheless, AIRBUS (2022) expects the air traffic to reach the year 2019 level between 2023 and 2025 and to continue to grow until 2040 (AIRBUS 2022). The demand for newly manufactured aircraft is forecast to be around 40,000 up to the year 2040 (AIRBUS 2022; BOEING 2022). At the same time, the goals for air traffic set in the European Union's Flightpath 2050 Agenda state that the CO₂ emissions per passenger kilometer have to be reduced by 75%, and the NO_x emissions by 90% compared to the year 2000 (ACARE 2017). Lightweight structures and efficient production systems are two key technological areas in the aircraft industry to remain competitive (VALDÉS et al. 2019) and reach these goals. Regarding lightweight structures, titanium alloys are the material of choice. BOYER (1995) states five reasons for their use:

- weight savings by replacing steel alloy components,
- space savings by replacing aluminium alloy components,
- higher operating temperatures,
- higher corrosion resistance than aluminium and low-steel alloys, and
- better composite compatibility than aluminium.

The last reason by BOYER (1995), better composite compatibility, further increases the attractiveness of titanium alloys for airplane production, since Carbon Fiber Reinforced Polymers (CFRPs) are a secondary option with a rising usage to decrease airplane mass (KARUPPANNAN GOPALRAJ et al. 2021). For the combination of CFRP with metals in the airframe, factors such as the corrosion potential and the thermal expansion have to be considered (INAGAKI et al. 2014). Here, titanium alloys are favorable in comparison to aluminum alloys (PETERS et al. 2003), such further increasing the amount of titanium alloys in use for airplane production. However, the efficiency of titanium airframes' production systems could be improved. One indicator of this is the Buy-to-Fly

(BTF) ratio. This is the ratio of the material mass bought for manufacturing of a component to the component mass in the finished aircraft. For complex shapes produced by forging and machining, the BTF reaches a value as high as 20 (SEMIATIN et al. 2001) or slightly higher. Reducing the BTF is one research interest (BOYER 2010). Its reduction has two benefits: reducing the amount of material needed and reducing the machining time (BOYER 2010). One process chain increasingly studied for this purpose is the combination of Wire and Arc Additive Manufacturing (WAAM) and machining. The WAAM process principle is based on the conventional welding process (DING et al. 2015b) and belongs to the category of metal Additive Manufacturing (AM) processes (*ISO/ASTM 52900* 2022). A metal wire is melted and deposited layer by layer, forming a near-net shape of the final component. Advantages of the WAAM process are its high deposition rates compared to other AM processes, such as Powder-bed Fusion of Metals with a Laser Beam (PBF-LB/M), its capability to produce large-size components, and its lower feedstock wastage (KHAN and JAPPES 2022). However, two major disadvantages are poor surface finish and poor resolution (KHAN and JAPPES 2022). Therefore, components are often milled to the final shape. CUNNINGHAM et al. (2017) and MARTINA and WILLIAMS (2015) showed the economic potential of this process chain. MARTINA and WILLIAMS (2015) demonstrated that the cost-saving potential was around 69% for a landing gear part made of titanium. The cost analysis by CUNNINGHAM et al. (2017) even indicated the potential for a cost reduction of 76% for a propeller if the initial BTF ratio was 20. A great deal of research has been conducted on improving the WAAM process concerning the cooling or the heating of setup and part, the shielding gas, the process parameters, and the process stability with various materials (RODRIGUES et al. 2019). The deposition strategy, the handling of residual stresses, heat treatments, and modeling and simulation were research interests as well (RODRIGUES et al. 2019). However, the subsequent milling process was the focus of only a limited amount of study, as was the full integration of WAAM and milling within the process planning.

1.2 Objective and structure

The objective of this publication-based thesis was to develop a methodology for the integrated process planning and an adapted operations planning for manufacturing Ti-6Al-4V components with WAAM and milling. The alloy Ti-6Al-4V was chosen since it is the most commonly used titanium alloy (LÜTJERING and WILLIAMS 2007). This means that, integrated into this context, the individual processes and their influence on each other are considered jointly. Integrated process planning is necessary since the accessibility of the part for the cutting tools needs to be respected for the WAAM process, and sufficient material has to be deposited for the subsequent machining process. Choosing the milling tools, the cutting conditions, and the path strategies is part of the milling operations planning (see Chapter 2). The machinability must be known to make

these choices. Possibly, the machinability of wire and arc additively manufactured material differs from conventionally produced material, since the material is melted during the WAAM process. Therefore, studies on the machinability of wire and arc additively manufactured material were conducted, and conclusions for the milling operations planning were drawn.

The objective is fulfilled with a top-down approach (VDI 3633-1 2014), by first analyzing the process chain of manufacturing airplane components with WAAM and machining, and, secondly, defining the process steps and interfaces between the individual steps. The results are addressed in five publications, which form the major part (Chapters 4 and 5) of this thesis:

- Publication ①: FUCHS, RODRÍGUEZ, et al. (2021),
- Publication ②: FUCHS, SEMM, et al. (2021),
- Publication ③: FUCHS et al. (2020),
- Publication ④: FUCHS et al. (2023), and
- Publication ⑤: FUCHS et al. (2022).

Initially, an introduction into this thesis was given in Chapter 1. This is followed by the necessary background information, in particular the fundamentals of WAAM and machining, and the state of the art of WAAM, machining, and process planning in Chapter 2. Based on the state of the art, two needs for action are identified. The two-part research objective and the four research questions, developed based on the need for action, and the research approach are discussed in depth in Chapter 3. Summaries of the embedded publications ① to ③, which address the integrated process planning, are given in Chapter 4. The results concerning the milling operations planning for wire and arc additively manufactured parts are summarized in Chapter 5 with the embedded publications ④ and ⑤. Finally, a discussion of the results and an analysis of the process chain's potential are given in Chapter 6. The thesis concludes with a summary and an outlook in Chapter 7.

Chapter 2

Background and Literature Review

This chapter provides background information on the WAAM process (Sec. 2.1.1) and the milling process (Sec. 2.2.1). The milling process is strongly influenced by the workpiece properties (TOENSHOFF 2014b), including the microstructure and mechanical properties. These properties, in turn, are influenced by the material's manufacturing process. In the conventional process chain for manufacturing airplane components, Ti-6Al-4V parts are machined from cast or wrought stock material. For the wire and arc additively manufactured material, different material properties are expected. Therefore, a literature review on the microstructure, mechanical properties and part geometry of wire and arc additively manufactured parts is presented (Sec. 2.1.2 – 2.1.3). The influence of the change from cast or wrought stock material to wire and arc additively manufactured material on the machining process is shown in the Section 2.2.3, after a general introduction to milling process challenges (Sec. 2.2.2). As described in Chapter 1, the objective of this thesis is to develop a methodology for integrated process planning. Therefore, the background information and current state of process chain design is reported in Section 2.3. The chapter concludes with summarizing the state of the art and formulating the need for action (Sec. 2.4).

2.1 Wire and arc additive manufacturing

All processes in which the material is successively added to build a 3D form based on a 3D model are considered as additive manufacturing (AM) processes (ISO/ASTM 52900 2022). Metal AM processes are characterized by the following six principles (ISO/ASTM 52900 2022):

- process category,
- source of fusion,
- basic AM principle,
- material feedstock,
- material distribution, and
- state of fusion.

WAAM belongs to the *process category* of directed energy input with an arc as the *source of fusion* instead of a laser or an electron beam. The *basic AM principle* is the selective deposition of material to a substrate, and the *material distribution* is done through a deposition nozzle. The *material feedstock* is a wire, with the melted state as the *state of fusion*. The detailed WAAM process operating principles and the characteristics of WAAM-components regarding their microstructure, mechanical properties, and geometry are discussed in the following sections (Sec. 2.1.1 – 2.1.3).

2.1.1 Principles of wire and arc additive manufacturing

The WAAM operating principle is based on the arc welding process. Generally, during arc welding, the workpiece is part of the electric circuit while the power supply and the current is passed from the electrode to the workpiece via the arc. The electrode is either a consumable or a non-consumable electrode. Processes with a consumable electrode are, among others, Gas Metal Arc Welding (GMAW) and Shielded Metal Arc Welding (SMAW). Those with a non-consumable electrode are Gas Tungsten Arc Welding (GTAW), and Plasma Arc Welding (PAW). (MESSLER 2011)

GMAW, GTAW, and PAW are the most commonly used welding processes for WAAM (NORRISH et al. 2021). In Figure 2.1, the three welding process principles, as they are used for wire and arc manufacturing, are shown.

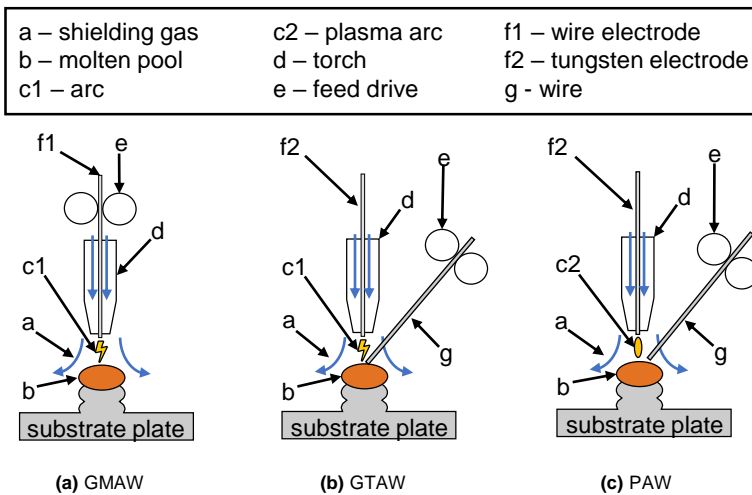


Figure 2.1: Schematic of the WAAM process principles based on DING et al. (2015d) and NORRISH et al. (2021)

A comparison of the three types of arc welding processes for various criteria relevant for AM as noted in literature is given in Table 2.1. The *weld quality* of GMAW is considered to be lower than that of GTAW and PAW, since the process tends to produce spatters (CONRARDY 2011). The *deposition rate* for GMAW processes is higher than the other processes' deposition rates with up to 5 kg/h depending on the material and parameters (MESSLER 2011; SINGH and KHANNA 2021). *Directional ease* describes the effort to change the welding direction. For GTAW and PAW, this effort is high since the welding torch has to be rotated to keep the wire feed direction constant in relation to the welding direction (DING et al. 2015d). Therefore, the directional ease is low. In GMAW processes, the wire is fed through the torch and the directional ease is higher. The *geometrical accessibility* is related to the external wire feed as well. It describes the effort required in manufacturing complex geometries. The external wire feeder increases this effort for GTAW and PAW. Therefore, their rating with respect to accessibility is lower than for GMAW. A cause for *distortion* is the thermal energy input resulting in non-uniform expansion and contraction of the workpiece (DING et al. 2015d). For PAW, the arc energy¹ is higher and more concentrated, resulting in less distortion than in GTAW and GMAW (DING et al. 2015d). The *capital equipment costs* are higher for the more complex PAW torch than for the GTAW torch (HARRIS 2011).

Table 2.1: Arc welding process advantages and disadvantages based on results by DING et al. (2015d), HARRIS (2011), MESSLER (2011), SINGH and KHANNA (2021), WILLIAMS et al. (2016), and ZHANG (2011); "-" – negative rating, "0" – neutral rating, "+" – positive rating

	GMAW	GTAW	PAW
weld quality	0	+	+
deposition rate	+	0	0
directional ease	+	-	-
geometrical accessibility	+	-	-
distortion of the workpiece	-	-	+
capital equipment costs	0	0	-

Theoretically, the WAAM process is applicable to all weldable materials, and its successful application has been shown for a number of materials. For aluminum and steel alloys, the GMAW process results in a good weld quality, while for titanium alloys arc wandering reduces the quality (WILLIAMS et al. 2016). However, for GMAW the deposition rate is higher, resulting in a higher production speed for large components and a more cost-effective production. Therefore, research has been conducted on using GMAW for additively manufacturing Ti-6Al-4V components.

For the GMAW process, three modes of how and when the droplet of molten material is transferred to the substrate are differentiated (CONRARDY 2011). Based on the three modes, several subtypes were developed to counter the ef-

¹in physical terms: the arc power

fects of unstable welding and the forming of spatters (ALMEIDA and WILLIAMS 2010). One subtype often used for WAAM is the Cold Metal Transfer (CMT) process (WILLIAMS et al. 2016). The CMT process is characterized by a reverse movement of the electrode. The moment of contact between the electrode wire and the molten pool is detected. Then, the electrode is retracted and the droplet is transferred. After the transfer, the electrode feed is reversed and directed towards the molten pool. The arc reignites. (NORRISH et al. 2021; ZHANG 2011)

The WAAM setup generally consists of a standard welding power source, a weld torch, and a wire feed drive (WILLIAMS et al. 2016). It is combined with a robotic arm or a Computerized Numerical Control (CNC) gantry to enable the feed motion (GIBSON et al. 2021; KNEZOVIC and TOPIC 2019). Such a process setup is shown in Figure 2.2.

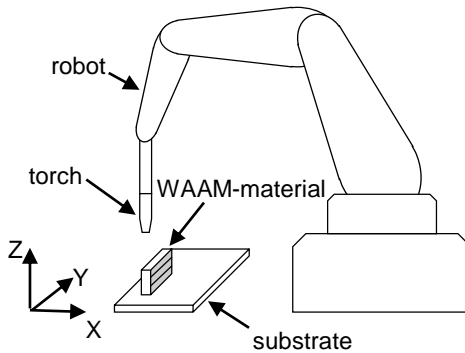


Figure 2.2: Schematic depiction of the WAAM setup

The process cycle described in the following is repeated until the desired shape is built. First, a layer of material is deposited on the substrate plate. In Figure 2.2, this layer is in the X-Y plane. The torch's feed direction within this layer is designated as the welding direction or the deposition direction (MARTINA et al. 2012). The speed of the torch movement is called the torch speed v_T or the travel speed (MARTINA et al. 2012). After the cooling of the layer, the torch is moved one layer up and the next layer is deposited. The direction in which the layers are stacked is known as the building direction (SCHMITZ et al. 2021). In Figure 2.2, this direction corresponds to the Z-direction. The deposited wire material is called wire and arc additively manufactured material (WAAM-material) in the following. Accordingly, the deposited shape is the WAAM-geometry. The welding torch can be inclined with respect to the welding direction. This inclination is designated as the travel angle δ (CONRARDY 2011) or the lead angle (REISCH et al. 2020). Additionally, the torch can be inclined perpendicular to the welding direction, which is called the tilt angle ζ (REISCH et al. 2020). In addition to the torch speed v_T and the travel angle δ , the wire feed speed v_W ,

the voltage U , the shielding gas flow rate \dot{V} and composition, and the stand-off distance b between the torch and the substrate are essential parameters for GMAW processes (CONRARDY 2011).

2.1.2 Ti-6Al-4V component microstructure and mechanical properties

The milling process is strongly influenced by the workpiece properties (TOENSHOFF 2014b). Therefore, in this section, the state of the art concerning the WAAM-component microstructure and its mechanical properties are discussed. Additionally, a comparison to wrought and cast Ti-6Al-4V is given.

Conventionally produced Ti-6Al-4V. Four main groups of titanium alloys are differentiated: α alloys, near α alloys, α - β alloys, and β alloys (EZUGWU and WANG 1997). This differentiation refers to the presence of the different microstructural phases of titanium. α references the close-packed hexagonal phase which is usually present at low temperatures. Meanwhile, β indicates the body-centered cubic phase existing at high temperatures (LÜTJERING and WILLIAMS 2007). Ti-6Al-4V belongs to the group of α - β alloys. The presence of both phases is possible by adding stabilizers, such as aluminum (α -stabilizer) and vanadium (β -stabilizer) (EZUGWU and WANG 1997). For Ti-6Al-4V, a wide range of microstructures is achievable depending on the processing of the raw materials (BOYER 1994). These microstructures include

- fully lamellar structures,
- fully equiaxed² structures, and
- bi-modal microstructures (LÜTJERING and WILLIAMS 2007).

The *lamellar* microstructure is characterized by α -colonies, which consist of parallel α -plates separated by the retained β -matrix. An example of such a microstructure is depicted in Figure 2.3. The size of the α -colonies and the α -plates decreases with an increased cooling rate, leading to the growth of α -plates perpendicular to another α -plate. The resulting microstructure is called Widmanstätten structure or basket-weave structure. (LÜTJERING and WILLIAMS 2007)

Alternatively, wrought Ti-6Al-4V often has an *equiaxed* structure (RAZAVI and BERTO 2019; SHUNMUGAVEL et al. 2015). This microstructure is depicted in Figure 2.4. The *bi-modal* microstructure contains equiaxed α in a lamellar $\alpha + \beta$ matrix (LÜTJERING and WILLIAMS 2007).

²“having approximately equal dimensions in all directions” (MERRIAM-WEBSTER DICTIONARY 2022b)

Additionally, two phase transition modes from β to α phase exist: martensite transformation and diffusion-controlled nucleation. The cooling rate and the alloy composition control the transition mode. The martensitically reached phase is designated as α' . Two morphologies, massive martensite and acicular³ martensite, are observed. (LÜTJERING and WILLIAMS 2007)

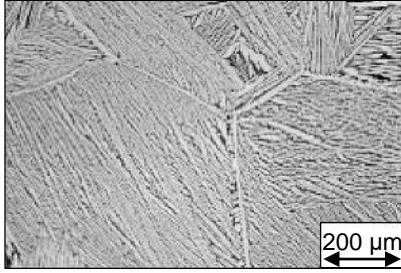


Figure 2.3: Lamellar α - β microstructure in Ti-6Al-4V, α – light and β – dark (LÜTJERING and WILLIAMS 2007); reprinted by permission from Springer Nature: Springer, Titanium by Gerd Lütjering and James C. Williams, Springer-Verlag Berlin Heidelberg (2007)

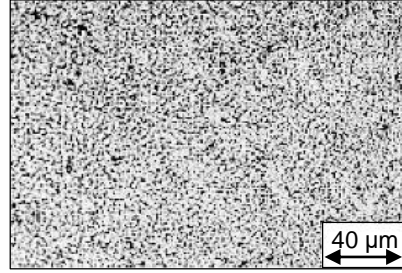


Figure 2.4: Fine grained, fully equiaxed microstructure in Ti-6Al-4V (LÜTJERING and WILLIAMS 2007); reprinted by permission from Springer Nature: Springer, Titanium by Gerd Lütjering and James C. Williams, Springer-Verlag Berlin Heidelberg (2007)

The mechanical properties of Ti-6Al-4V, along with some material properties, are listed in Table 2.2. They have been studied in a number of publications and have been published in industrial standards.

Table 2.2: The material properties of conventionally manufactured Ti-6Al-4V (DAVIM 2018; GROPPE 2014; VAZQUEZ et al. 2021; VENKATESH et al. 2001; WANG et al. 2013) (see also glossary: stress-strain-diagram)

Material properties	Unit	Value
density ρ	g/cm^3	4.43
modulus of elasticity (Young's modulus) E	GPa	108 – 113
ultimate tensile strength (UTS) R_m	MPa	900 – 1180
yield strength (YS) R_{p02}	MPa	830 – 1030
elongation at break e_{break}	%	8 – 15
Vickers hardness	HV	330 – 425
specific heat capacity c_p	J/(kg K)	500 – 567
heat conductivity λ	W/mK	6.5 – 7.6
minimum YS (investment casting) R_{p02min}	MPa	827
minimum YS (wrought) R_{p02min}	MPa	860
minimum elongation (investment casting) e_{min}	%	6
minimum elongation (wrought) e_{min}	%	10

³“shaped like a needle” (MERRIAM-WEBSTER DICTIONARY 2022a)

The microstructure, macrostructure and mechanical properties of wire and arc additively manufactured Ti-6Al-4V have been reported by several studies in recent years. The weldability of Ti-6Al-4V with GMAW is considered worse (see Section 2.1.1). Therefore, until now, most research in this field has been conducted on GTAW-produced Ti-6Al-4V. Some characteristics of both processes (GMAW and GTAW) are similar, e.g., the layer dimensions, the energy source, and the raw material shape. Consequently, similarities between the resulting microstructures are expected. Therefore, in the following, the resulting microstructures of the GTAW, the GMAW, and the PAW process are reported. Since controlling the WAAM process is not within the scope of this thesis, the state of the art is presented to show the differences and the similarities between WAAM-material and conventionally manufactured material.

WAAM-microstructure and macrostructure. For CMT-processed Ti-6Al-4V, TIAN et al. (2019) reported a basket-weave structure. With the same deposition process, GOU et al. (2019) found a fine acicular α' martensite within the basket-weave structure on the side of the deposited wall. On the top of the wall, GOU et al. (2019) observed a basket-weave microstructure with large columnar grains. The micrographs are shown in Figure 2.5.

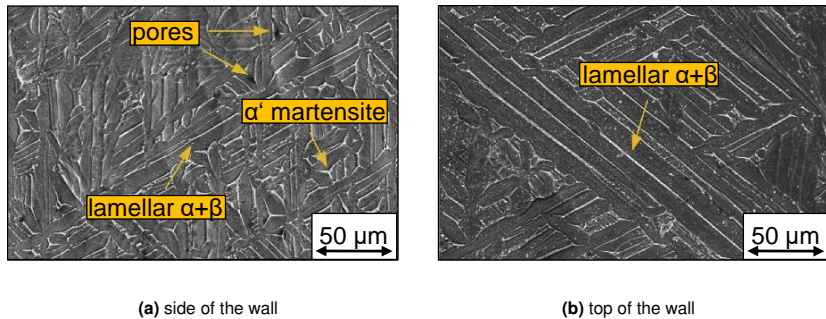


Figure 2.5: Micrographs of a wall deposited with CMT (GOU et al. 2019); reprinted from Journal of Manufacturing Processes, 42, Jian Gou, Junqi Shen, Shengsun Hu, Yinbao Tian, and Ying Liang, Microstructure and mechanical properties of as-built and heat-treated Ti-6Al-4V alloy prepared by cold metal transfer additive manufacturing, pp. 41–50, Copyright (2019), with permission from Elsevier

The CMT process was also used by VÁZQUEZ et al. (2020) to study the influence of the cooling conditions on the microstructure. The longer the time interval between the deposition of the layers is, the further the deposited material cools down between two manufactured layers. In that case, the authors observed an increase in the α' martensite microstructure within a Widmanstätten structure. With forced cooling, VÁZQUEZ et al. (2020) could speed up this behavior and consequently reduce the time interval between the deposition of different layers.

For the GTAW process of Ti-6Al-4V, similar results concerning the microstructure were found. BAUFELD et al. (2009) found a coarse Widmanstätten microstructure with acicular lamellae in the bottom of the part close to the substrate. The top layers showed a needle-like microstructure. The thickness of the top layer increased with the height of the wall. The authors concluded that the Widmanstätten structure was likely linked to sequential heat treatment by the deposition of the individual layers. In 2011 (BAUFELD et al. 2011), the same authors observed elongated β -grains growing epitaxially⁴ through the deposited layers. The microstructure consisted of a Widmanstätten structure. Slender lamellae were present at the top, while at the bottom the lamellae were thicker. The authors linked the thickening of the lamellae to the repeated heat treatment of the lower layers due to the deposition of the top layers.

Similar macrostructural grain growth was also reported by WANG et al. (2013), who found large epitaxial columnar β -grains grown from the substrate to the top of the deposited wall. Each deposition pass was detectable as well in the macrostructure. Concerning the microstructure, the authors found a coarse Widmanstätten structure over most of the wall. Only in the transition zone between individual layers, a fine Widmanstätten microstructure was observed.

ZHOU et al. (2020) detected a Widmanstätten structure in the bottom of the parts as well. In the top layers, the authors noted an acicular α -phase interwoven with a basket-weave microstructure, while in the middle of the parts, a basket-weave microstructure developed. The authors found these microstructural developments to be independent of the deposition strategy. The same microstructure was observed by YI et al. (2020). They refined this Widmanstätten structure using a cooling system for the deposited material.

For the PAW process, both Widmanstätten and basket-weave structures were also observed (LIN et al. 2016).

In addition to the research on as-deposited material, several post-processing techniques have been studied to refine the microstructure and enhance the mechanical properties, such as interpass-rolling (MARTINA et al. 2013; MCANDREW et al. 2018), cooling (YI et al. 2020), and subsequent heat treatment (VAZQUEZ et al. 2021).

Mechanical properties. The mechanical properties of metals are influenced by their microstructure. As presented, the microstructure of WAAM-Ti-6Al-4V differs from the microstructure of conventionally produced Ti-6Al-4V. Therefore, research is presented in the following on the achievable mechanical properties.

Even though the GMAW process is less common for Ti-6Al-4V than is the GTAW process, some researchers have already studied its resulting mechanical properties. VAZQUEZ et al. (2021) observed anisotropy in the tensile behavior. The YS

⁴“The growth of a thin layer on the surface of a crystal so that the layer has the same structure as the underlying crystal” (COLLINS ENGLISH DICTIONARY 2022)

in the welding direction ($884.9 \text{ MPa} \pm 10.3 \text{ MPa}$) was lower than in the building direction ($917.5 \text{ MPa} \pm 8.1 \text{ MPa}$). The same held true for the Ultimate Tensile Strength (UTS) and the elongation. The authors decreased the YS and the UTS, but increased the elongation using heat treatments. Increased tensile properties were observed for a strategy using overlapping beads within each layer. ZHANG et al. (2021) analyzed the influence of the deposition rate on the mechanical properties. The authors increased the deposition rate by increasing the wire feed rate. They observed a decrease in the UTS of around 100 MPa to approximately 900 MPa. This behavior was linked to the higher thermal energy input and to a lower cooling rate.

Initial studies on the mechanical properties of GTAW manufactured Ti-6Al-4V were conducted by BRANDL et al. (2010). The authors measured a hardness of $(337 \pm 14) \text{ HV } 0.1$ in the center of the investigated part. The hardness increased at the top to $(346 \pm 16) \text{ HV } 0.1$. The YS reached 856 MPa to 915 MPa and the UTS 930 MPa to 981 MPa. The elongation was between 6.6% and 20.5%. The high cycle fatigue was higher than that of cast material. At the same research facility, in 2011, a UTS between 880 MPa and 1054 MPa was observed. The strain at failure depended significantly on the sample orientation. In the building direction, much higher strains were observed than in the welding direction. (BAUFELD et al. 2011)

An anisotropy of the tensile properties was reported by YI et al. (2020) as well. The authors studied the influence of the cooling rate. Overall, a lower YS and UTS in the building direction were detected than in the welding direction. With an increased cooling rate, a higher YS and UTS, along with a decreased elongation, were noticed.

WANG et al. (2013) studied the tensile and fatigue behavior of PAW manufactured Ti-6Al-4V. The authors observed an average YS of 950 MPa in the welding direction, while the YS in the building direction was 803 MPa. Accordingly, the tensile properties are dependent on the orientation of the sample relative to the orientation of the deposition process.

For fatigue testing, no dependence on the orientation of the samples was detected. On average, the high cycle fatigue resistance of the WAAM-samples was better than the authors' reference material. The authors linked this to the different microstructure of the reference material. The UTS and YS for PAW-manufactured Ti-6Al-4V were studied by LIN et al. (2016) as well. At a YS of $909 \text{ MPa} \pm 13.6 \text{ MPa}$ and a UTS of $988 \text{ MPa} \pm 19.2 \text{ MPa}$, the authors' as-deposited material had a higher mechanical resistance than the standard for cast material given by the American Society for Testing and Materials (ASTM).

In summary, all authors reported the YS and the UTS to be within the range according to the state of the art for conventionally manufactured Ti-6Al-4V (see Table 2.2). This held true for the hardness as well. The elongation ϵ , however, was described with a larger interval.

2.1.3 WAAM-part geometry

WAAM-component geometries have been experimentally characterized, and several authors developed models to describe the expected geometry based on the welding parameters. Within the literature, two important research areas were identified: the study of abnormal⁵ areas of the weld bead, and the research into the geometry of stacked weld beads.

Study of abnormal areas. The focus of research of TANG et al. (2019) was the abnormal area of the weld bead at the arc striking point (start of the weld) and the extinguishing point (end of the weld). The authors studied the influence of the welding parameters on the weld bead geometry. Without an adaption of the parameters, the beginning of the weld beads tended to be wider and higher than the middle area, while the ends of the weld bead were wider and flatter. The authors developed a so-called burning back method, going back over the flatter area to equalize the abnormal areas to the middle of the weld bead. The authors' validation showed a successful application of the method. In 2020, members of the same research group determined regression equations for the abnormal bead areas and used these models to optimize the welding parameters (TANG et al. 2020). Finally, in 2021, they presented a closed-loop control system to control the height and width of the weld bead by adjusting the welding parameters (TANG et al. 2021).

Research into the geometry of stacked weld beads. Research into the geometry of stacked weld beads has been focused on developing geometrical models to describe the resulting part geometry (KAZANAS et al. 2012) and to predict the part geometry based on the welding parameters. The latter is classifiable with a definition of terms by the author of this thesis relating to the type of deposition that was studied (see Figure 2.6):

- T1 *single-layer, single-bead deposition*: one weld bead is deposited on the substrate (DING et al. 2015a; GENG et al. 2017; KARMUHILAN and SOOD 2018),
- T2 *single-layer, multi-bead deposition*: several intersecting or adhering weld beads are deposited in one layer on the substrate (DING et al. 2015a),
- T3 *multi-layer, single-bead deposition*: one weld bead is stacked in multiple layers on the substrate (ABE and SASAHARA 2015; ALMEIDA and WILLIAMS 2010; SZOST et al. 2016), and
- T4 *multi-layer, multi-bead deposition*: several intersecting or adhering weld beads are stacked in multiple layers on the substrate (DING et al. 2015a; LI et al. 2018).

⁵“abnormal” refers to areas where the geometry differs from the geometry of most areas of the weld. The term was formulated by TANG et al. (2019).

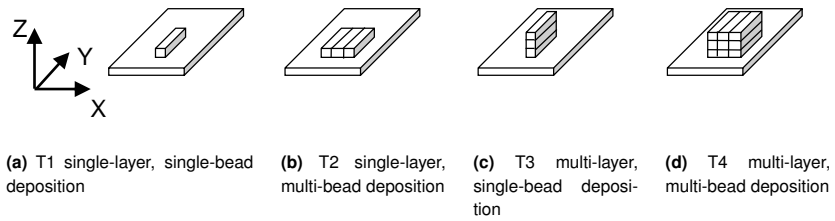


Figure 2.6: Schematic of the types of deposition

A comparability of the geometry of stacked weld beads for different materials and welding processes is expected, since the deposition process flow from wire to molten material to weld bead is similar. Therefore, the following research is presented independently of the materials and the welding process.

DING et al. (2015c) concluded that parabola and cosine functions most accurately represented the cross-sectional area of a single-layer, single-bead deposit (T1). Based on these results, the authors developed a model for single-layer, multi-bead cross-sections (T2). The authors realized that the distance d between the beads was critical for achieving a stable surface. Their model was verified by producing multi-layer, multi-bead deposits (T4) showing a stable surface with a periodically varying surface height $H(x)$, dependent on the position. The resulting surface profile is depicted in Figure 2.7. The profile is shown as a cut through the part parallel to the X-Z plane (see Figure 2.2). With the distance d below the critical distance, the surface enveloping plane is inclined with the angle η towards the horizontal line. With the distance d equal to the critical distance, the resulting enveloping plane is horizontal. The surface height $H(x)$ periodically varies. In the context of wire and arc additive manufacturing, this is considered as a stable surface, since there is no inclination η . The distance d above the critical distance would likely also result in an inclination of the surface enveloping plane, since the material spreads out further and further, though this case was not presented by the authors.

Challenges in manufacturing sharp angles and large curvatures (in T1) were addressed by GENG et al. (2017). They determined a minimum angle for sharp corners and a minimum radius for the curve. With angles smaller than the minimum angle, they showed that a wetting of the initial side occurred during the deposition of the terminal side, which led to a build-up of material. For the curvature, radii smaller than the minimum radius led to a material accumulation on the weld bead side oriented towards the center of the curvature. They concluded that both would lead to varying heights when stacking several layers (T3).

Another challenge concerning the height of the deposited surface H was addressed by ABE and SASAHARA (2015). The authors showed that for an inclined multi-layer, single-bead deposition (T3), the deposited height varied compared to a deposition with a similar number of layers perpendicular to the substrate.

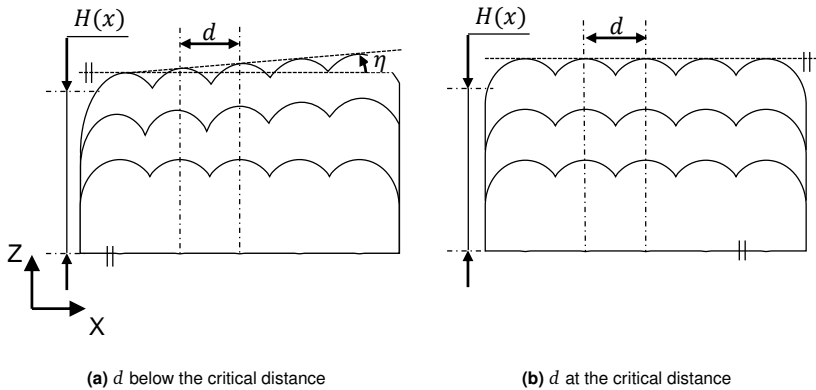


Figure 2.7: Schematic depiction of a multi-layer, multi-bead cross section based on the experimental results according to DING et al. 2015c

They proposed a model of intersecting symmetric parabolas (Figure 2.8) to enable the calculation of the component height and the single-layer height h_{layer} depending on the welding torch speed and the inclination angle Θ . The model was then used to develop CAM-software to compensate for the height error in inclined models by adjusting the welding torch speed v_T . This was successfully applied in the manufacture of a part. Figure 2.8 shows that even in the modeling a varying cross-section is expected since round shapes are stacked on each other.

The varying cross-section of deposited weld beads was studied by KAZANAS et al. (2012). The authors showed that a multi-layer, single-bead deposit's cross-section (T3) does not resemble a rectangle, but is similar to the schematic depictions in Figure 2.8 and 2.9 by the presence of a number of indented areas. Thereby, the effective wall thickness w_e (= maximum constant wall thickness after milling) varies depending on the welding parameters.

The degree of the variation was studied by SZOST et al. (2016). They stated that it could be specified by a deviation from the ideal flat surface and linked it to the deposited layers. On their sample, the periodicity was 1 mm, in agreement with the offset between layers which was 1 mm as well.

LI et al. (2018) also studied the cross-section. The authors observed that with an increasing built height the width of the deposited beads increased, while their individual height decreased. They linked this observation to the slower solidification of the molten pool due to lower heat transfer the further the deposition is away from the substrate. This was solved by developing a thermoelectric cooling system which resulted in a 56.8% decrease in bead width deviation.

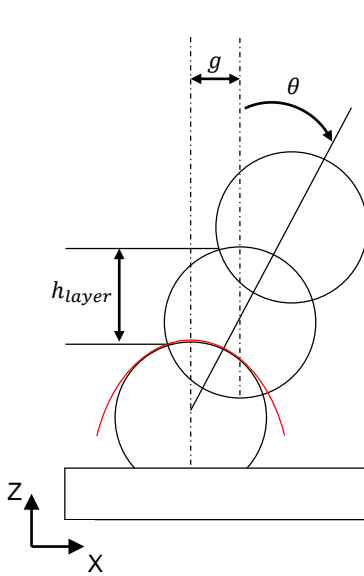


Figure 2.8: Schematic depiction of the weld bead cross section based on ABE and SASA-HARA (2015)

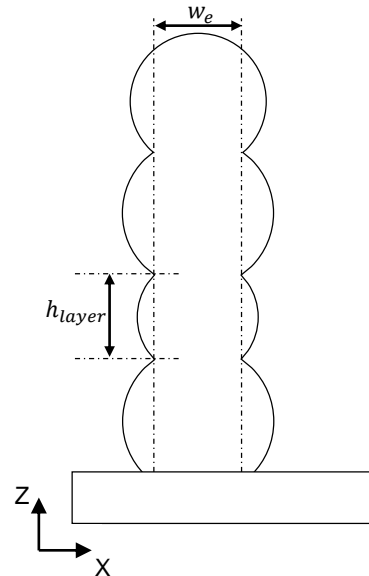


Figure 2.9: Schematic depiction of the effective wall width based on results by KAZANAS et al. (2012)

An additional area of study concerning both the WAAM-part geometry and the microstructure is the quality control during the deposition process. BAIER et al. (2020) presented a method to ensure a high quality of geometrically complex components by splitting them into geometrically simple shapes, such as blocks, walls, and cylinders, and validating deposition parameters individually for each shape. The authors' method enables the control of the microstructure and the WAAM-geometry.

In summary, the literature on WAAM-part microstructure, mechanical properties, and part geometry properties is listed in Table 2.3. Visibly, considerable research has already been performed on the microstructure and mechanical properties of wire and arc additively manufactured Ti-6Al-4V, while research on the part geometry obtained by WAAM is scarce. These properties are expected to influence the milling process. Therefore, the background and state of the art on the machining of WAAM-material is presented in the following Section 2.2.

Table 2.3: Overview of the publications presenting research on the microstructure, mechanical properties and geometry of wire and arc additively manufactured Ti-6Al-4V; ● – the topic is the research focus, ◐ – the topic is (partially) included, ○ – the topic is not addressed

Material	Publication	Macro- and microstructure	Mechanical properties	WAAM-geometry
Ti-6Al-4V	BAUFELD et al. 2009	◐	●	○
	ALMEIDA and WILLIAMS 2010	●	○	◐
	BRANDL et al. 2010	◐	●	○
	BAUFELD et al. 2011	●	●	○
	WANG et al. 2013	●	●	○
	MARTINA et al. 2013	●	●	○
	SZOST et al. 2016	●	◐	◐
	LIN et al. 2016	●	●	○
	MCANDREW et al. 2018	●	○	○
	TIAN et al. 2019	●	●	○
	GOU et al. 2019	●	●	○
	VÁZQUEZ et al. 2020	●	●	○
	ZHOU et al. 2020	●	●	○
	YI et al. 2020	●	●	○
	BAIER et al. 2020	○	○	●
	VAZQUEZ et al. 2021	●	●	○
ZHANG et al. 2021	●	●	○	
Steel	KAZANAS et al. 2012	○	○	●
	ABE and SASAHARA 2015	○	○	●
	DING et al. 2015c	○	○	●
	KARUHILAN and SOOD 2018	○	○	●
	TANG et al. 2019	○	○	●
	TANG et al. 2020	○	○	●
	TANG et al. 2021	○	○	●
Al alloy	GENG et al. 2017	○	●	●
	LI et al. 2018	○	○	●

2.2 Machining

Most metallic airplane surfaces are machined to minimize the airplane mass and to enhance the fatigue properties (SARH et al. 2009). For non-rotationally symmetric parts, milling is one of the most common machining processes for air-frame components (EZUGWU and WANG 1997). Therefore, it is the one which is researched within this thesis, and its process principles are discussed in Section 2.2.1. However, challenges arise when milling Ti-6Al-4V. These are addressed in Section 2.2.2. Several key characteristics of the milling process are similar to those of other metal cutting processes. Therefore, in Section 2.2.3, the state of the art concerning the machining in general of wire and arc additively manufactured Ti-6Al-4V is presented.

2.2.1 Principles of the milling process

Milling is categorized as a cutting process with a defined cutting edge (DIN 8580 2020). During the process, material is removed from the raw material by the tool's cutting edges in the form of chips (TOENSHOFF 2014a). Milling is characterized by the cutting speed resulting from the tool's rotation and a feed movement along, oblique, or perpendicular to the tool's rotational axis (DIN 8589-3 2003). Accordingly, to accommodate the feed movement oblique or perpendicular to the rotational axis, milling tools have two types of cutting edges: the primary cutting edge and the secondary cutting edge. A schematic of a milling tool is depicted in Figure 2.10. Several types of cutting are differentiated, depending on the direction of the feed relative to the tool's axial direction and the cutting edges involved in the cutting process. Peripheral milling is commonly used for aircraft structural components (RATCHEV et al. 2004). The process schematic as well as the kinematic and geometric parameters are depicted in Figure 2.11.

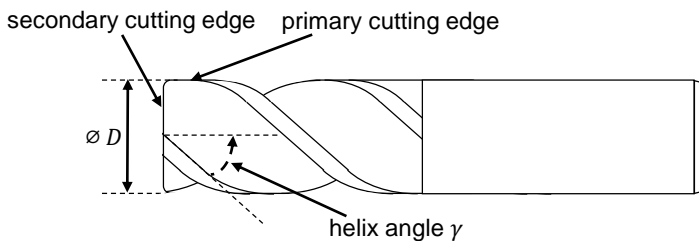


Figure 2.10: Schematic of a milling tool, D – tool diameter, depiction based on (ALTINTAS 2012; BÖGE 2017)

The kinematic and geometric parameters are part of the process input, along with the workpiece properties, the tool properties, and environmental influences (TOENSHOFF 2014a). Kinematic parameters are the cutting speed v_c and

the feed velocity v_f , with their control variables spindle speed n , tool diameter D , feed rate per tooth f_z , and the number of cutter teeth z . The cutting speed v_c is defined as

$$v_c = n \cdot D \cdot \pi , \quad (2.1)$$

where n denotes the spindle speed, and D denotes the tool diameter (GROOVER 2011). The feed velocity v_f is calculated from the feed per tooth f_z , the number of teeth z , and the spindle speed n as

$$v_f = f_z \cdot n \cdot z \quad (\text{GROOVER 2011}) . \quad (2.2)$$

From the feed per tooth f_z and the cutter angle Φ , the uncut chip thickness h can be determined as

$$h(\Phi) = f_z \cdot \sin(\Phi) \quad (\text{ALTINTAS 2012}) . \quad (2.3)$$

The productivity of the process can be quantified by the volumetric material removal rate MRR_{vol} , which is defined as

$$MRR_{vol} = v_f \cdot a_p \cdot a_e , \quad (2.4)$$

where $a_p \cdot a_e$ denotes the area of the cut. a_p and a_e are, therefore, geometric parameters defining the engagement of the tool and the workpiece (GROOVER 2011). This tool engagement is also depicted in Fig. 2.11.

Three strategies are differentiated for the milling process based on the cutter's angle of entry Φ_e of the cutter's teeth into the workpiece: face milling, up-milling, and down-milling. For up-milling operations, the feed direction of the workpiece is opposite to the spindle rotational direction (*DIN 8589-3 2003*). In this case, the entry angle of the cutter is 0° . A schematic of the up-milling kinematics is depicted in Figures 2.11 and 2.12. For down-milling operations, the spindle direction is inverse to the one marked in Figure 2.12. The exit angle is then 0° .

The workpiece properties are also inputs for the milling process (TOENSHOFF 2014a). The workpiece characteristics and properties are summarized by its machinability (GROOVER 2011), which is determined from the tool life, the surface finish, the cutting forces, the power consumption, and the ease of chip disposal (GROOVER 2011; HUDA 2021). A short tool life, a low surface finish, high cutting forces, a high power consumption and a low ease of chip disposal constitute low machinability.

The cutting forces F are produced as a part of the process interactions (TOENSHOFF 2014a). Each tooth experiences these forces in the tangential (t), the radial (r), and the axial (a) direction of the tool during the shearing motion to cut the material. According to ALTINTAS (2012), these cutting forces are expressible as

$$\begin{aligned} F_t(\Phi) &= K_{tc} \cdot c \cdot h(\Phi) + K_{te} \cdot c , \\ F_r(\Phi) &= K_{rc} \cdot c \cdot h(\Phi) + K_{re} \cdot c , \text{ and} \\ F_a(\Phi) &= K_{ac} \cdot c \cdot h(\Phi) + K_{ae} \cdot c , \end{aligned} \quad (2.5)$$

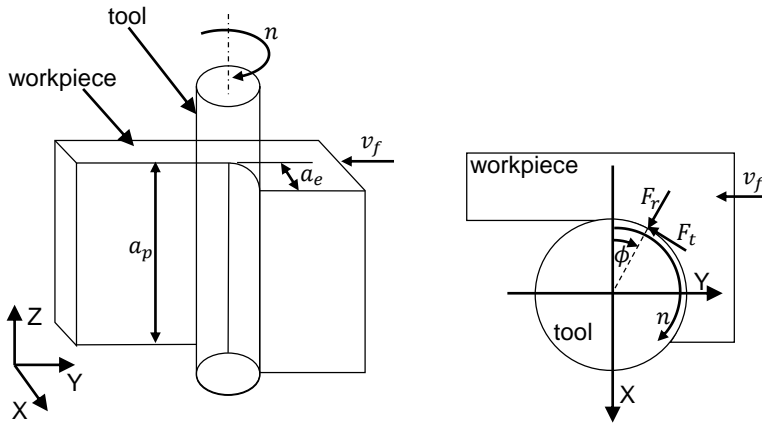


Figure 2.11: Schematic of the peripheral milling **Figure 2.12:** Schematic of the up-milling process with geometric parameters based on *DIN 6580* (1985), *DIN 8589-3* (2003), and *ALTINTAS* (2012). GROOVER (2011).

where K_{tc} , K_{rc} , and K_{ac} denote the cutting force coefficients for the shearing action, and K_{te} , K_{re} , and K_{ae} represent the edge constants. The cutting forces are dependent on the uncut chip area $c \cdot h(\Phi)$ and the edge contact length c . The six cutting force coefficients K must be determined by milling tests or calculated from previously determined coefficients and are constant for a workpiece and tool combination. (ALTINTAS 2012)

Based on the schematic shown in Figure 2.12, the cutting forces are also expressible in the X-Y coordinate system using horizontal (feed), normal and axial components (ALTINTAS 2012) as

$$\begin{aligned} F_x(\Phi) &= -F_t \cdot \sin(\Phi) + F_r \cdot \cos(\Phi) , \\ F_y(\Phi) &= -F_t \cdot \cos(\Phi) - F_r \cdot \sin(\Phi) \text{ and} \\ F_z(\Phi) &= +F_a . \end{aligned} \quad (2.6)$$

Notably, the equations presented here are simplifications and are only valid for cutters with a helix angle γ of zero. For more complex cutter geometries, the cutting forces must be expressed as an integral along the cutting edge. (ALTINTAS 2012)

In addition to the equations presented here for the mechanistic identification of cutting forces, several more representations for the calculation and simulation of cutting forces exist. Examples are the equations by Kienzle and Victor or Ernst

and Merchant (GROOVER 2011; TOENSHOFF 2014a)⁶. The process output are the chip form and the effects on the workpiece, the tool, and on the environment (TOENSHOFF 2014a).

2.2.2 Milling process challenges

Several challenges are generally associated with controlling the machining process interactions and effects, such as the forces, the temperature, the vibrations, and the stresses and deflections (TOENSHOFF 2014a). In this section, the challenges, especially for milling Ti-6Al-4V, are addressed and state of the art solutions are presented.

Forces and temperature. Titanium and its alloys are usually considered as materials with a low machinability (GROPPE 2014; NIKNAM et al. 2014). One reason for the low machinability is the low thermal conductivity, resulting in a high thermal load on the tool (GROPPE 2014). Furthermore, the material has a low modulus of elasticity and a high tensile strength, leading to only minor plastic deformations (GROPPE 2014). This results in high mechanical loads on the flanks of the cutting tool (GROPPE 2014). Titanium alloys also tend to react with the cutting tool materials. This adversely affects the tool life. At the same time, protective tool coatings fail rapidly due to the high temperatures during the cut (NIKNAM et al. 2014). The high cutting forces are linked to strain rate hardening⁷ (NIKNAM et al. 2014). Segmented chip formation is often reported, which is why localized shearing exists and the effective chip thickness varies (PRAMANIK 2014). The chip thickness variation leads to a cyclic force on the tool, which may lead to rough machined surfaces, chatter, and tool breakage (PRAMANIK 2014).

Vibrations. Vibrations in machine tools are induced by various sources, such as the process, the environment, and the machine tool itself (SHAMOTO and SENCER 2014). Every vibration is caused by an exciting force or displacement and results in a deterioration of the machined surface or shortened tool life (SHAMOTO and SENCER 2014). Additionally, self-excited vibrations may occur in machining processes, known as chatter (ALTINTAS and WECK 2004). Periodicity in the cutting forces instigates process-induced vibrations. This periodicity is either process inherent or induced by tool runout, imbalance or non-symmetric cutting teeth. The forced vibrations then occur at the tooth passing frequency or at the spindle frequencies including their harmonics (ALTINTAS 2012).

⁶The equations from the original publications (likely ERNST and MERCHANT 1941; KIENZLE and VICTOR 1957) were reproduced many times and their formatting transformed into today's mathematical formulae. Therefore, textbooks on basic machining principles are given as references here.

⁷The faster the deformation, the more stress needs to be applied to achieve the deformation (ATZEMA 2017).

Chatter can occur when the chip thickness varies. Initially, one structural mode is forcibly excited, which results in a wavy surface. The next tooth, which also oscillates due to forced vibrations, removes a chip thickness that varies. In turn, this leads to oscillating cutting forces in case this waviness is removed with the next cut or by the next tooth. These excitation effects can build up and lead to tool breakage or jumping out of the cut. (ALTINTAŞ and BUDAK 1995) The milling process stability for chatter depends on the spindle speed and the axial depth of the cut (BUDAK 2014).

Deflections. As within any mechanical system, the applied forces lead to a deflection of the parts involved in the cutting process. In the machining process, these deflections lead to errors in the geometric form of the workpiece (ALTINTAS 2012; RATCHEV et al. 2004). A schematic of such deflections of the workpiece is depicted in Figure 2.13. The tool is depicted in the schematic in a simplified rigid manner. In reality, the tool could also be deflected.

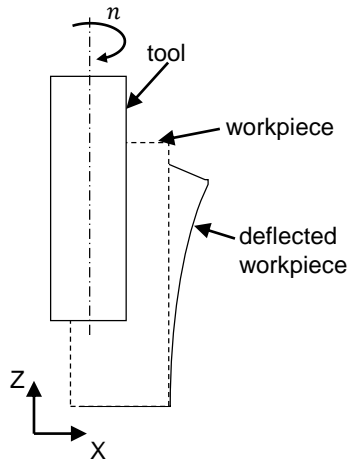


Figure 2.13: Schematic depiction of deflections due to the cutting forces based on RATCHEV et al. (2004), with the assumption of a stiff tool

Additionally, the thermal heat input into the workpiece may also lead to deflections (LOEHE et al. 2012). Specific to titanium alloys are the deformations that are caused by its low modulus of elasticity E , which results in a bouncing action when the cutter enters the cut (CAMPBELL 2006). According to LOEHE and ZAEH (2014), two approaches are in use to reduce deflections during the milling process: a process-related approach and compensation strategies.

Within the process-related approach, kinematic and geometric process parameters (v_c , v_f , a_e , and a_p) are sought to reduce deflections. For example, BUDAK and ALTINTAS (1995) developed a model to predict the form error and to lower

it by choosing an appropriate feed rate and radial depth of cut. By scheduling the feed rate along the plate that was machined, narrowing the tolerance of the form error from $300\ \mu\text{m}$ to $80\ \mu\text{m}$ was possible with only a slight increase in the machining time. The machining strategy was addressed by HERRANZ et al. (2005). The authors proposed a strategy of switching the cutting from side to side several times during machining for milling thin-walled parts, and successfully applied it to machine an aluminum alloy into a wall with a thickness of 0.3 mm. The form error was reduced to $4\ \mu\text{m}$. The authors also suggested using the up-milling strategy. In up-cut milling, the force component in the normal direction, which is mainly responsible for deflections, pulls the workpiece into the tooth, helping to reduce deflections.

Compensation strategies are based on the adaption of the tool path trajectory. DÉPINCÉ and HASCOËT (2006b) presented such a compensation strategy. The authors proposed a computational method based on calculating the cutting forces and the tool deflection in the normal direction. Then, a compensation value was calculated from the expected tool deflection and the part's tolerances, which was applied in the opposite direction of the expected error. The authors successfully applied the method to manufacture an industrial part, reducing the overall surface error to reach the tolerance zone.

WIMMER (2020) incorporated a flexible workpiece into a similar approach. The author simulated the cutting forces and the workpiece deflection. Based on the simulation results, he adapted the tool's path by discretizing the poses and adjusting the tool's position and axis orientation. The form error was significantly reduced on an aluminum part using his method.

For nearly all deflection reduction methods, it is necessary to determine the cutting forces and estimate the tool and/or the workpiece deflections. The cutting forces are obtainable from either

- *empirical models* which are derived from experimental cutting data or analytical models based on elementary plastomechanics, or
- *Finite Element (FE) methods* (TOENSHOFF 2014a).

Based on these cutting force estimations, several options exist to approximate the tool deflection:

- *geometrical modeling*: cylindrical model, equivalent tool diameter model, and Computer-Aided Design (CAD) model
- *cutting force modeling*: concentrated forces, and distributed forces
- *deflection calculation*: cantilever beam model based on solid mechanics and FE methods (DÉPINCÉ and HASCOËT 2006a)

The workpiece deflections are usually determined by FE simulation. This is necessary since during the milling process the material is removed from the workpiece, and thus, stiffness and deflection behavior are time-dependent. (WIMMER 2020)

2.2.3 Machinability of material manufactured with wire-based processes

Several researchers have already conducted investigations on the topic of the machinability of WAAM-material. In the following, their research is discussed for various WAAM-materials. Investigations into the machinability of materials manufactured by AM processes other than WAAM are omitted, since the microstructure, which has a significant influence on the machinability, is influenced by the AM process.

Steel. MONTEVECCHI et al. (2016) compared the machinability of wrought, laser additively manufactured and wire and arc additively manufactured AISI H13 steel. Their results showed higher average cutting forces for the AM-materials. At the same time, the hardness of the AM-materials was higher than that of the wrought material. The authors concluded that this was the likely reason for their results. Due to the higher cutting forces, the machinability of the AM-materials could be considered lower. Contrastingly, MASEK et al. (2019) determined that the machinability based on the surface quality was higher for WAAM than for a hot rolled rod made of American Iron and Steel Institute (AISI) 316L. The authors also measured a higher hardness for the WAAM-material and concluded that machinability could not be determined based on hardness alone, since the material composition and microstructure also influence the results.

LOPES et al. (2020) also detected an influence of the microstructure. The authors carried out slot milling experiments on High-strength low-alloy steel (HSLA steel) parts manufactured by GMAW. Seemingly, the microstructure did not influence the cutting forces, but significant tool wear was detected, which was assumed to be caused by strong fluctuations in the microstructure. The cutting forces and the tool wear were also studied by DTTMANN and GOMES (2021). The authors conducted milling experiments on GMAW-manufactured ER70S-6 steel parts with three cutting speeds. The cutting force decreased with increased cutting speed, while the tool wear increased. These results were in accordance with the state of the art for milling conventionally manufactured material.

The influence of the WAAM-part geometry on the orthogonal cutting process was shown by ESCHELBACHER and MÖHRING (2021). The experiments were conducted on a test bench and the authors analyzed the structure-borne sound and the cutting forces. They concluded that the WAAM-geometry influenced the structure-borne sounds. Therefore, the structure-borne sound and the cutting force signals can be used to detect defects in the welded material. The geometry of the WAAM-parts was also a focus of a study by CHERNOVOL et al. (2021). The authors studied the WAAM process and the influence of the cutting parameters on the milling process stability. The material was EN ISO 14341-A (G 42 4/M21 3Si1), and the process was GMAW. The authors detected a relation between the WAAM process parameters and the milling process stability, mainly

due to the difference in microstructures and deposited wall widths. It was concluded that a shorter cooling time leads to a decreased component stiffness and thus provoked chatter during the milling process in their case.

Titanium alloys. ALONSO et al. (2020) compared the machinability of PAW-manufactured Ti-6Al-4V to the machinability of a conventionally manufactured plate. The results showed a higher cutting torque for the PAW-manufactured titanium than for conventional material, which was in agreement with the higher hardness of the material. The cutting torque for three milling strategies, up-milling, down-milling, and slot-milling, was analyzed by VEIGA et al. (2020). The authors conducted peripheral milling experiments in PAW-manufactured Ti-6Al-4V. They showed that the variations in the hardness had no significant influence on the cutting forces. The torque difference between up-milling and down-milling was statistically insignificant, however, slot milling led to tool breakage. This was linked to the direction of the tool path, which was perpendicular to the deposited layers.

The literature on the machinability of WAAM-material is summarized in Table 2.4.

Table 2.4: Overview of the publications presenting research on the machinability of WAAM-material, and the topics studied in connection with the machinability; ● – the topic is the research focus, ◐ – the topic is (partially) included, ○ – the topic is not addressed

Material	Publication	Machinability	Microstructure	Mechanical properties	WAAM-geometry
Steel	MONTEVECCHI et al. 2016	●	○	◐	○
	MASEK et al. 2019	●	◐	◐	○
	LOPES et al. 2020	●	◐	○	◐
	DTTMANN and GOMES 2021	●	◐	◐	◐
	ESCHELBACHER and MÖHRING 2021	●	○	◐	◐
	CHERNOVOL et al. 2021	●	○	◐	◐
Ti-6Al-4V	ALONSO et al. 2020	●	◐	◐	○
	VEIGA et al. 2020	●	◐	◐	○

Visibly, only a small amount of research has been conducted up until present. Therefore, it was chosen to be a topic of research for this thesis. However, before a manufacturing process can be conducted, it must be planned. Consequently, the background and state of the art of process planning, which is a part of process chain design, is presented in the following Section 2.3.

2.3 Process chain design

Process chain design needs to be conducted in order to achieve an efficient production (DENKENA and TÖNSHOFF 2011). Within this section, the terms related to process chain design are first defined. Then, the state of the art on process chain design for the combination of AM and machining is presented. Finally, the Process and Operations Planning (POP) within such a process chain is discussed.

2.3.1 Definition of terms and general considerations

Within the manufacturing context, a *process chain* is defined as "a sequence of process elements with the objective of transforming certain items from an input state into a conformable [desired] output state" (HENJES 2014). *Processes* are the most minor and impartible parts of such a process chain (DENKENA and TÖNSHOFF 2011). They are defined by their input and output parameters (HENJES 2014) and use "one or more physical mechanisms to transform a material's shape and/or properties" (CHRYSSOLOURIS 1992). The *technological interfaces* define the transfer of information and material between the processes (DENKENA and TÖNSHOFF 2011). Transferred information can include surface quality, part dimensions, or processing temperatures, for example (DENKENA and TÖNSHOFF 2011). The task of the *process chain design* is to identify and to arrange processes to achieve specific product characteristics and efficient production (DENKENA and TÖNSHOFF 2011). If a previous process chain exists, three options are available to remodel the process chain:

- *adaption*: adjusting sequential processes for higher efficiency or higher quality,
- *substitution*: replacing one process with another, and
- *integration*: conducting one process together with another one (HENJES 2014).

Planning steps must be conducted before a component is manufactured with a specific process chain. The planning steps are part of the *production planning* (DENKENA and TÖNSHOFF 2011; SCALLAN 2010). Planning steps to select and sequence processes are considered *process planning* (D'ADDONA and TETI 2014;

SCALLAN 2010). How each process is carried out is defined during the *operations planning* (D'ADDONA and TETI 2014; EVERSHEIM 2002). This contains, for example, the selection of tools and tool holders and the process parameter selection. It is carried out individually for each process. Within this thesis, defining how the POP must be conducted is considered part of the process chain design. Overall, production planning considers a broader context. Scheduling machines and people, coordinating suppliers, and deciding what is to be produced where, when, and how are also production planning activities (D'ADDONA and TETI 2014). Process chains, in which the main processes are additive manufacturing and machining, are designated additive-subtractive process chains within the thesis. However, the thesis presents only research concerning the WAAM process as the AM process. To enable a comparison of the researchers' results, they are clustered with the above introduced definitions. However, the publication authors' original terms for the process steps are retained, in order to showcase the confusion within the state of the art. A listing by the author of this thesis of the actions within the steps is given in the Appendix A.1.

2.3.2 Process chain design for additive-subtractive manufacturing

Several researchers have already studied the process chain design for additive-subtractive manufacturing. Two types of additive-subtractive process chains were identified by the author of this thesis within the state of the art: sequential and hybrid process chains. Within sequential process chains, additive and subtractive processes are carried out in two different machining centers. First, the part is manufactured entirely by additive manufacturing, and subsequently it is milled or cut by some other process. An adaption of the processes is usually necessary for this type of process chain remodeling. This process chain might also be conducted on one machining center, provided the tool is changeable from a welding torch to a milling spindle. Based on the definitions by DENKENA and TÖNSHOFF (2011), if the conventional process chain included the manufacturing of a near-net shape by a forming process such as forging, the remodeling type may be considered a substitution, replacing the forming process by AM. Hybrid process chains incorporate both processes within one machining center, and the operations are carried out iteratively: one layer is deposited and machined before the next layer is deposited. The remodeling type is then an integration, not a substitution. Both process chain types may include further processes, such as heat treatment, process planning steps, and waste material processing, but the main shaping processes are AM and machining.

Sequential process chain. Applications and considerations for the sequential additive-subtractive process chain are described in the literature. The technological interfaces for a WAAM-based sequential process chain were documented by BUSACHI et al. (2015). The authors listed five processes in their process chain:

1. *WAAM system*,
2. *heat treatment*,
3. *machining*,
4. *wire electrical discharge machining*, and
5. *argon recovery**

They divided the process outputs into critical (i.e., noise and vibrations) and non-critical outputs (i.e., waviness resulting in chips, heat, and supports). The connection between the processes was realized by the product flow, whose properties were not described in-depth.

The successful application of a sequential process chain was shown by YA and HAMILTON (2018), for example. The authors focused their research on manufacturing conventionally hard-to-machine propeller designs and explored CNC milling and manual grinding as subtractive machining processes. For the deposition process, the authors used GMAW with a steel wire.

An adaption of the GMAW process for additive manufacturing was proposed by CHERNOVOL et al. (2020), and the setup requirements for sequential manufacturing were documented by REISCH et al. (2020). A total of 15 requirements were collected, including *multi-axis deposition* and the capability of *detecting anomalies*. Based on these requirements, the authors developed a WAAM setup with the CMT process and studied the influence of different lead angles on the deposited walls. They concluded that a lead angle of 0° was preferable since it eased automation and path planning, while its influence on the weld quality was negligible. Finally, REISCH et al. (2020) presented a system architecture for the process chain and used it to document computing needs within the control system. Notably, REISCH et al. (2020) combined the process planning for WAAM and milling within one step.

Hybrid process chain. Several applications of the hybrid additive-subtractive process chain are described in literature. KARUNAKARAN et al. (2010) developed a machining center and software framework for a component's hybrid deposition and finish machining. The authors integrated GMAW equipment into a CNC machining center. The process steps are then deposition of one layer and face milling of this layer until the final height is reached, and peripheral milling to final shape. The successful application of this process chain was shown for manufacturing injection mold dies.

For the fabrication of stiffened panels, LI et al. (2017) developed a two-robot hybrid manufacturing system to fabricate stiffened panels. One robot was equipped with a GMAW welding torch, while the other was outfitted with a spindle and a milling tool. The process chain consisted of the following steps: repeated deposition of one layer and face and peripheral milling of that layer until the deposit reached the desired height. The authors studied the effect of

*For a brief description of the process steps, the reader is kindly referred to Appendix A.1.

the deposition parameters and milling parameters on the surface quality and material utilization. They improved the material utilization from 34% to 91% in comparison to conventional machining.

2.3.3 Process and operations planning for sequential additive-subtractive manufacturing

Substantial research was conducted on the POP for the individual processes WAAM and milling.

WAAM process. DING, PAN, CUIURI, LI, et al. (2016) identified six steps for an automated WAAM process planning:

1. *CAD modeling,*
2. *3D slicing,*
3. *2D path planning,*
4. *bead modeling,*
5. *weld setting,* and
6. *robot code generation*.*

The authors' focus was the bead modeling, which they identified as crucial to achieving geometrical accuracy and which is an input into 2D path planning and weld setting. They implemented a neural network to predict the bead geometry and developed a path planning algorithm based on the Medial Axis Transformation (MAT). (DING, PAN, CUIURI, LI, et al. 2016)

The first step of CAD modeling was, among others, addressed by LOCKETT et al. (2017), who defined design rules for WAAM parts, including part dimensions, symmetry, and machining considerations such as accessibility for the tool. The authors also developed a methodology to determine the build orientation during the WAAM process. The possible build orientations are chosen by guidelines and assessed using five criteria: the deposited material, the number of build operations, the build complexity, the symmetry and the substrate waste. The methodology was applied to two case studies and reviewed by experts, proving that viable build orientations were chosen.

Another framework for the POP was developed by URBANIC et al. (2017). It is applicable to all bead-based additive manufacturing processes, including WAAM. The authors' framework includes five steps:

1. *project setup,*
2. *travel path strategy [selection],*
3. *definition of process-specific parameters,*
4. *travel path simulation and verification,* and
5. *generation of the Numerical Control (NC) code*.*

*For a brief description of the process steps, the reader is kindly referred to Appendix A.1

The machine, the process type, the substrate material, the material and the travel path strategy are considered within the *project setup*. Here, the research is not conclusive, since the *travel path strategy* is also the second item in the framework and thus considered twice. Process-specific parameters are the speed v_T and feed parameters v_W , the substrate heat input parameters, transient conditions, and profile and fill parameters. Simulation modules and CAM path planning modules were developed for the additive processes and linked with a database containing knowledge such as on material parameters and build rules.

In 2020, DAI et al. (2020) stated that planning for the WAAM process generally consists of

1. *modeling*,
2. *slicing*,
3. *path filling*,
4. *tool-path generation*,
5. *weld setting*,
6. *weld code generation*,
7. *welding*, and
8. *machining*^{*}.

According to the previously introduced definitions (see Section 2.3.1), *welding* and *machining* are not part of the planning steps but are manufacturing steps. DAI et al. (2020) studied the steps *slicing*, *path filling*, and *tool-path generation* for the deposition on conical substrates and proposed an algorithm to calculate the tool paths. The authors applied this algorithm to the manufacture of an underwater thruster and achieved a dimensional accuracy of roughly ± 0.55 mm.

An example of a POP method based on the control of the heat input was presented by CUI (2020). The authors investigated in which component areas a higher or a lower heat input was necessary to influence the bead geometry for an improved shape. They demonstrated a successful application of their method by manufacturing an L-shape.

Milling process. For the milling process, a high amount of research was conducted for the POP. In the following, a short overview of the necessary steps is given, along with current research trends.

Generally, XU (2009) defined four steps for the POP in manufacturing:

1. *specification and requirement[s] analysis*,
2. *operation selection and sequencing*,
3. *resource selection*, and
4. *determination of operational parameters*^{*}.

^{*}For a brief description of the process steps, the reader is kindly referred to Appendix A.1

In the first step, the component design is analyzed, and features⁸ are identified. Appropriate manufacturing operations and their sequence are identified in the second step. The resource selection comprises decisions such as the selection of the machine tools, the cutting tools, the fixtures, and the clamps. Operational parameters for machining operations include the process parameters and the tool engagement parameters. (ELMARAGHY and NASSEHI 2014; XU 2009)

More specific to machining processes, HALEVI and WEILL (1995) identified ten steps for the POP. These steps are:

1. *input specifications and interpretation,*
2. *selection of primary processes,*
3. *determination of production tolerances,*
4. *selection of holding devices and datums,*
5. *selection and grouping of operations,*
6. *selection of [the] machine and [the] sequence of operations,*
7. *selection of cutting tools,*
8. *selection of quality assurance methods,*
9. *time and cost module, and*
10. *editing of [the] process sheet*.*

The order of the steps is not fixed. The processing conditions (speeds, tool engagement, etc.) are chosen within the time and cost module. (HALEVI and WEILL 1995)

This approach has shortcomings, such as the fact that the results are depending on the process planner, and that they are incomplete or inconsistent. Also, an extended pre-production time is to be accepted. Therefore, the main research focus is the replacement of manual labor by automation of the planning activities. Research interests in this field are studied under the topic of Computer-Aided Process Planning (CAPP). (HALEVI and WEILL 1995)

Two main approaches are researched within the topic of CAPP: the variant approach and the generative approach (ELMARAGHY and NASSEHI 2014). Already existing process plans for similar parts are used to generate a new process plan within the variant approach (XU et al. 2011). The generative approach uses decision logic and process knowledge to develop process plans (XU et al. 2011). For this purpose, feature-based or knowledge-based systems were developed, and the benefits of machine learning algorithms such as neural networks and genetic algorithms were studied (XU et al. 2011). In specific regard to the milling POP for the post-processing of WAAM-components, no research was identified at this time.

⁸“A feature is a physical constituent of a part, which is mappable to a generic shape, has engineering significance, and has predictable properties.” (SHAH and MÄNTYLÄ 1995).

*For a brief description of the process steps, the reader is kindly referred to Appendix A.1

Process chain. However, some research was found for the POP for the complete additive-subtractive process chain with WAAM and milling. Along with the technological interfaces, BUSACHI et al. (2015) also defined and documented process steps within the POP for the WAAM process. However, their design lacked the consideration of the milling process within the WAAM process operations planning.

PRADO-CERQUEIRA et al. (2017) proposed an eight-step methodology to manufacture parts with the additive-subtractive process chain. Part of it, the steps

1. *3D modeling,*
2. *slicing in layers,*
3. *programming the path in each layer,*
4. *CNC code generation, and*
5. *adjustment of welding parameters*,*

are attributable to the POP, although the authors make no such distinction. These five steps are followed by the steps *manufacture by addition, post-machining, and final result.*

As mentioned in Section 2.3.2, REISCH et al. (2020) defined one combined process planning step for both the WAAM and the milling process. Within this step, the workpiece model should be divided into segments, deposition strategies and parameters chosen for each segment, and milling operations defined on all surfaces requiring post-processing. The path planning should also be conducted, along with a collision check.

A summary of the literature on process planning for WAAM and machining is listed in Table 2.5. Visibly, research on process planning for a sequential process chain, as studied in this thesis, is scarce, while for both individual processes, WAAM and milling, detailed research results are already available.

*For a brief description of the process steps, the reader is kindly referred to Appendix A.1

Table 2.5: Overview of the publications presenting research on the process chain design and process planning of WAAM-material; ● – the topic is the research focus, ◐ – the topic is (partially) included, ○ – the topic is not addressed

Process (chain) type	Publication	Successful application	Process steps and requirements	Process planning steps and interfaces
Hybrid	KARUNAKARAN et al. 2010	●	◐	○
	LI et al. 2017	●	◐	○
Sequential	BUSACHI et al. 2015	○	●	◐
	PRADO-CERQUEIRA et al. 2017	◐	◐	○
	YA and HAMILTON 2018	●	◐	○
	CHERNOVOL et al. 2020	●	◐	○
	REISCH et al. 2020	○	◐	●
WAAM	DING, CHEN, et al. 2016	◐	◐	◐
	LOCKETT et al. 2017	○	◐	●
	URBANIC et al. 2017	○	◐	●
	DAI et al. 2020	○	◐	●
	CUI 2020	◐	○	●
Milling	HALEVI and WEILL 1995	○	◐	●
	XU 2009	○	○	●
	XU et al. 2011	○	◐	●
	ELMARAGHY and NASSEHI 2014	○	◐	●

2.4 Summary and need for action

The background and state of the art presented in the previous sections are summarized in this section with key facts, and the need for action is formulated.

Summary. The following four key facts (Sx) summarize the state of the art:

- S1 The process chain for aircraft structural components by WAAM and milling uses substitution to remodel the process chain. Before the substitution, a (titanium) slab was used as a raw part for the milling process. A WAAM-component replaces this slab. Successful applications of this process chain were shown in literature.
- S2 POP was studied for the individual processes. In regard to the operations planning for the WAAM process, algorithms for the orientation of the build (LOCKETT et al. 2017), path planning strategies (DING et al. 2015c), quality control (BAIER et al. 2022), and a framework for simulation models (URBANIC et al. 2017) have been developed. Ten steps were identified by HALEVI and WEILL (1995) for the manual milling operations planning.
- S3 The WAAM process can produce near-net shaped parts of Ti-6Al-4V, with mechanical properties comparable to those of conventionally manufactured Ti-6Al-4V.
 - S3.1 All the models presented in the literature show that individual weld beads are expected to be identifiable in the WAAM deposition, resulting in geometric deviations from ideal shapes.
 - S3.2 Abnormal areas on the weld beads are likely. They are adjustable to the rest of the weld bead with additional effort, such as with the so-called burning back method.
 - S3.3 The WAAM-microstructure differs from the microstructure of conventionally produced Ti-6Al-4V. The microstructure depends on the position within the part (top or bottom), and instead of a lamellar or equiaxed microstructure, a Widmanstätten structure is often found.
 - S3.4 The properties of wire and arc additively manufactured Ti-6Al-4V are dependent on the orientation within the part (anisotropy). Furthermore, the YS and UTS are often above the minimally required strength, but the elongation is not.
- S4 Milling Ti-6Al-4V presents challenges. The material is mostly difficult to machine due to its properties (see Section 2.2.2). Furthermore, vibrations and deformations need to be controlled during the machining

process. Vibrations are expected due to an excitation force or a variation of the chip thickness. Deformation occurs due to the cutting forces and affects the cutting tool and the workpiece. For wire and arc additively manufactured Ti-6Al-4V, one publication showed a higher cutting torque than for conventional material. Additionally, a dependency of tool wear on the tool path directions was speculated. The results were not consistent for steel, however, the authors realized that a study of the microstructure and the material's hardness was necessary to compare the machinability of conventional and additively manufactured steel alloys.

Need for action. From this state of art, two areas necessitating action (Nx) were identified.

- N1 There is no consideration of the subsequent milling process during the WAAM POP, except by LOCKETT et al. (2017), who state that cutting tool accessibility needs to be ensured for the WAAM design. Additional research should be carried out, especially regarding the machining allowance which is the amount of material additionally deposited to ensure a stable surface quality after machining. No further research concerning this topic could be identified at this time.
- N2 There is no adaption of the milling operations planning to WAAM-components.
 - N2.1 A part of the operations planning is selecting cutting tools and parameters. This cannot be successful if the machinability of the material is unknown. Therefore, the machinability of wire and arc additively manufactured Ti-6Al-4V has to be determined.
 - N2.2 Tool path strategies also have to be chosen during operations planning. Generally, vibrations are induced by a variation of the cutting force. Due to the WAAM-geometry, a variation of the cutting forces is expected, which should be considered for the tool path strategy.

Chapter 3

Objective and Research Approach

The following sections present the objective, the scope, and the approach of this publication based thesis. The chapter concludes with the author's contributions to the listed publications.

3.1 Objective and scope

The objectives (Ox) of this thesis were developed based on the areas necessitating action N1 to N4 (Sec. 2.4).

O1 Methodology for integrated process planning

Integrated in this context means that the individual processes and their influence on each other are considered jointly. An integrated process planning is necessary since, for example, accessibility for the tools needs to be considered for the WAAM process, and sufficient material needs to be deposited for the subsequent machining process.

O2 Milling operations planning adapted for WAAM-components of Ti-6Al-4V

Choosing tools, cutting conditions, and path strategies is part of the operations planning. For these choices, the machinability has to be known. As presented in Chapter 2, the machinability of WAAM-components is still undetermined but likely differs from the machinability of conventional Ti-6Al-4V.

To fulfill these objectives, four research questions (Rx) were defined as follows:

- R1 What are the steps of the integrated process planning?
- R2 How can a sufficient machining allowance be ensured?
- R3 How does the WAAM-material's machinability differ from conventional material?
- R4 How does the WAAM-part geometry influence the milling process?

The relations between the objectives and the research questions are depicted in Figure 3.1, along with the respective chapters in which the results are presented. The WAAM process is a new process which is studied by a large research community and its process stability is relatively low compared to the milling process. The WAAM process parameters are therefore chosen for process stability, while the milling process, with its higher process capability, reacts to the resulting WAAM-component characteristics. Consequently, operations planning for the WAAM process and improving the WAAM process by adapting the process parameters are outside the scope of this thesis. The WAAM-part geometry and properties presented in Chapter 2 show considerable variability. Therefore, within this thesis, a milling operations planning is to be developed which is adaptable to changing WAAM-component characteristics. Accordingly, specifying cutting conditions or tools are outside the scope of this thesis.

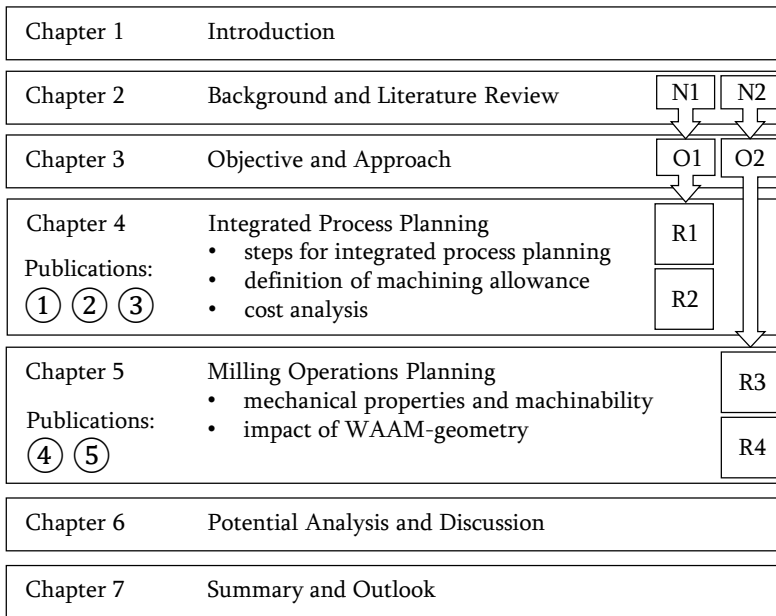


Figure 3.1: Methodology of this dissertation thesis

3.2 Research approach

The technological interfaces between the processes need to be determined to enable this type of integrated process planning. Therefore, this thesis presents a process chain model developed by system analysis. The top-down approach is

used for the system analysis. The schematic of the top-down approach is shown in Figure 3.2. The advantages of this approach are a rapid comprehension of the interdependencies of the processes, while the effort can be limited since the detailing is only conducted to the level required to achieve the objective (VDI 3633-1 2014). Steps for the integrated process planning are developed based on the process chain model. Furthermore, studies on the machinability of WAAM-material were conducted, and conclusions for the milling operations planning are drawn.

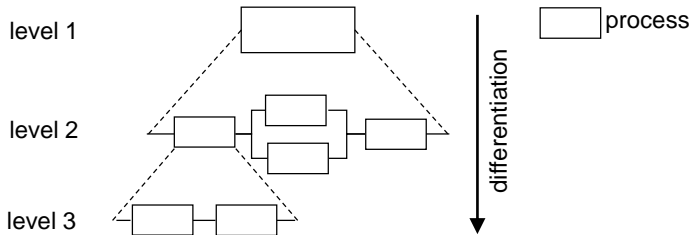


Figure 3.2: Schematic depiction of the top-down approach for system analysis based on VDI 3633-1 (2014)

The approach was pursued in the five publications, which this dissertation thesis is based on. Using the following bibliographical information, the full publications can be found in the respective journals or online:

- ① FUCHS, C., RODRÍGUEZ, I., et al., (2021). “Process Planning for the Machining of Ti-6Al-4V Near-net Shaped Components”. In: *Procedia CIRP* vol. 101, pp. 58–61. ISSN: 22128271. DOI: 10.1016/j.procir.2020.03.155
- ② FUCHS, C., SEMM, T., et al., (2021). “Decision-based process planning for wire and arc additively manufactured and machined parts”. In: *Journal of Manufacturing Systems* vol. 59, pp. 180–189. ISSN: 02786125. DOI: 10.1016/j.jmsy.2021.01.016
- ③ FUCHS, C. et al., (2020). “Determining the machining allowance for WAAM parts”. In: *Production Engineering* vol. 14.5–6, pp. 629–637. ISSN: 0944-6524. DOI: 10.1007/s11740-020-00982-9
- ④ FUCHS, C. et al., (2023). “Investigation into the influence of the interlayer temperature on machinability and microstructure of additively manufactured Ti-6Al-4V”. in: *Production Engineering* vol. 17.5, pp. 703–714. ISSN: 0944-6524. DOI: 10.1007/s11740-023-01192-9
- ⑤ FUCHS, C. et al., (2022). “Impact of wire and arc additively manufactured workpiece geometry on the milling process”. In: *Production Engineering* vol. 17.3–4, pp. 415–424. ISSN: 0944-6524. DOI: 10.1007/s11740-022-01153-8

Following the top-down approach, the first part of Publication ①, Chapter 4 introduces the process chain and defines technological interfaces within the process chain. Based on the definition of the interfaces, three steps for the integrated process planning are developed in the second part of Publication ① in Chapter 4, and the first step is specified. This publication answers the research question R1. In Publications ② and ③, the other two steps for integrated process planning are detailed. The research question R2 is addressed in Publication ③ by defining a method to determine the necessary machining allowance based on surface profile measurements. This is followed by Publications ④ and ⑤, which address the operations planning for milling of WAAM-parts. The results are described in Chapter 5. The research question R3 of how the WAAM-material's machinability differs from conventional Ti-6Al-4V is answered in Publication ④. The influence of the WAAM-part geometry on the milling process (R4) is studied in Publication ⑤. Finally, in Chapter 6, an exemplary application of the process chain to two test parts is described, and an analysis of the process chain potential is performed. The methodology of this dissertation thesis is depicted in Figure 3.1, along with the respective publications.

An overview of this author's contributions to the publications is depicted in Figure 3.3.

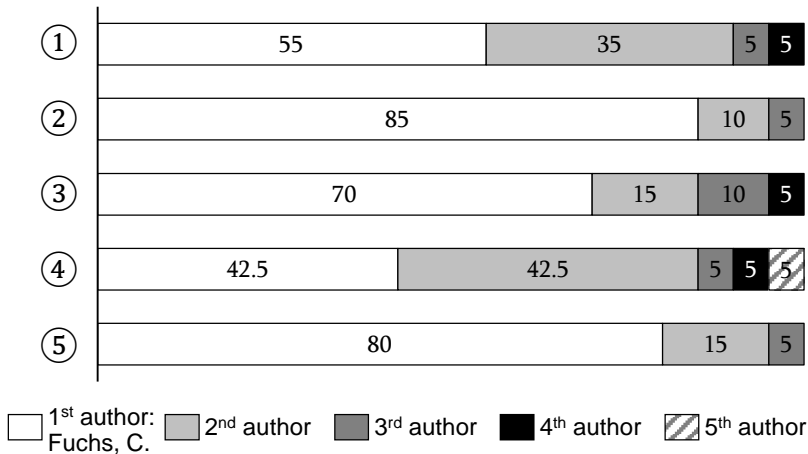


Figure 3.3: Overview of this author's contribution percentages to the publications

The individual contributions of the author are based on the Contributor Roles Taxonomy (CRediT) categories (ALLEN et al. 2019). The following categories were used to define the authorship:

- conceptualization and methodology,
- investigation and validation, and
- writing and visualization.

If categories are not applicable for the author in any publication, they are not given. Except for Publication ④, the majority of the work was conducted by the author of this thesis. In Publication ④, this author shared the work equally with the second author.

Chapter 4

Integrated Process Planning for WAAM and Milling

The integrated process planning considers both the WAAM and the milling process. To achieve this, technological interfaces in the process chain must initially be defined, and then the planning process steps must be developed. Publication ① addresses this topic and details the first planning step. Publications ② and ③ present methods for individual steps of the integrated process planning.

4.1 Process planning and orientation – Publication ①

Publication ① presents the process chain with its technological interfaces. The process chain was detailed following the top-down approach. Initial input into the production is a model of the desired workpiece. The output is the finished workpiece. For manufacturing, six processes are necessary: process planning, WAAM operations planning, WAAM, heat treatment, milling operations planning, and machining.

Further detailing the model, the integrated process planning is presented in Publication ①. In Figure 4.1, the three processes, part orientation, manufacturability analysis, and surface offset, are depicted in the flow chart of the planning process. Subsequently, the part orientation process is further detailed in Publication ①. In Publication ②, the cost analysis as part of the manufacturability analysis is specified. The surface offset determination, necessary for the third process, is described in Publication ③.

During the definition of the part orientation, the build direction is determined from four parameters. These four parameters include the substrate utilisation in parameter P_1 , the deposited material (parameter P_2), the build time (parameter P_3), and the build complexity (parameter P_4)¹. The determination requires

¹For the equations to calculate P_1 to P_4 and in-depth explanations the reader is kindly referred to the Publication ①.

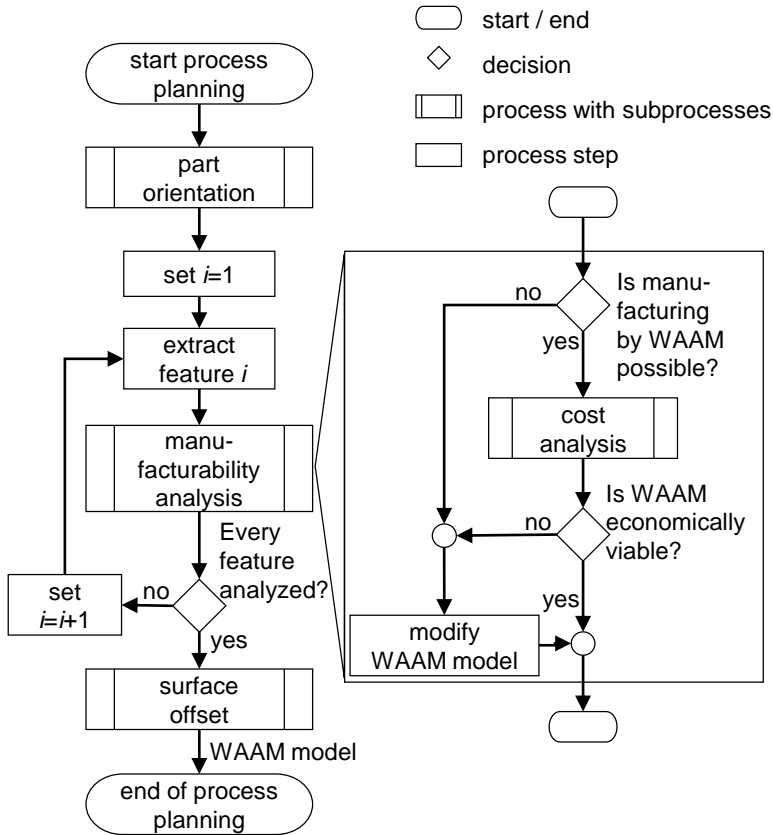


Figure 4.1: Flow chart of the integrated process planning (FUCHS, RODRÍGUEZ, et al. 2021); licensed under the Creative Commons License CC BY 4.0

that the desired mechanical properties and microstructure are achievable independent of the orientation. The determination parameters were adapted from LOCKETT et al. (2017) for a 3-axis welding setup. This determination is possible when using gantry machines or welding robots without a turn-tilt table, because the calculation is only valid for an unchanged build direction. The calculation of the part orientation was conducted for one generic aerospace component as a validation.

The following achievements were obtained through Publication ①:

- The additive-subtractive process chain with WAAM and milling and its technological interfaces were defined.
- Processes within the integrated process planning for the sequential WAAM and milling process chain were determined.

- The first process, the determination of the part orientation, was detailed and validated with an exemplary component.

In Figure 4.2, the author's contributions to the publication are specified.

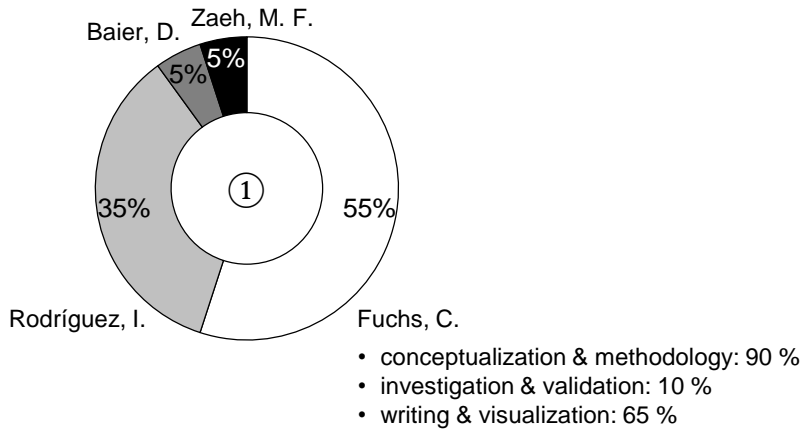


Figure 4.2: Individual contributions of the authors to Publication ①

4.2 Feature-based sequence definition by performing a cost analysis – Publication ②

The manufacturability analysis is the second part of integrated process planning (see Figure 4.1). Two questions need to be answered within this step:

- "Is manufacturing by WAAM possible?", and
- "Is WAAM economically viable?".

The first question is answerable by the state of the art. However, a cost analysis has to be conducted to answer the second question. Notably, the economic viability does not refer to the component as a whole but refers to each subtractive geometric feature. A method for the cost analysis is presented in Publication ②. For each geometric subtractive feature of a component, the decision of which work sequence to use has to be made based on economic considerations. The sequences are: premanufacturing the feature with WAAM and milling from a near-net shape (Sequence X) or filling the feature with material during the WAAM process and milling from a conventional shape (Sequence Y). Examples of these work sequences for manufacturing a hole are shown in Figure 4.3.

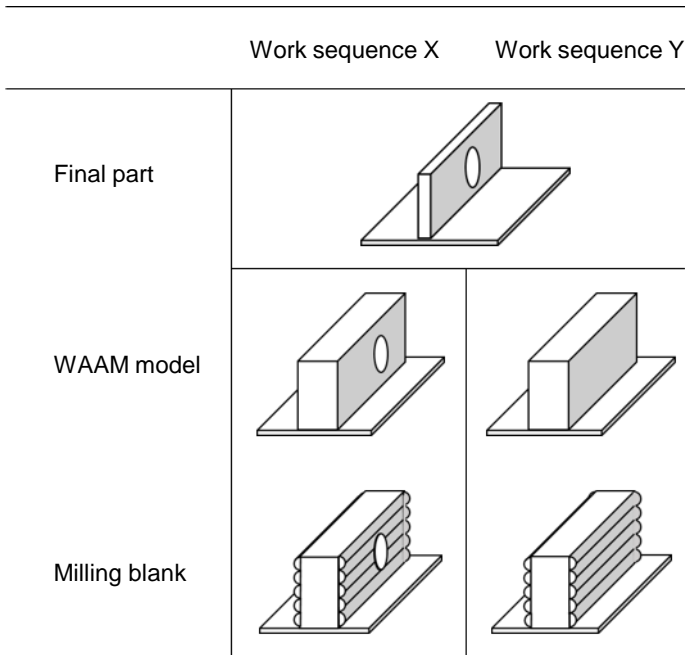


Figure 4.3: Work sequences for the cost analysis (FUCHS, SEMM, et al. 2021)

A cost model, based on the deposition and material removal rates, was developed in Publication ② for each work sequence. The model was applied to the manufacture of generic features. Additionally, the influence of model parameters on the decision of which work sequence to use was determined. The results showed that the machining allowance had the greatest influence, followed by the diameter of the hole.

The following achievements were obtained through Publication ②:

- The second process planning step, manufacturability analysis, was detailed by developing a method for the cost analysis of sequentially manufacturing with WAAM and milling.
- The cost analysis enables a decision on how each geometric feature should be manufactured.

In Figure 4.4, the author's contributions to the publication are specified.

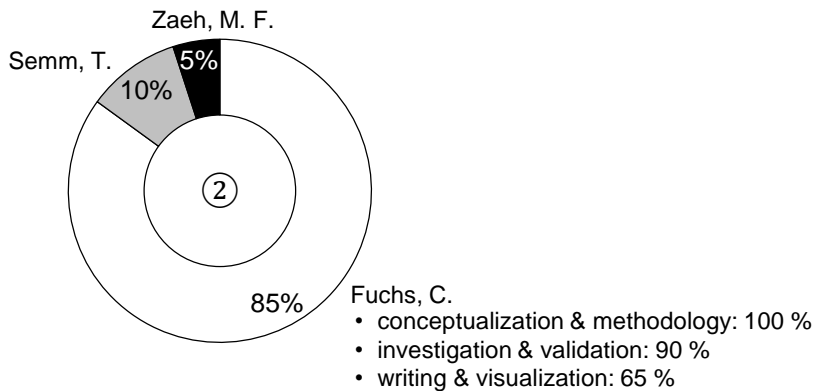


Figure 4.4: Individual contributions of the authors to Publication ②

4.3 Determining the machining allowance – Publication ③

Publication ③ focuses on the determination of the machining allowance. The machining allowance is defined as the additional material deposited during the WAAM process and removed during the milling process to achieve a defect-free surface with a surface quality acceptable for the application. The publication presents research on how much material must be removed until a defect-free surface is reached.

The amount of material removed is given with regard to the initial surface roughness. Notably, a connection between the deposition strategy and the surface waviness was found in the study. In the welding direction, the periodicity of the waviness corresponds to the deposition's zig-zag pattern. The deposition layers are found in the periodicity in the building direction. With the proposed method, the machining allowance can be determined based on surface profile measurements. This results in a faster determination of an acceptable amount compared to trial and error. In the study, surface parameters such as maximum height of the roughness profile R_z , maximum height of the waviness profile W_z , maximum surface waviness S_z , maximum height of the primary profile P_z and form deviations were determined. Of those, the maximum surface waviness S_z exceeded the other deviations and was therefore, according to the method, chosen as the reference for the necessary material removal. A surface was considered defect-free, when no remnants of the welded surface remained. The results are depicted in Figure 4.5.

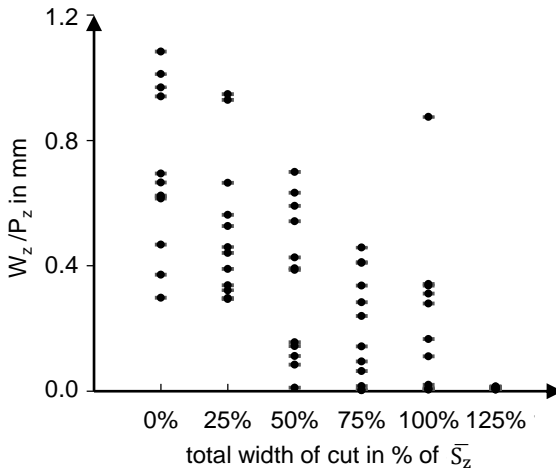


Figure 4.5: Surface quality after milling (FUCHS et al. 2020); licensed under the Creative Commons License CC BY 4.0

On each part of the twelve parts, six areas with different depths of material removal (total width of cut) were machined. At a material removal depth of 125% of the initial waviness, the surfaces are defect-free. Notably, 125% exceeds the method's proposed 100% of the maximum surface deviation. As likely reasons, deviations in the workpiece datum axis and measurement inaccuracies due to spatter were identified. However, the study showed that determination of the machining allowance based on measured surface profiles values is possible and that the method was applicable.

The following achievements were obtained through Publication ③:

- The relationship between the surface waviness and the deposition strategy was described.
- It was shown that removing the waviness is key to achieving even surfaces.
- A method to determine the necessary machining allowance, based on measured surface roughness and waviness values, was presented.

In Figure 4.6, the author's contributions to the publication are specified.

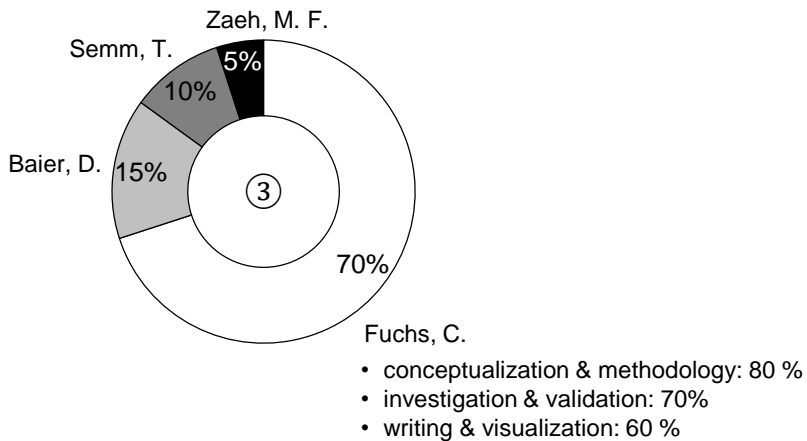


Figure 4.6: Individual contributions of the authors to Publication ③

4.4 Summary of the integrated process planning

The objective O1 was to develop a methodology for integrated process planning, which considers both the WAAM and the milling process. The methodology is supposed to enable the consideration of the accessibility for the tool and sufficient deposited material for the subsequent machining. The first step of this objective was achieved by Publication ①. Within the publication, the technological interfaces of the additive-subtractive process chain were defined, and the individual processes within the integrated process planning were determined. Furthermore, the first process of the integrated process planning was detailed and validated. The second process of the integrated process planning was studied in Publication ②. Here, the manufacturability analysis was detailed, which enables a decision on how each geometric feature should be manufactured. The deposition of sufficient material was the focus of Publication ③. Within the publication, a method to determine the necessary machining allowance based on measured surface roughness and waviness values was presented. With these three publications, a complete methodology for the integrated process planning is presented. The difference between the WAAM-material's machinability and conventional material and the influence of the WAAM-part geometry on the milling process are issues that need to be answered for the second objective O2. These issues are addressed in the following chapter.

Chapter 5

Considerations for the Milling Operations Planning

The tools, the cutting conditions, and the cutting strategy must be defined in the milling operations planning. Tools and cutting conditions are only definable if the machinability of the WAAM-material is known. Publication ④ addresses this topic and is described in Section 5.1. Aside from that, there is a difference between the near-net-shaped WAAM-components' and the conventional material's geometry (see Chapter 2). The difference influences the cutting strategy and the cutting conditions. Therefore, milling operations planning should consider the geometry of the WAAM-parts. This topic is addressed in Publication ⑤ (Sec. 5.2).

5.1 Connection between microstructure, mechanical properties and machinability – Publication ④

The material's heat cycles influence the microstructure of WAAM-components significantly. As shown by various researchers, the heat cycles are dependent on the interlayer temperature. Therefore, Publication ④ focuses on the influence of the interlayer temperature¹ on the microstructure, the mechanical properties, and the machinability. Two samples each with three different interlayer temperatures (200°C, 350°C and 500°C) were manufactured, peripherally milled, and their properties were analyzed. A Widmanstätten structure was found in all samples. This is consistent with the state of the art (see Section 2.1.2). The β -lamellae were coarser at the bottom of the samples than at the top. The hardness of the samples was similar, except for the top layer. Here, the hardness slightly increased with increasing interlayer temperature. The tension tests showed uniform yield strength and ultimate tensile strength for all samples, comparable to the state of the art for Ti-6Al-4V. The waviness was removed on

¹The interlayer temperature is the temperature of the weld bead before depositing the next layer.

the samples before the cutting force measurements were made. During the measurements, no influence of the interlayer temperature was detected. Additionally, substrate material was also milled, and the cutting forces were measured. The comparison between the cutting forces of WAAM-material and substrate material, which can be considered as conventionally produced Ti-6Al-4V, show no discernible difference. The results in the direction perpendicular to the part are depicted in Figure 5.1.

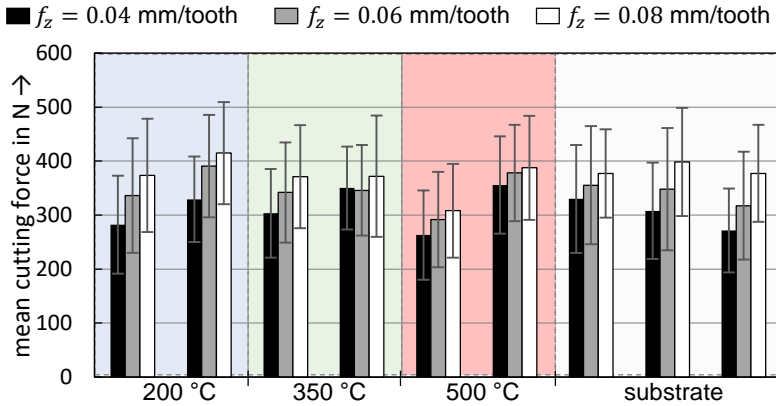


Figure 5.1: Cutting forces in normal direction for three different interlayer temperatures and for the substrate material (FUCHS et al. 2023); licensed under the Creative Commons License CC BY 4.0

This publication shows that mechanical properties similar to conventional Ti-6Al-4V are achievable by WAAM. Secondly, if the mechanical properties are similar, the influence of the interlayer temperature on the cutting forces is negligible. Thirdly, the cutting forces are comparable to those of conventionally manufactured Ti-6Al-4V, even though the microstructure differs. Therefore, for milling operations planning, similar cutting conditions are advisable as for conventionally manufactured Ti-6Al-4V.

The following achievements were obtained through this Publication (4):

- The microstructure was shown to be similar to the microstructure described in the chapters on the state of the art for WAAM-components.
- The mechanical properties of the WAAM-samples were similar to conventionally manufactured Ti-6Al-4V, except for the top layer, where an influence of the interlayer temperature was detected.
- The cutting forces were determined to have no discernible difference from the cutting forces in conventionally manufactured Ti-6Al-4V.

In Figure 5.2, the author's contributions to the publication are specified.

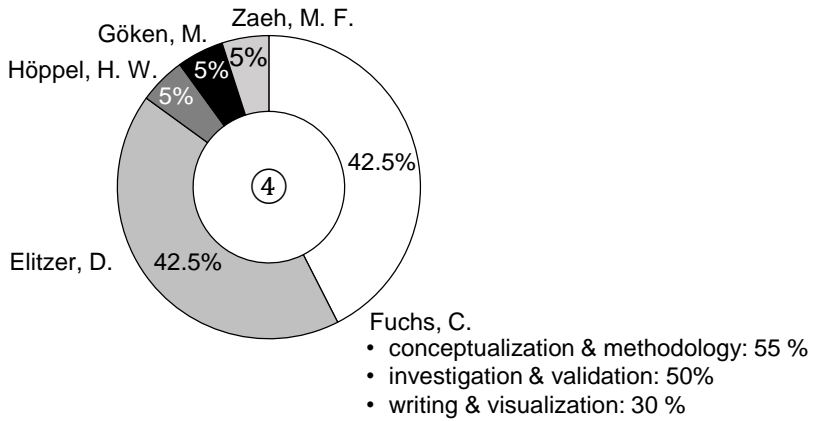


Figure 5.2: Individual contributions of the authors to publication ④

5.2 Impact of the WAAM-geometry on the milling process

– Publication ⑤

Publication ⑤ focuses on the WAAM-geometry's impact on the milling process. The surface quality of three sample sets was analyzed. The samples were manufactured with different parameters and their profile visibly differed. Details of the surfaces are depicted in Figure 5.3. Next, the surfaces were peripherally milled, and the resulting cutting forces were analyzed. Notably, the surface profile waviness was detectable in the mean cutting forces, which vary with the modulation frequency, which is calculable from the surface waviness and the feed velocity.

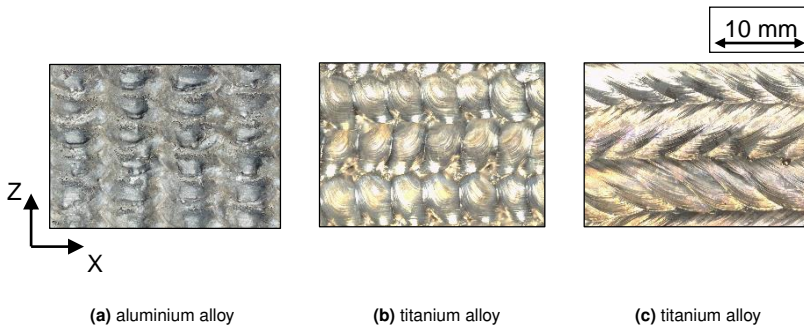


Figure 5.3: Surfaces of three types of WAAM components without post-processing, and manufactured using three different WAAM strategies (FUCHS et al. 2022); licensed under the Creative Commons License CC BY 4.0

The impact of the force modulation on the milling process was analyzed. It was concluded that forced vibrations might occur if the modulation frequency coincides with a natural frequency of the setup. This is especially likely for milling with robots since their first mode natural frequency lies between 5.5 and 10 Hz. Additionally, the modulation led to periodic deflections found on the aluminum samples. On these samples, the surface waviness after milling corresponded to the waviness before the milling process, even though the deposited surface was completely removed by the cuts. A likely reason for that is to be seen in the tool and the workpiece deflections due to the modulation of the mean cutting force.

Guidelines for the milling process were determined from these results. They include choosing a cutting strategy with the feed direction parallel to the smallest measured waviness value, ensuring that the modulation frequency, the natural frequency of the setup, and the spindle rotational frequency do not coincide, and choosing a strategy with a finishing cut.

In summary, these results give guidelines for milling operations planning. An improved cutting strategy is proposed, and recommendations for choosing cutting conditions such as spindle speed n , and feed rate f_z are given. Combined with the results from Publication (4), the milling operations planning has been adapted from conventional material to WAAM-components.

The following achievements were obtained through this Publication (5):

- The impact of the surface profile of WAAM-components on the cutting forces was determined. This shows that the surface profile waviness leads to a modulation of the mean cutting force.
- The influence of the modulation (fluctuation) of the mean cutting force on the vibration and deflection behavior was demonstrated.
- Guidelines for the milling process planning to counteract the impact of the WAAM-geometry were derived and proposed.

In Figure 5.4, the author's contributions to the publication are specified.

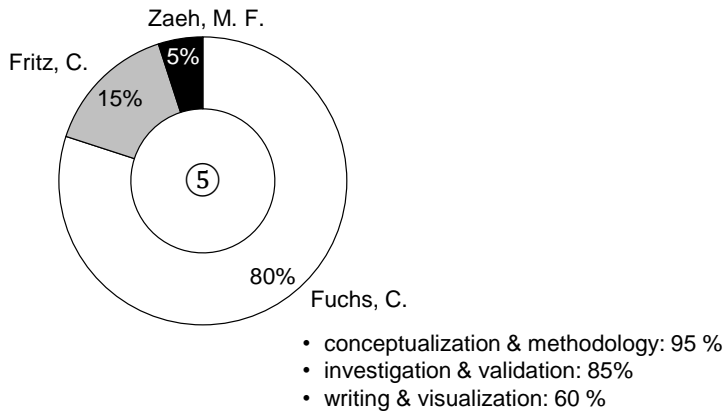


Figure 5.4: Individual contributions of the authors to Publication (5)

5.3 Summary of the considerations for the milling operations planning

The objective O2 was to adapt the milling operations planning for WAAM components of Ti-6Al-4V. For that purpose, the machinability of the wire and arc additively manufactured material had to be determined. This determination of the machinability was performed in Publication (4). For the publication, the macro- and microstructure of wire and arc additively manufactured Ti-6Al-4V were analyzed, and the mechanical properties were determined for samples manufactured with different interlayer temperatures. Furthermore, the machinability of these samples was ascertained by determining the cutting forces. The machinability of conventionally manufactured Ti-6Al-4V and the samples' machinability were compared to each other. The results show that it is possible to manufacture Ti-6Al-4V with WAAM with a machinability comparable to that of conventional Ti-6Al-4V. Therefore, similar cutting conditions are advisable as for conventionally manufactured Ti-6Al-4V. However, in Chapter 2, it was shown that the stock material geometry for the machining process differs, when machining near-net shaped WAAM-material compared to the conventional process chain. The impact of this difference was studied in Publication (5). The wavy surface profile due to the WAAM process leads to a modulation of the mean cutting force. It was demonstrated, that, in turn, this influences the vibration and deflection behavior. And finally, guidelines for the milling process planning were derived. The milling operations planning was adapted to the WAAM process with these two publications. Combined with Chapter 4, the objective of this thesis is achieved. However, no analysis of the potential and the applicability was conducted so far. Therefore, this topic is addressed in Chapter 6, along with a discussion of the results of the thesis compared to the literature.

Chapter 6

Potential Analysis and Discussion

This chapter presents an analysis of the potential of the process chain developed in this thesis. It serves the dual purpose of showing the applicability of the process steps to parts having an engineering significance and of illustrating the process chain's economic impact in comparison to a trial-and-error-based process planning approach. In Section 6.1, the parts and fundamental equations for the analysis are initially introduced. This is followed by the analysis of potential, which is carried out for each step of the developed process planning procedure. In Section 6.2, the thesis results are compared to the objectives, and the research limitations are pointed out.

6.1 Potential analysis

Several publications address the economic and environmental potential of an additive-subtractive process chain consisting of WAAM and machining. An early-stage assessment of the economic feasibility of such a process chain and a sensitivity analysis was given by MARTINA and WILLIAMS (2015). CUNNINGHAM et al. (2017) presented a more in-depth study. The energy efficiency was studied by CAMPATELLI et al. (2020), for example. Overall, the results by all authors show that the process chain consisting of WAAM and machining has great economic and environmental potential. Above all, saved material compared to machining the components from slabs leads to the process chain being the more economical decision every time, provided that the WAAM equipment is inexpensive compared to machining centers. Even the additional welding time does not change this outcome.

All aforementioned authors assumed that the process chain is conducted with optimal parameters within their studies. As shown in Chapter 2, the process planning for a combination of WAAM and milling is still in the early stages. Therefore, a methodology for integrated process planning was developed in this thesis. The potential of this methodology is analyzed in this section. The possibility of losses due to process planning with a trial-and-error method is

determined for that purpose. The basis for the calculations are two test components. Both are depicted in Figure 6.1. The dimensions of the parts are found in Appendix A.2.

The first part is based on a structural aircraft component. A similar part was developed for the research project REGULUS (Federal Ministry for Economic Affairs and Climate Action (BMWK), Grant Nr. 20W1709D) in cooperation with the industrial partners. The second component is based on a bleed air leak detect bracket. The bracket was presented in a case study by DEHOFF et al. (2013). The authors showed the potential of Powder-bed Fusion of Metals with an Electron Beam (PBF-EB/M) for decreasing the BTF ratio. Initially, the BTF ratio was around 33 and was speculated to decrease to fairly close to 1. Since no scale was given for the part, its appearance was recreated.

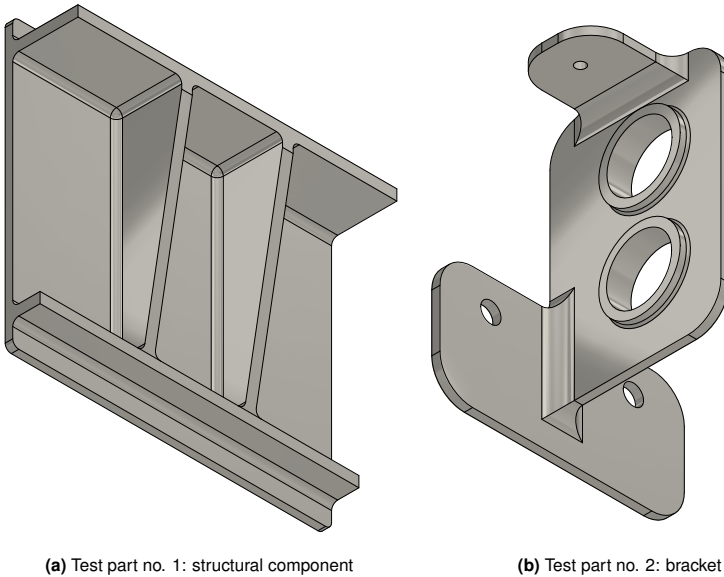


Figure 6.1: Isometric view of the two test parts for the analysis of the potential

Since the lesser material consumption of the process chain is crucial for its economic potential, the BTF ratio is used for the analysis. Additionally, manufacturing time is a concern. Therefore, an estimation of the manufacturing time based on the deposition rate and the material removal rate is given. Theoretically, if the manufacturing time is strongly increased by the additive-subtractive process chain, any economic gains due to the lesser material consumption can be canceled out by the costs for the increased manufacturing time. Consequently, both parameters are considered in the potential analysis. All calculations are based on the initial parameters given in the appendix in Table A.2.

The following assumptions were made for the calculations:

- The clamping is ideal, and the substrate is no larger than necessary for the part dimensions.
- Only a deposition of geometrically simple shapes such as straight walls is conducted. No tapering, cylinders or unsupported features are considered.
- The machining allowance is added globally to all surfaces, even to the substrate. This machining allowance on the substrate accounts for the fact that raw material slabs likely have to be milled to remove the rolled skin and unevenness.
- The idle and setup times are not considered.

Based on these assumptions, the models for the deposition were determined. They are shown in Figure 6.2.

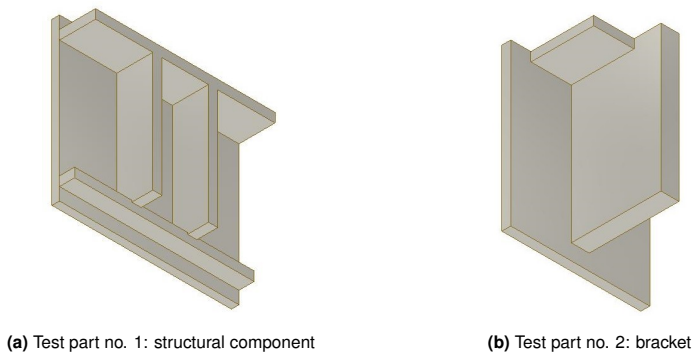


Figure 6.2: Depictions of the part geometries that should be deposited

The component mass for the potential analysis was determined by modeling all parts in CAD and calculating it based on the volumes. The BTF ratio BTF was determined from the material's mass used for production M_p divided by the material's mass of the final component M_f

$$BTF = \frac{M_p}{M_f}, \quad (6.1)$$

where M_p is the sum of the deposited material's mass M_d and the substrate material's mass M_s according to

$$M_p = M_d + M_s. \quad (6.2)$$

The manufacturing time T is the sum of the time for deposition T_d and the time for milling T_m according to

$$T = T_d + T_m. \quad (6.3)$$

T_d is a function of the deposition rate DR_{mass} and the mass of the deposited material M_d :

$$T_d = \frac{M_d}{DR_{mass}}, \quad (6.4)$$

while T_m is dependent on the material removal rate MRR_{mass} and the mass of the machining allowance M_a :

$$T_m = \frac{M_a}{MRR_{mass}}. \quad (6.5)$$

The relation between the volumetric material removal rate MRR_{vol} (see Eq. 2.4) and the material removal rate MRR_{mass} is defined by the density ρ as

$$MRR_{mass} = MRR_{vol} \cdot \rho. \quad (6.6)$$

The initial BTF ratio and machining time are listed in Table 6.1. The objective of a substitution of the conventional manufacturing route is to reduce both or, if that proves impossible, to find an optimal point between increasing costs due to one factor and decreasing costs due to the other.

Table 6.1: Initial BTF ratio and machining time for the test parts

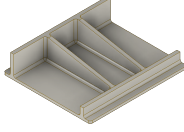
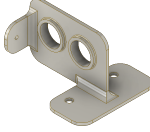
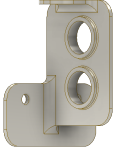
Parameter	Unit	Structural component	Bracket
BTF	-	6.01	21.13
T_m	h	3.16	2.69

6.1.1 Part orientation

The first step within the integrated process planning is determining the part orientation. For both test parts, a suitable build orientation according to Publication ① was determined. Based on the guidelines for choosing preliminary build orientations, only one orientation is feasible for the structural component. It is denominated as $OR1_1$. However, at least two orientations are possible for the Test part no.2 (bracket), denominated $OR1_2$ and $OR2_2$. The results of the evaluation are listed in Table 6.2. The layer height h_{layer} was assumed to be 5 mm. To determine the optimal build orientation, four parameters P_1 to P_4 are calculated from the component's characteristics (see Publication ①). The optimal orientation is reached at the maximum of the sum of the four parameters. Therefore, as the bracket's sum of P_1 to P_4 for $OR2_2$ exceeds the one for $OR1_2$, it was chosen as the optimal build orientation.

Table 6.3 lists the results of the potential analysis for the orientation of the two test parts. The initial BTF ratio of the structural component was 6.01. It was decreased to 1.83 with the additive-subtractive process chain. The BTF ratio was

Table 6.2: Results of the orientation evaluation based on Publication ①

Parameter	Structural component $OR1_1$	Bracket	
		$OR1_2$	$OR2_2$
↑ building direction			
P_1	0.56	1.88	1.15
P_2	0.87	0.88	0.82
P_3	1.00	1.00	0.59
P_4	0.62	0.40	0.44
Sum	3.05	4.16	3.00

also significantly reduced for the bracket, from initially 21.13 to around 5. However, for $OR1_2$, the BTF is lower than for $OR2_2$ by 13%. Even more significant is the difference concerning the manufacturing time T_d . Here, $OR1_2$'s time is shorter than $OR2_2$'s time by 35%. This demonstrates that the calculation of the build orientation leads to significantly better results than a trial-and-error-based approach. The guidelines for choosing preliminary build orientations enable a brief definition of possible orientations and show that only one orientation is feasible in the case of the structural component. With other orientations, overhanging areas cannot be minimized, which is why they are not considered for the evaluation.

Table 6.3: Comparison between BTF and manufacturing time T (the sum of T_d and T_m) for different part orientations

Parameter	Unit	Structural component $OR1_1$	Bracket	
			$OR1_2$	$OR2_2$
M_d	kg	1.23	0.84	1.29
M_s	kg	1.64	0.63	0.39
M_a	kg	1.29	1.14	1.34
M_p	kg	2.87	1.47	1.68
M_f	kg	1.57	0.33	0.33
BTF	-	1.83	4.45	5.09
T_d	h	2.46	1.68	2.58
T_m	h	0.52	0.46	0.54

6.1.2 Cost analysis

Publication ② presents a decision-based method to minimize production costs. The method was applied to both test parts. The constants of the method were set to the values originally specified in Publication ②, which are listed in Appendix A.3. The same assumptions as made in the publication were applied to calculate the optimal sequence. The manufacturing time and material consumption are regarded within the publication's calculation method. Based on these characteristics, the costs for manufacturing near-net shaped or prefilled features (see Figure 4.3 on page 46) were determined and their ratio is illustrated with the cost coefficient Q_c . The cost coefficient Q_c gives the ratio between the manufacturing costs for work sequence X divided by the costs for work sequence Y. If Q_c exceeds 1, the costs for work sequence X are larger than the costs for manufacturing the feature with work sequence Y. Consequentially, the feature should be manufactured with work sequence Y. If the cost coefficient Q_c is smaller than 1, the opposite applies.

The determinations are based on the identification of subtractive features, which was the first step conducted in this potential analysis. For the structural component, only one relevant feature was identified. For the bracket, five features were found where a decision between deposition and milling has to be made. In Figure 6.3, the features are depicted.

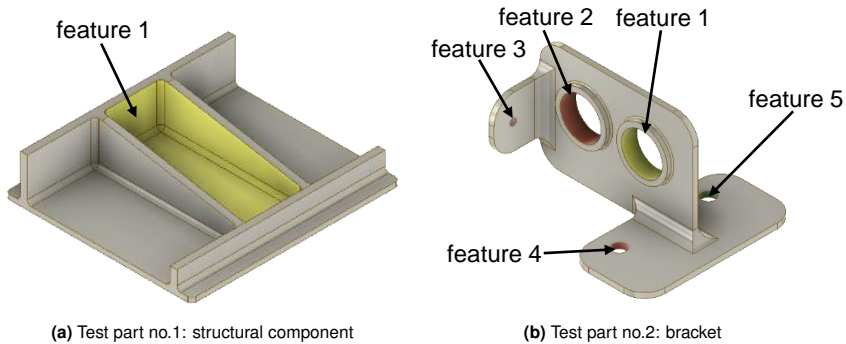


Figure 6.3: Test parts with the identified features that require a decision between the work sequences X and Y

The resulting cost coefficients Q_c for each feature are listed in Table 6.4, along with the mass and BTF ratio. An in-depth description of the work sequences and the calculation method is included in Publication ②.

For the structural component's Feature 1, the chosen work sequence is Sequence X – near-net shape manufacturing with WAAM and milling to shape (see Figure 4.3 on page 46). This is equal to the one used for the orientation evaluation in Section 6.1.1. Therefore, the resulting BTF ratio remains at 1.83.

Table 6.4: Comparison of the work sequences for the test parts

Feature no.	Unit	Structural compo- nent	Bracket				
			1	2	3	4	5
Cost coefficient Q_c	–	0.090	0.361	0.361	1.002	0.950	0.950
Work sequence	–	X	X	X	Y	X	X
M_d	kg	1.23			0.72		
M_s	kg	1.64			0.63		
M_a	kg	1.29			1.02		
M_p	kg	2.87			1.35		
<i>BTF</i>	–	1.83			4.09		

For the bracket's Feature 3, the chosen work sequence is the Sequence Y instead of the Sequence X. Sequence X is chosen for all other features. Consequently, the WAAM model to be deposited during the WAAM process would have a prefilled Feature 3, but would have near-net shaped holes for Features 1, 2, 4, and 5.

In comparison to the assumed WAAM model of Section 6.1.1 (page 60), this is a difference. One premise for the determination of the orientation was that only geometrically simple shapes are deposited, with no unsupported features or cylinders (see Figure 6.2). Therefore, originally, for the orientation determination, the Sequence Y for all features – prefilling the features and milling from a conventional shape – was chosen.

The BTF ratio of Test Part no. 2 after the cost analysis would be 4.09. Previously it was at 4.45. Consequently, the BTF ratio is reducible by considering the individual features. At the same time, the manufacturing time is also decreased.

In reality, however, it is unlikely that a deposition with the calculated work sequences for the all features would be performed. Due to the part's orientation, the plate containing Features 4 and 5 would be part of the substrate. Therefore, using Sequence X for these features would be unlikely since the substrate is usually a rolled slab without holes. Therefore, if the original premise of the deposition of simple shapes is omitted, Features 1 and 2 would be deposited with work sequence X, while Feature 4 and 5 would be prefilled (Sequence Y) opposite to the evaluation results. A comparison of the resulting WAAM model and the originally assumed model for the orientation determination is depicted in Figure 6.4.

The cost analysis method leads to better results than a trial-and-error approach for the determination of the work sequence. In the case of the structural component, the method confirms the preliminary assumptions of Section 6.1 for the

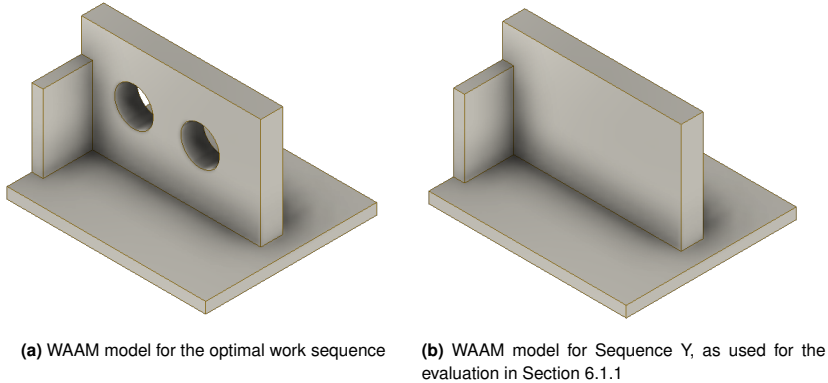


Figure 6.4: Comparison of the WAAM models for the bracket

WAAM model. However, the BTF ratio is further reducible for the bracket by depositing near-net-shaped holes. Here, the method rejects the initial design of the WAAM model.

6.1.3 Machining allowance

The third step within the process planning is to include the necessary machining allowance. A method to determine the machining allowance was presented in Publication ③. The impact of the machining allowance's size on the process chain's potential was determined by analyzing the BTF ratio and the manufacturing time for the two test parts (Fig. 6.1) for two machining allowances a . They are set at $a = 2$ mm and $a = 4$ mm. According to the method, they would be chosen based on measured surface quality values. The optimal orientation based on Publication ① and ② was chosen for the calculation.

The results are listed in Table 6.5. The structural component's BTF ratio increases by 44% and the manufacturing time by 36%. The bracket's BTF ratio increases by 44% and the manufacturing time by 30%. Conclusively, employing a method to determine the necessary machining allowance increases the potential of the process chain. Both material consumption and manufacturing time can be reduced.

6.1.4 Milling operations planning

Guidelines for the milling operations planning are determined in Publications ④ and ⑤. These include the milling strategy and the cutting conditions. Both influence the material removal rate MRR_{mass} of the milling process. Therefore, the influence of the MRR_{mass} on the process chain's potential is analyzed in the

Table 6.5: Comparison between BTF ratio and machining time for different machining allowances

Parameter	Unit	Structural component		Bracket	
		$a = 2 \text{ mm}$	$a = 4 \text{ mm}$	$a = 2 \text{ mm}$	$a = 4 \text{ mm}$
Machining allowance					
M_d	kg	1.23	1.67	0.72	0.93
M_s	kg	1.64	2.46	0.63	1.01
M_a	kg	1.30	2.56	1.02	1.61
M_p	kg	2.87	4.13	1.35	1.94
BTF	–	1.83	2.63	4.09	5.88
T_d	h	2.46	3.35	1.44	1.87
T_m	h	0.52	1.02	0.41	0.64

following. However, the material removal rate MRR_{mass} does not influence the BTF ratio. Consequently, in this section, only its influence on the manufacturing time T is studied. For the evaluation, Equation 2.4 and the Equations 6.3 to 6.5 with the initial parameters given in Appendix A.2 were used.

The relationship between the manufacturing time T and the material removal rate MRR_{mass} is depicted in Figure 6.5. The comparison between the manufacturing from a rolled slab and the manufacturing with the additive-subtractive process chain is shown for each test part (see Fig. 6.1). The deposition rate DR_{mass} was fixed at 0.5 kg/h. Visibly, for a small MRR_{mass} , the manufacturing time with the conventional process chain is higher than for the additive-subtractive process chain. A reason for this is the deposition time. However, at a MRR_{mass} of 2.8 kg/h for the structural component and 4.0 kg/h for the bracket, this is reversed, and the conventional process chain is faster than the additive-subtractive process chain. In this scenario, the DR_{mass} stays constant. Therefore, the deposition times are constantly 2.46 h and 1.68 h, respectively. At a MRR_{mass} higher than 2.0 kg/h, the milling time's share of the manufacturing time is smaller than 25%. Conclusively, the influence of the DR_{mass} exceeds that of the MRR_{mass} . However, if the MRR_{mass} for the additive-subtractive process chain is consistently lower than for the conventional process, no switch from the conventional process to the process chain is recommended, based on the manufacturing time. Therefore, the material removal rate significantly influences the process chain's potential.

Consequently, the potential of the process chain is increased by the results concerning the milling operations planning. Within the studies presented in Publications (4) and (5), a MRR_{mass} of 0.65 kg/h and 1.75 kg/h was applied respectively. At these values of MRR_{mass} , the additive-subtractive process chain has a lower manufacturing time than conventional manufacturing (see Figure 6.5). It was shown that these values of MRR_{mass} lead to acceptable results concerning the cutting forces and are applicable for manufacturing. However, due to the relatively small volume machined in the additive-subtractive process chain, there

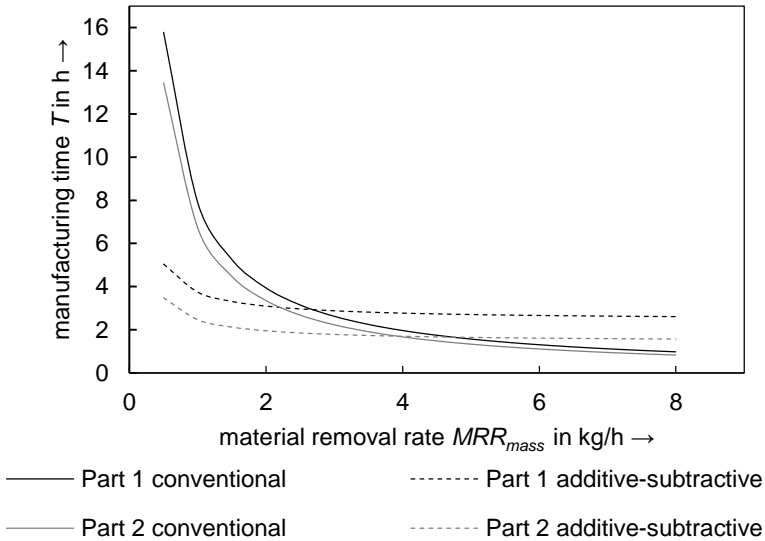


Figure 6.5: Influence of the material removal rate MRR_{mass} on the manufacturing time T for both test parts with a conventional and an additive-subtractive process chain

is a limit on improving the manufacturing time by increasing the MRR_{mass} . As demonstrated for the test parts, the deposition time is a significant factor concerning the manufacturing time and needs to be considered for improvement.

Overall, it was shown with the potential analysis that the application of the proposed method results in a BTF ratio equal to or better than the trial-and-error approach. For the structural component, the BTF ratio was lowered from 6.01 to 1.83. Here, the trial-and-error approach might have achieved the same outcome. For the bracket, the BTF ratio was reduced from 21.13 to 4.09. Here, each step of the process planning decreased the BTF ratio further, likely producing a better result than the trial-and-error approach.

6.2 Discussion

This section discusses the main contributions of the publications compared to the state of the art. The limitations of each result are published in the respective publications. Therefore, in this section, the results of this dissertation thesis as a whole are discussed and their limitations are pointed out.

In Publications ① to ③, steps for an integrated process planning were developed. For the additive-subtractive process chain, this enhances the state of the art by jointly considering WAAM and milling. The method for decision-based process planning, described in Publication ②, facilitates the optimization of the work sequence for each geometric feature based on the manufacturing costs. Overall, in combination with the calculation of the part orientation ① and the method for determining the minimal machining allowance ③, integrated process planning strives to minimize the manufacturing costs within the additive-subtractive process chain. These results address the first need for action N1. With integrated process planning, the milling process is considered before the WAAM process is conducted. The results also answer the research questions R1, "What are the steps of integrated process planning?", and R2, "How can sufficient machining allowance be ensured?", and thus fulfill the objective O1. However, process planning strongly relies on expert knowledge in several steps:

- Build orientation:
This method determines the optimal orientation based on a set of possible orientations.
- Manufacturability by WAAM:
Parts should be modified if the manufacturability is not assured.
- Modification of the WAAM model:
The manufacturability analysis necessitates adapting the WAAM model if a feature is not manufacturable or not economically viable.

Disadvantages of the fact that there is expert knowledge necessary are the need for skilled production planners and the possibility of non-optimal solutions because the number of possible solutions is too large for an individual person to consider.

Publications ④ and ⑤ address the milling operations planning for the additive-subtractive process chain. While Publication ④ shows that a comparable machinability for WAAM-material is achievable, Publication ⑤ points out the differences in milling strategies and parameters which need to be considered for WAAM-material. These publications address the second need for action N2 and answer the research questions R3, "How does the WAAM-material's machinability differ from that of conventional material?", and R4, "How does the WAAM-part geometry influence the milling process?". The results fulfill

the objective O2. Nevertheless, several aspects of milling operations planning which are specified in the steps of HALEVI and WEILL (1995) were not addressed in the thesis:

- Holding devices and datum axes:
Due to switching between production processes and the characteristic geometry of the WAAM-component, clamping was identified as a challenge during the research activities. The selection of datum axes is complicated by the WAAM-geometry as well.
- Sequence of operations:
Sequencing milling operations for maximum efficiency and sufficient quality was beyond the scope of this thesis, since not a single specific WAAM-component was studied. The milling strategy sometimes needs to be adapted in order to avoid deformations. This could lead to excessive repositioning moves of the cutting tool.
- Time and cost module:
Due to the fact that the proposed guidelines for milling operations planning are of a general nature and not part-specific, no optimization of the milling parameters was conducted.

Chapter 7

Summary and Outlook

7.1 Summary

A sequential process chain with WAAM and machining has economic and environmental benefits for manufacturing aircraft components. While the successful application of such a process chain was shown in literature, subsequent milling was not considered during the WAAM process planning. Likewise, the milling operations planning was not adapted to WAAM-components. This necessitates process planning by trial and error and could possibly lead to economic losses.

Therefore, within this thesis, the process chain design was conducted through an adaption of the WAAM and milling process for manufacturing in a sequential additive-subtractive process chain. Two objectives were defined for the research: the development of a methodology for integrated process planning and the adaption of the milling operations planning.

A top-down approach was chosen to fulfill these objectives. The approach was pursued in five publications. First, a process chain model was derived, and technological interfaces between the processes were defined. Second, the steps for the process planning were detailed, and a methodology to determine the necessary machining allowance was developed combined with a decision-based method to reduce the manufacturing costs. Third, the machinability of wire and arc additively manufactured Ti-6Al-4V was determined, and the influence of the WAAM-component geometry on the milling process was investigated. The key results were:

- The integrated process planning consists of three steps: the determination of the part orientation, the manufacturability analysis, and the determination of surface offset.
- A cost analysis within the manufacturability analysis enables the minimization of the manufacturing costs. A decision-based method for this step was developed.
- The minimal necessary machining allowance is an input parameter for the surface offset. A method was developed to determine this from the measured surface profile.

- A machinability comparable to conventionally manufactured Ti-6Al-4V parts was proven to be achievable with WAAM. Therefore, cutting conditions similar to those for conventionally manufactured Ti-6Al-4V are possible.
- The WAAM-component geometry leads to a modulation of the mean cutting force. This modulation needs to be considered for the selection of the cutting parameters and the tool path strategy.

The thesis closes with an analysis of the methodology's potential and applicability. Compared to process planning with the trial-and-error method, the developed methodology performs better.

7.2 Outlook

With this dissertation, integrated process planning for a process chain of WAAM and machining is available. Besides the application for manufacturing aircraft components, the process chain is already studied for manufacturing in the automotive sector, the nautical sector and the aerospace sector. An application in the automotive sector could be the production of the chassis, while in the nautical sector parts of the hull structures could be manufactured. The integrated process planning, as proposed within this thesis, can be used to plan the production of these components and shorten the time from design to production considerably, by providing a methodical approach to production, which is better than the trial-and-error method. Findings on the milling process behavior of WAAM-parts can be generalized to other materials than Ti-6Al-4V, as it was shown in this thesis that some characteristics remain the same for an aluminum alloy and Ti-6Al-4V (FUCHS et al. 2022). Some topics were not addressed within this thesis. Clamping must be chosen during milling operations planning, since the modulation of the cutting forces might excite the clamping to vibrations. Additionally, repositioning between the two manufacturing processes complicates the definition of datum axes. Future research should address both aspects using a clamping strategy specific for this process chain. This aspect is included in the research project adDEDValue funded by the Federal Ministry for Economic Affairs and Climate Action (German: Bundesministerium für Wirtschaft und Klimaschutz (BMWK)) in the initiative “digitalisation of the vehicle manufacturers and supplier industry” (German: Digitalisierung der Fahrzeughersteller und Zulieferindustrie). Its results are expected to be published in 2024. Furthermore, the process planning method relies on expert knowledge to determine the building orientation and perform the manufacturability analysis. In the future, these aspects should be incorporated in a CAPP software to decrease the involvement of experts. Finally, while cutting conditions similar to those for conventionally manufactured Ti-6Al-4V are possible, the impact of the force modulation on the tool wear has not been studied so far. Changing tool engagement, the root cause of the force modulation, might increase the tool

wear. Further research activities should address this aspect by developing a tool wear model for changing tool engagement and employing this model to choose cutting strategies and cutting parameters to minimize the tool wear. Since one-sided optimization could lead to a decrease in profitability, the manufacturing time should be simultaneously considered. However, with the results presented in this thesis, a considerable step has been taken from a trial-and-error-based process chain planning towards sophisticated process planning, resulting in reduced manufacturing costs.

Bibliography

- ABE, T. and SASAHARA, H., (2015). “Development of the shell structures fabrication CAM system for direct metal lamination using arc discharge – lamination height error compensation by torch feed speed control –”. In: *International Journal of Precision Engineering and Manufacturing* vol. 16.1, pp. 171–176. ISSN: 2234-7593. DOI: 10.1007/s12541-015-0022-4.
- ACARE, ed., (2017). *Strategic Research & Innovation Agenda. 2017 Update | Executive Summary*. URL: https://www.acare4europe.org/sites/acare4europe.org/files/attachment/acare-strategic-research-innovation-summary-2-interactive-fin_0.pdf (visited on 02/15/2019).
- AIRBUS, ed., (2022). *Aviation connects and unites us! Airbus Global Market Forecast 2021 - 2040*. URL: <https://www.airbus.com/sites/g/files/jlcbita136/files/2021-07/GMF-2019-2038-Airbus-Commercial-Aircraft-book.pdf> (visited on 11/22/2022).
- ALLEN, L., O’CONNELL, A., and KIERMER, V., (2019). “How can we ensure visibility and diversity in research contributions? How the Contributor Role Taxonomy (CRediT) is helping the shift from authorship to contributorship”. In: *Learned Publishing* vol. 32.1, pp. 71–74. ISSN: 09531513. DOI: 10.1002/leap.1210.
- ALMEIDA, P. S. and WILLIAMS, S., (2010). “Innovative Process Model of Ti-6Al-4V Additive Layer Manufacturing Using Cold Metal Transfer (CMT)”. In: *Proceedings for the 2010 International Solid Freeform Fabrication Symposium*. Ed. by UNIVERSITY OF TEXAS, pp. 25–36. DOI: 10.26153/tsw/15162.
- ALONSO, U., VEIGA, F., SUÁREZ, A., and ARTAZA, T., (2020). “Experimental investigation of the influence of wire arc additive manufacturing on the machinability of titanium parts”. In: *Metals* vol. 10.24. DOI: 10.3390/met10010024.
- ALTINTAS, Y. and WECK, M., (2004). “Chatter Stability of Metal Cutting and Grinding”. In: *CIRP Annals* vol. 53.2, pp. 619–642. ISSN: 00078506. DOI: 10.1016/S0007-8506(07)60032-8.
- ALTINTAS, Y., (2012). *Manufacturing automation. Metal cutting mechanics, machine tool vibrations, and CNC design*. 2. ed. Cambridge: Cambridge University Press. ISBN: 978-1-107-00148-0.

- ALTINTAŞ, Y. and BUDAK, E., (1995). “Analytical Prediction of Stability Lobes in Milling”. In: *CIRP Annals* vol. 44.1, pp. 357–362. ISSN: 00078506. DOI: 10.1016/S0007-8506(07)62342-7.
- ATZEMA, E. H., (2017). “Formability of auto components”. In: *Automotive Steels*. Elsevier, pp. 47–93. ISBN: 9780081006382. DOI: 10.1016/B978-0-08-100638-2.00003-1.
- BAIER, D., BACHMANN, A., and ZAEH, M. F., (2020). “Towards Wire and Arc Additive Manufacturing of High-Quality Parts”. In: *Procedia CIRP* vol. 95, pp. 54–59. ISSN: 22128271. DOI: 10.1016/j.procir.2020.01.180.
- BAIER, D., WOLF, F., WECKENMANN, T., LEHMANN, M., and ZAEH, M. F., (2022). “Thermal process monitoring and control for a near-net-shape Wire and Arc Additive Manufacturing”. In: *Production Engineering* vol. 16.6, pp. 811–822. ISSN: 0944-6524. DOI: 10.1007/s11740-022-01138-7.
- BAUFELD, B., VAN DER BIEST, O., and GAULT, R., (2009). “Microstructure of Ti-6Al-4V specimens produced by shaped metal deposition”. In: *International Journal of Materials Research* vol. 100.11, pp. 1536–1542. ISSN: 1862-5282. DOI: 10.3139/146.110217.
- BAUFELD, B., VAN DER BIEST, O., GAULT, R., and RIDGWAY, K., (2011). “Manufacturing Ti-6Al-4V Components by Shaped Metal Deposition: Microstructure and Mechanical Properties”. In: *IOP Conference Series: Materials Science and Engineering* vol. 26.012001. DOI: 10.1088/1757-899X/26/1/012001.
- BOEING, ed., (2022). *Commercial Market Outlook 2021 - 2040*. URL: <https://www.boeing.com/commercial/market/commercial-market-outlook/> (visited on 07/11/2022).
- BÖGE, W., (2017). “Fräsen”. In: *Handbuch Maschinenbau*. Ed. by BÖGE, A. and BÖGE, W. Wiesbaden: Springer Fachmedien Wiesbaden, pp. 1289–1298. ISBN: 978-3-658-12528-8. DOI: 10.1007/978-3-658-12529-5_77.
- BOYER, R. R., (1995). “Titanium for aerospace: Rationale and applications”. In: *Advanced Performance Materials* vol. 2.4, pp. 349–368. ISSN: 0929-1881. DOI: 10.1007/BF00705316.
- BOYER, R. R., (2010). “Attributes, characteristics, and applications of titanium and its alloys”. In: *JOM* vol. 62.5, pp. 21–24. ISSN: 1047-4838. DOI: 10.1007/s11837-010-0071-1.
- BOYER, R., ed., (1994). *Materials properties handbook*. Materials Park, Ohio: ASM International. ISBN: 978-0-87170-481-8.
- BRANDL, E., BAUFELD, B., LEYENS, C., and GAULT, R., (2010). “Additive manufactured Ti-6Al-4V using welding wire: comparison of laser and arc beam deposition and evaluation with respect to aerospace material specifications”. In: *Physics Procedia* vol. 5, pp. 595–606. ISSN: 18753892. DOI: 10.1016/j.phpro.2010.08.087.

- BUDAK, E., (2014). “Chatter”. In: *CIRP Encyclopedia of Production Engineering*. Ed. by LAPERRIÈRE, L. and REINHART, G. Berlin, Heidelberg: Springer, pp. 163–169. DOI: 10.1007/978-3-642-20617-7_6523.
- BUDAK, E. and ALTINTAS, Y., (1995). “Modeling and avoidance of static form errors in peripheral milling of plates”. In: *International Journal of Machine Tools and Manufacture* vol. 35.3, pp. 459–476. ISSN: 08906955. DOI: 10.1016/0890-6955(94)P2628-S.
- BUSACHI, A., ERKOYUNCU, J., COLEGROVE, P., MARTINA, F., and DING, J., (2015). “Designing a WAAM Based Manufacturing System for Defence Applications”. In: *Procedia CIRP* vol. 37, pp. 48–53. ISSN: 22128271. DOI: 10.1016/j.procir.2015.08.085.
- CAMPATELLI, G., MONTEVECCHI, F., VENTURINI, G., INGARAO, G., and PRIARONE, P. C., (2020). “Integrated WAAM-Subtractive Versus Pure Subtractive Manufacturing Approaches: An Energy Efficiency Comparison”. In: *International Journal of Precision Engineering and Manufacturing-Green Technology* vol. 7.1, pp. 1–11. ISSN: 2288-6206. DOI: 10.1007/s40684-019-00071-y.
- CAMPBELL, F. C., (2006). *Manufacturing technology for aerospace structural materials*. Aerospace engineering materials science. Amsterdam: Elsevier. ISBN: 9781856174954.
- CHERNOVOL, N., SHARMA, A., TJAHJOWIDODO, T., LAUWERS, B., and VAN RYMENANT, P., (2021). “Machinability of wire and arc additive manufactured components”. In: *CIRP Journal of Manufacturing Science and Technology* vol. 35, pp. 379–389. ISSN: 17555817. DOI: 10.1016/j.cirpj.2021.06.022.
- CHERNOVOL, N., LAUWERS, B., and VAN RYMENANT, P., (2020). “Development of low-cost production process for prototype components based on Wire and Arc Additive Manufacturing (WAAM)”. In: *Procedia CIRP* vol. 95, pp. 60–65. ISSN: 22128271. DOI: 10.1016/j.procir.2020.01.188.
- CHRYSSOLOURIS, G., (1992). *Manufacturing systems. Theory and practice*. 2., corr. printing. Springer texts in mechanical engineering. New York: Springer. ISBN: 3540977546.
- COLLINS ENGLISH DICTIONARY, (2022). *Definition of 'epitaxy'*. URL: <https://www.collinsdictionary.com/us/dictionary/english/epitaxy> (visited on 05/19/2022).
- CONRARDY, C., (2011). “Gas Metal Arc Welding”. In: *Welding fundamentals and processes*. Ed. by LIENERT, T. J., BABU, S. S., SIEWERT, T. A., and ACOFF, V. L. ASM Handbook. Ohio: ASM International. ISBN: 978-1-61344-660-7.
- CUI, J., (2020). “WAAM process for metal block structure parts based on mixed heat input”. PhD thesis. Wollongong: University of Wollongong, Australia. DOI: 10.1007/s00170-021-06654-x.

- CUNNINGHAM, C. R., WIKSHÅLAND, S., XU, F., KEMAKOLAM, N., SHOKRANI, A., DHOKIA, V., and NEWMAN, S. T., (2017). “Cost Modelling and Sensitivity Analysis of Wire and Arc Additive Manufacturing”. In: *Procedia Manufacturing* vol. 11, pp. 650–657. ISSN: 23519789. DOI: 10.1016/j.promfg.2017.07.163.
- D’ADDONA, D. M. and TETI, R., (2014). “Planning”. In: *CIRP Encyclopedia of Production Engineering*. Ed. by LAPERRIÈRE, L. and REINHART, G. Berlin, Heidelberg: Springer, pp. 946–950. DOI: 10.1007/978-3-642-20617-7_6566.
- DAI, F., ZHANG, H., and LI, R., (2020). “Process planning based on cylindrical or conical surfaces for five-axis wire and arc additive manufacturing”. In: *Rapid Prototyping Journal* vol. 26.8, pp. 1405–1420. ISSN: 1355-2546. DOI: 10.1108/RPJ-01-2020-0001.
- DAVIM, J. P., (2018). *Introduction to Mechanical Engineering*. Cham: Springer International Publishing. DOI: 10.1007/978-3-319-78488-5.
- DEHOFF, R., DUTY, C., PETER, W., YAMAMOTO, Y., CHEN, W., and BUE, C., (2013). “Case Study: Additive Manufacturing of Aerospace Brackets”. In: *Advanced Materials & Processes* vol. 171.3, pp. 19–22.
- DENKENA, B. and TÖNSHOFF, H. K., (2011). *Spanen. [Machining]*. Berlin, Heidelberg: Springer. ISBN: 978-3-642-19771-0. DOI: 10.1007/978-3-642-19772-7.
- DÉPINCÉ, P. and HASCOËT, J.-Y., (2006a). “Active integration of tool deflection effects in end milling. Part 1. Prediction of milled surfaces”. In: *International Journal of Machine Tools and Manufacture* vol. 46.9, pp. 937–944. ISSN: 08906955. DOI: 10.1016/j.ijmachtools.2005.08.005.
- DÉPINCÉ, P. and HASCOËT, J.-Y., (2006b). “Active integration of tool deflection effects in end milling. Part 2. Compensation of tool deflection”. In: *International Journal of Machine Tools and Manufacture* vol. 46.9, pp. 945–956. ISSN: 08906955. DOI: 10.1016/j.ijmachtools.2005.08.014.
- DIN 6580 (1985). *Terminology of chip removing: movements and geometry of the chip removing process*. Deutsches Institut für Normung.
- DIN 8580 (2020). *Manufacturing processes - Terms and definitions, division*. Deutsches Institut für Normung.
- DIN 8589-3 (2003). *Manufacturing processes chip removal Part 3: Milling — Classification, subdivision, terms and definitions*. Deutsches Institut für Normung.
- DING, D., PAN, Z., CUIURI, D., and LI, H., (2015a). “A multi-bead overlapping model for robotic wire and arc additive manufacturing (WAAM)”. In: *Robotics and Computer-Integrated Manufacturing* vol. 31, pp. 101–110. ISSN: 07365845. DOI: 10.1016/j.rcim.2014.08.008.

- DING, D., PAN, Z., CUIURI, D., and LI, H., (2015b). “A practical path planning methodology for wire and arc additive manufacturing of thin-walled structures”. In: *Robotics and Computer-Integrated Manufacturing* vol. 34, pp. 8–19. ISSN: 07365845. DOI: 10.1016/j.rcim.2015.01.003.
- DING, D., PAN, Z., CUIURI, D., and LI, H., (2015c). “Process planning for robotic wire and arc additive manufacturing”. In: *2015 IEEE 10th Conference on Industrial Electronics and Applications (ICIEA)*.
- DING, D., PAN, Z., CUIURI, D., and LI, H., (2015d). “Wire-feed additive manufacturing of metal components: technologies, developments and future interests”. In: *The International Journal of Advanced Manufacturing Technology* vol. 81, pp. 465–481. ISSN: 0268-3768. DOI: 10.1007/s00170-015-7077-3.
- DING, D., PAN, Z., CUIURI, D., LI, H., VAN DUIN, S., and LARKIN, N., (2016). “Bead modelling and implementation of adaptive MAT path in wire and arc additive manufacturing”. In: *Robotics and Computer-Integrated Manufacturing* vol. 39, pp. 32–42. ISSN: 07365845. DOI: 10.1016/j.rcim.2015.12.004.
- DING, X., CHEN, T. T., YANG, Y. F., and LI, L., (2016). “Process Optimization for Milling Deformation Control of Titanium Alloy Thin-Walled Web”. In: *Materials Science Forum* vol. 836-837, pp. 147–154. DOI: 10.4028/www.scientific.net/MSF.836-837.147.
- DTTMANN, A. and GOMES, J. O., (2021). “Evaluation of additive manufacturing parts machinability using automated gmaw er70s-6 with nodular cast iron”. In: *U.Porto Journal of Engineering* vol. 7.2, pp. 88–97. DOI: 10.24840/2183-6493_007.002_0011.
- ELMARAGHY, H. and NASSEHI, A., (2014). “Computer-Aided Process Planning”. In: *CIRP Encyclopedia of Production Engineering*. Ed. by LAPERRIÈRE, L. and REINHART, G. Berlin, Heidelberg: Springer, pp. 266–271. DOI: 10.1007/978-3-642-20617-7_6551.
- ERNST, H. J. and MERCHANT, M. E., (1941). “Chip formation, friction and finish”. In: *Transactions of the ASME* vol. 29, pp. 299–378.
- ESCHELBACHER, S. and MÖHRING, H.-C., (2021). “Hardness and Orthogonal Cutting Analyses of a Wire and Arc Additive Manufactured (WAAM) Sample”. In: *Procedia CIRP* vol. 101, pp. 26–29. ISSN: 22128271. DOI: 10.1016/j.procir.2021.02.005.
- EVERSHEIM, W., (2002). *Organisation in der Produktionstechnik - Arbeitsvorbereitung. [Organisation in production engineering - work planning]*. 4 ed. Berlin: Springer. ISBN: 978-3-642-62640-1.
- EZUGWU, E. O. and WANG, Z. M., (1997). “Titanium alloys and their machinability—a review”. In: *Journal of Materials Processing Technology* vol. 68.3, pp. 262–274. ISSN: 09240136. DOI: 10.1016/S0924-0136(96)00030-1.

- FUCHS, C., KICK, L., LEPREVOST, O., and ZAEH, M. F., (2021). "ASSESSMENT OF FINISH MACHINING AND MASS FINISHING AS POST-PROCESSING METHODS FOR PBF-LB/M-MANUFACTURED 316L". In: *MM Science Journal* vol. 2021.5, pp. 5187–5194. ISSN: 18031269. DOI: 10.17973/MMSJ.2021_11_2021137.
- FUCHS, C., BAIER, D., ELITZER, D., KLEINWORT, R., BACHMANN, A., and ZÄH, M. F., (2019). "Additive Fertigung für Flugzeug-Strukturkomponenten. [Additive Manufacturing for Structural Components in Aerospace Engineering]". In: *ZWF Zeitschrift für wirtschaftlichen Fabrikbetrieb* vol. 114.7-8, pp. 431–434. ISSN: 0947-0085. DOI: 10.3139/104.112124.
- FUCHS, C., BAIER, D., SEMM, T., and ZAEH, M. F., (2020). "Determining the machining allowance for WAAM parts". In: *Production Engineering* vol. 14.5–6, pp. 629–637. ISSN: 0944-6524. DOI: 10.1007/s11740-020-00982-9.
- FUCHS, C., ELITZER, D., HÖPPEL, H. W., GÖKEN, M., and ZAEH, M. F., (2023). "Investigation into the influence of the interlayer temperature on machinability and microstructure of additively manufactured Ti-6Al-4V". In: *Production Engineering* vol. 17.5, pp. 703–714. ISSN: 0944-6524. DOI: 10.1007/s11740-023-01192-9.
- FUCHS, C., FRITZ, C., and ZAEH, M. F., (2022). "Impact of wire and arc additively manufactured workpiece geometry on the milling process". In: *Production Engineering* vol. 17.3–4, pp. 415–424. ISSN: 0944-6524. DOI: 10.1007/s11740-022-01153-8.
- FUCHS, C., RODRÍGUEZ, I., BAIER, D., and ZAEH, M. F., (2021). "Process Planning for the Machining of Ti-6Al-4V Near-net Shaped Components". In: *Procedia CIRP* vol. 101, pp. 58–61. ISSN: 22128271. DOI: 10.1016/j.procir.2020.03.155.
- FUCHS, C., SEMM, T., and ZAEH, M. F., (2021). "Decision-based process planning for wire and arc additively manufactured and machined parts". In: *Journal of Manufacturing Systems* vol. 59, pp. 180–189. ISSN: 02786125. DOI: 10.1016/j.jmsy.2021.01.016.
- GENG, H., LI, J., XIONG, J., LIN, X., and ZHANG, F., (2017). "Geometric Limitation and Tensile Properties of Wire and Arc Additive Manufacturing 5A06 Aluminum Alloy Parts". In: *Journal of Materials Engineering and Performance* vol. 26.2, pp. 621–629. ISSN: 1059-9495. DOI: 10.1007/s11665-016-2480-y.
- GIBSON, I., ROSEN, D., STUCKER, B., and KHORASANI, M., (2021). *Additive Manufacturing Technologies*. Cham: Springer International Publishing. DOI: 10.1007/978-3-030-56127-7.
- GOU, J., SHEN, J., HU, S., TIAN, Y., and LIANG, Y., (2019). "Microstructure and mechanical properties of as-built and heat-treated Ti-6Al-4V alloy prepared by cold metal transfer additive manufacturing". In: *Journal of Manufacturing Processes* vol. 42, pp. 41–50. ISSN: 15266125. DOI: 10.1016/j.jmapro.2019.04.012.

- GROOVER, M. P., (2011). *Fundamentals of modern manufacturing. Materials, processes, and systems*. 4th ed. Hoboken, NJ: J. Wiley & Sons. ISBN: 978-0470-467002.
- GROPPE, M., (2014). "Milling of Titanium". In: *CIRP Encyclopedia of Production Engineering*. Ed. by LAPERRIÈRE, L. and REINHART, G. Berlin, Heidelberg: Springer, pp. 883–887. DOI: 10.1007/978-3-642-20617-7_6409.
- HALEVI, G. and WEILL, R. D., (1995). *Principles of Process Planning. A logical approach*. Dordrecht and s.l.: Springer Netherlands. ISBN: 978-94-010-4544-5. DOI: 10.1007/978-94-011-1250-5.
- HARRIS, I. D., (2011). "Plasma Arc Welding". In: *Welding fundamentals and processes*. Ed. by LIENERT, T. J., BABU, S. S., SIEWERT, T. A., and ACOFF, V. L. ASM Handbook. Ohio: ASM International. ISBN: 978-1-61344-660-7.
- HENJES, J., (2014). "Process Chain Design". In: *CIRP Encyclopedia of Production Engineering*. Ed. by LAPERRIÈRE, L. and REINHART, G. Berlin, Heidelberg: Springer, pp. 975–978. DOI: 10.1007/978-3-642-20617-7_6694.
- HERRANZ, S., CAMPA, F. J., LACALLE, L. N. L. de, RIVERO, A., LAMIKIZ, A., UKAR, E., SÁNCHEZ, J. A., and BRAVO, U., (2005). "The milling of airframe components with low rigidity: A general approach to avoid static and dynamic problems". In: *Proceedings of the Institution of Mechanical Engineers, Part B: Journal of Engineering Manufacture* vol. 219.11, pp. 789–801. ISSN: 0954-4054. DOI: 10.1243/095440505X32742.
- HUDA, Z., (2021). *Machining Processes and Machines. Fundamentals, Analysis, and Calculations*. Milton: Taylor & Francis Group. ISBN: 9781000284799.
- IATA, (2022). *Anzahl der Flüge in der weltweiten Luftfahrt von 2014 bis 2021 (in Millionen)*. [Number of flights in global aviation from 2014 to 2021 (in millions).] Ed. by STATISTA. Statista GmbH. URL: <https://de-statista-com.eaccess.ub.tum.de/statistik/daten/studie/411620/umfrage/anzahl-der-weltweiten-fluege/> (visited on 06/02/2022).
- INAGAKI, I., SHIRAI, Y., TAKECHI, T., and ARIYASU, N., (2014). "Application and Features of Titanium for the Aerospace Industry". In: *NIPPON STEEL & SUMITOMO METAL TECHNICAL REPORT* 106. URL: <https://www.nipponsteel.com/en/tech/report/nssmc/pdf/106-05.pdf>.
- ISO/ASTM 52900 (2022). *Additive manufacturing - General Principles - Fundamentals and vocabulary*.
- KARMUHILAN, M. and SOOD, A. K., (2018). "Intelligent process model for bead geometry prediction in WAAM". In: *Materials Today: Proceedings* vol. 5.11, pp. 24005–24013. ISSN: 22147853. DOI: 10.1016/j.matpr.2018.10.193.
- KARUNAKARAN, K. P., SURYAKUMAR, S., PUSHPA, V., and AKULA, S., (2010). "Low cost integration of additive and subtractive processes for hybrid layered manufacturing". In: *Robotics and Computer-Integrated Manufacturing* vol. 26.5, pp. 490–499. ISSN: 07365845. DOI: 10.1016/j.rcim.2010.03.008.

- KARUPPANNAN GOPALRAJ, S., DEVIATKIN, I., HORTTANAINEN, M., and KÄRKI, T., (2021). "Life Cycle Assessment of a Thermal Recycling Process as an Alternative to Existing CFRP and GFRP Composite Wastes Management Options". In: *Polymers* vol. 13.24. DOI: 10.3390/polym13244430.
- KAZANAS, P., DEHERKAR, P., ALMEIDA, P., LOCKETT, H., and WILLIAMS, S., (2012). "Fabrication of geometrical features using wire and arc additive manufacture". In: *Proceedings of the Institution of Mechanical Engineers, Part B: Journal of Engineering Manufacture* vol. 226.6, pp. 1042–1051. ISSN: 0954-4054. DOI: 10.1177/0954405412437126.
- KHAN, M. A. and JAPPES, J. T. W., (2022). *Innovations in Additive Manufacturing*. Springer eBook Collection. Cham: Springer International Publishing and Imprint Springer. ISBN: 978-3-030-89400-9. DOI: 10.1007/978-3-030-89401-6.
- KIENZLE, O. and VICTOR, H., (1957). "Spezifische Schnittkräfte bei der Metallbearbeitung". In: *Werkstofftechnik und Maschinenbau* vol. 47.5, pp. 224–225.
- KNEZOVIĆ, N. and TOPIĆ, A., (2019). "Wire and Arc Additive Manufacturing (WAAM) – A New Advance in Manufacturing". In: *New Technologies, Development and Application*. Ed. by KARABEGOVIĆ, I. Vol. vol. 42. Cham: Springer International Publishing, pp. 65–71. DOI: 10.1007/978-3-319-90893-9_7.
- LI, F., CHEN, S., SHI, J., ZHAO, Y., and TIAN, H., (2018). "Thermoelectric cooling-aided bead geometry regulation in wire and arc-based additive manufacturing of thin-walled structures". In: *Applied Sciences (Switzerland)* vol. 8.2. DOI: 10.3390/app8020207.
- LI, F., CHEN, S., SHI, J., TIAN, H., and ZHAO, Y., (2017). "Evaluation and Optimization of a Hybrid Manufacturing Process Combining Wire Arc Additive Manufacturing with Milling for the Fabrication of Stiffened Panels". In: *Applied Sciences* vol. 7.12.1233. DOI: 10.3390/app7121233.
- LIN, J. J., LV, Y. H., LIU, Y. X., XU, B. S., SUN, Z., LI, Z. G., and WU, Y. X., (2016). "Microstructural evolution and mechanical properties of Ti-6Al-4V wall deposited by pulsed plasma arc additive manufacturing". In: *Materials & Design* vol. 102, pp. 30–40. ISSN: 02613069. DOI: 10.1016/j.matdes.2016.04.018.
- LOCKETT, H., DING, J., WILLIAMS, S., and MARTINA, F., (2017). "Design for Wire + Arc Additive Manufacture: design rules and build orientation selection". In: *Journal of Engineering Design* vol. 28.7-9, pp. 568–598. ISSN: 0954-4828. DOI: 10.1080/09544828.2017.1365826.
- LOEHE, J. and ZAEH, M. F., (2014). "A New Approach to Build a Heat Flux Model of Milling Processes". In: *Procedia CIRP* vol. 24, pp. 7–12. ISSN: 22128271. DOI: 10.1016/j.procir.2014.08.003.

- LOEHE, J., ZAEH, M. F., and ROESCH, O., (2012). “In-Process Deformation Measurement of Thin-walled Workpieces”. In: *Procedia CIRP* vol. 1, pp. 546–551. ISSN: 22128271. DOI: 10.1016/j.procir.2012.04.097.
- LOPES, J. G., MACHADO, C. M., DUARTE, V. R., RODRIGUES, T. A., SANTOS, T. G., and OLIVEIRA, J. P., (2020). “Effect of milling parameters on HSLA steel parts produced by Wire and Arc Additive Manufacturing (WAAM)”. In: *Journal of Manufacturing Processes* vol. 59, pp. 739–749. ISSN: 15266125. DOI: 10.1016/j.jmapro.2020.10.007.
- LÜTJERING, G. and WILLIAMS, J. C., (2007). *Titanium*. 2. ed. Engineering materials and processes. Berlin and Heidelberg: Springer. ISBN: 978-3-540-71397-5.
- MARTINA, F., MEHNEN, J., WILLIAMS, S. W., COLEGROVE, P., and WANG, F., (2012). “Investigation of the benefits of plasma deposition for the additive layer manufacture of Ti-6Al-4V”. In: *Journal of Materials Processing Technology* vol. 212.6, pp. 1377–1386. ISSN: 09240136. DOI: 10.1016/j.jmatprotec.2012.02.002.
- MARTINA, F. and WILLIAMS, S., (2015). *Wire + arc additive manufacturing vs. traditional machining from solid: a cost comparison*. URL: <https://waammat.com/documents> (visited on 09/10/2019).
- MARTINA, F., WILLIAMS, S. W., and COLEGROVE, P., (2013). “Improved Microstructure and Increased Mechanical Properties of Additive Manufacture Produced Ti-6Al-4V By Interpass Cold Rolling”. In: DOI: 10.26153/tsw/15574.
- MASEK, P., FORNUSEK, T., ZEMAN, P., BUCKO, M., SMOLIK, J., and HEINRICH, P., (2019). “MACHINABILITY THE AISI 316 STAINLESS STEEL AFTER PROCESSING BY VARIOUS METHODS OF 3D PRINTING”. In: *MM Science Journal* vol. 2019.04, pp. 3338–3346. ISSN: 18031269. DOI: 10.17973/MMSJ.2019_11_2019091.
- MCANDREW, A. R., ALVAREZ ROSALES, M., COLEGROVE, P. A., HÖNNIGE, J. R., HO, A., FAYOLLE, R., EYITAYO, K., STAN, I., SUKRONGPANG, P., CROCHEMORE, A., and PINTER, Z., (2018). “Interpass rolling of Ti-6Al-4V wire + arc additively manufactured features for microstructural refinement”. In: *Additive Manufacturing* vol. 21, pp. 340–349. ISSN: 22148604. DOI: 10.1016/j.addma.2018.03.006.
- MERRIAM-WEBSTER DICTIONARY, (2022a). *Definition of 'acicular'*. URL: <https://www.merriam-webster.com/dictionary/acicular> (visited on 06/13/2022).
- MERRIAM-WEBSTER DICTIONARY, (2022b). *Definition of 'equiaxed'*. URL: <https://www.merriam-webster.com/dictionary/equiaxed> (visited on 05/19/2022).
- MESSLER, R. W., (2011). “Overview of Welding Processes”. In: *Welding fundamentals and processes*. Ed. by LIENERT, T. J., BABU, S. S., SIEWERT, T. A., and ACOFF, V. L. ASM Handbook. Ohio: ASM International, pp. 13–26. ISBN: 978-1-61344-660-7. DOI: 10.31399/asm.hb.v06a.a0005552.

- MONTEVECCHI, F., GROSSI, N., TAKAGI, H., SCIPPA, A., SASAHARA, H., and CAMPATELLI, G., (2016). “Cutting Forces Analysis in Additive Manufactured AISI H13 Alloy”. In: *Procedia CIRP* vol. 46, pp. 476–479. ISSN: 22128271. DOI: 10.1016/j.procir.2016.04.034.
- NIKNAM, S. A., KHETTABI, R., and SONGMENE, V., (2014). “Machinability and Machining of Titanium Alloys: A Review”. In: *Machining of titanium alloys*. Ed. by DAVIM, J. P. Vol. vol. 68. Materials Forming, Machining and Tribology. Heidelberg: Springer, pp. 1–30. ISBN: 978-3-662-43901-2. DOI: 10.1007/978-3-662-43902-9_1. (Visited on 02/27/2019).
- NORRISH, J., POLDEN, J., and RICHARDSON, I., (2021). “A review of wire arc additive manufacturing: development, principles, process physics, implementation and current status”. In: *Journal of Physics D: Applied Physics* vol. 54.47.473001. ISSN: 0022-3727. DOI: 10.1088/1361-6463/ac1e4a.
- PETERS, M., KUMPFERT, J., WARD, C. H., and LEYENS, C., (2003). “Titanium Alloys for Aerospace Applications”. In: *Advanced Engineering Materials* vol. 5.6, pp. 419–427. ISSN: 1438-1656. DOI: 10.1002/adem.200310095.
- PRADO-CERQUEIRA, J. L., DIÉGUEZ, J. L., and CAMACHO, A. M., (2017). “Preliminary development of a Wire and Arc Additive Manufacturing system (WAAM)”. In: *Procedia Manufacturing* vol. 13, pp. 895–902. ISSN: 23519789. DOI: 10.1016/j.promfg.2017.09.154.
- PRAMANIK, A., (2014). “Problems and solutions in machining of titanium alloys”. In: *The International Journal of Advanced Manufacturing Technology* vol. 70.5-8, pp. 919–928. ISSN: 0268-3768. DOI: 10.1007/s00170-013-5326-x.
- RATCHEV, S., LIU, S., HUANG, W., and BECKER, A. A., (2004). “Milling error prediction and compensation in machining of low-rigidity parts”. In: *International Journal of Machine Tools and Manufacture* vol. 44.15, pp. 1629–1641. ISSN: 08906955. DOI: 10.1016/j.ijmactools.2004.06.001.
- RAZAVI, S. M. J. and BERTO, F., (2019). “Directed Energy Deposition versus Wrought Ti–6Al–4V: A Comparison of Microstructure, Fatigue Behavior, and Notch Sensitivity”. In: *Advanced Engineering Materials* vol. 21.8. ISSN: 1438-1656. DOI: 10.1002/adem.201900220.
- REISCH, R., HAUSER, T., KAMPS, T., and KNOLL, A., (2020). “Robot Based Wire Arc Additive Manufacturing System with Context-Sensitive Multivariate Monitoring Framework”. In: *Procedia Manufacturing* vol. 51, pp. 732–739. ISSN: 23519789. DOI: 10.1016/j.promfg.2020.10.103.
- RODRIGUES, T. A., DUARTE, V., MIRANDA, R. M., SANTOS, T. G., and OLIVEIRA, J. P., (2019). “Current Status and Perspectives on Wire and Arc Additive Manufacturing (WAAM)”. In: *Materials* vol. 12.7. DOI: 10.3390/ma12071121.

- SARH, B., BUTTRICK, J., MUNK, C., and BOSSI, R., (2009). "Aircraft Manufacturing and Assembly". In: *Springer handbook of automation*. Ed. by NOF, S. Y. Dordrecht and Heidelberg: Springer, pp. 893–910. ISBN: 978-3-540-78830-0. DOI: 10.1007/978-3-540-78831-7_51.
- SCALLAN, P., (2010). *Process planning. The design/manufacture interface*. Amsterdam et al.: Butterworth-Heinemann, an imprint of Elsevier. ISBN: 0750651296.
- SCHMITZ, M., WIARTALLA, J., GELFGREN, M., MANN, S., CORVES, B., and HÜSING, M., (2021). "A Robot-Centered Path-Planning Algorithm for Multidirectional Additive Manufacturing for WAAM Processes and Pure Object Manipulation". In: *Applied Sciences* vol. 11.13. DOI: 10.3390/app11135759.
- SEMIATIN, S. L., KOBRYN, P. A., ROUSH, E. D., FURRER, D. J., HOWSON, T. E., BOYER, R. R., and CHELLMAN, D. J., (2001). "Plastic flow and microstructure evolution during thermomechanical processing of laser-deposited Ti-6Al-4V preforms". In: *Metallurgical and Materials Transactions A* vol. 32.7, pp. 1801–1811. ISSN: 1073-5623. DOI: 10.1007/s11661-001-0156-0.
- SHAH, J. J. and MÄNTYLÄ, M., (1995). *Parametric and feature-based CAD CAM. Concepts, techniques, and applications*. A Wiley-Interscience publication. New York: Wiley. ISBN: 0471002143.
- SHAMOTO, E. and SENCER, B., (2014). "Vibration". In: *CIRP Encyclopedia of Production Engineering*. Ed. by LAPERRIÈRE, L. and REINHART, G. Berlin, Heidelberg: Springer, pp. 1289–1294. DOI: 10.1007/978-3-642-20617-7_6547.
- SHUNMUGAVEL, M., POLISHETTY, A., and LITTLEFAIR, G., (2015). "Microstructure and Mechanical Properties of Wrought and Additive Manufactured Ti-6Al-4V Cylindrical Bars". In: *Procedia Technology* vol. 20, pp. 231–236. ISSN: 22120173. DOI: 10.1016/j.protcy.2015.07.037.
- SINGH, S. R. and KHANNA, P., (2021). "Wire arc additive manufacturing (WAAM): A new process to shape engineering materials". In: *Materials Today: Proceedings* vol. 44, pp. 118–128. ISSN: 22147853. DOI: 10.1016/j.matpr.2020.08.030.
- SZOST, B. A., TERZI, S., MARTINA, F., BOISSELIER, D., PRYTULIAK, A., PIRLING, T., HOFMANN, M., and JARVIS, D. J., (2016). "A comparative study of additive manufacturing techniques: Residual stress and microstructural analysis of CLAD and WAAM printed Ti-6Al-4V components". In: *Materials & Design* vol. 89, pp. 559–567. ISSN: 02613069. DOI: 10.1016/j.matdes.2015.09.115.
- TANG, S., WANG, G., HUANG, C., LI, R., ZHOU, S., and ZHANG, H., (2020). "Investigation, modeling and optimization of abnormal areas of weld beads in wire and arc additive manufacturing". In: *Rapid Prototyping Journal* vol. 26.7, pp. 1183–1195. ISSN: 1355-2546. DOI: 10.1108/RPJ-08-2019-0229.

- TANG, S., WANG, G., HUANG, C., and ZHANG, H., (2019). "Investigation and control of weld bead at both ends in waam". In: *Proceedings of the 30th Annual International Freeform Fabrication Symposium*. Ed. by LABORATORY FOR FREEFORM FABRICATION AND UNIVERSITY OF TEXAS AT AUSTIN, pp. 693–702.
- TANG, S., WANG, G., SONG, H., LI, R., and ZHANG, H., (2021). "A novel method of bead modeling and control for wire and arc additive manufacturing". In: *Rapid Prototyping Journal* vol. 27.2, pp. 311–320. ISSN: 1355-2546. DOI: 10.1108/RPJ-05-2020-0097.
- TIAN, Y., SHEN, J., HU, S., WANG, Z., and GOU, J., (2019). "Microstructure and mechanical properties of wire and arc additive manufactured Ti-6Al-4V and AlSi5 dissimilar alloys using cold metal transfer welding". In: *Journal of Manufacturing Processes* vol. 46, pp. 337–344. ISSN: 15266125. DOI: 10.1016/j.jmapro.2019.09.006.
- TOENSHOFF, H. K., (2014a). "Cutting, Fundamentals". In: *CIRP Encyclopedia of Production Engineering*. Ed. by LAPERRIÈRE, L. and REINHART, G. Berlin, Heidelberg: Springer, pp. 345–357. DOI: 10.1007/978-3-642-20617-7_6633.
- TOENSHOFF, H. K., (2014b). "Machinability". In: *CIRP Encyclopedia of Production Engineering*. Ed. by LAPERRIÈRE, L. and REINHART, G. Berlin, Heidelberg: Springer, pp. 769–770. DOI: 10.1007/978-3-642-20617-7_6704.
- URBANIC, R. J., HEDRICK, R. W., and BURFORD, C. G., (2017). "A process planning framework and virtual representation for bead-based additive manufacturing processes". In: *The International Journal of Advanced Manufacturing Technology* vol. 90.1-4, pp. 361–376. DOI: 10.1007/s00170-016-9392-8.
- VALDÉS, R. M. A., BURMAOGLU, S., TUCCI, V., DA BRAGA COSTA CAMPOS, L. M., MATTERA, L., and GOMEZ COMENDADOR, V. F., (2019). "Flight Path 2050 and ACARE Goals for Maintaining and Extending Industrial Leadership in Aviation: A Map of the Aviation Technology Space". In: *Sustainability* vol. 11.7. ISSN: 2071-1050. DOI: 10.3390/su11072065.
- VAZQUEZ, L., RODRIGUEZ, M. N., RODRIGUEZ, I., and ALVAREZ, P., (2021). "Influence of Post-Deposition Heat Treatments on the Microstructure and Tensile Properties of Ti-6Al-4V Parts Manufactured by CMT-WAAM". In: *Metals* vol. 11.8. DOI: 10.3390/met11081161.
- VÁZQUEZ, L., RODRÍGUEZ, N., RODRÍGUEZ, I., ALBERDI, E., and ÁLVAREZ, P., (2020). "Influence of interpass cooling conditions on microstructure and tensile properties of Ti-6Al-4V parts manufactured by WAAM". In: *Welding in the World* vol. 64.8, pp. 1377–1388. ISSN: 0043-2288. DOI: 10.1007/s40194-020-00921-3.
- VDI 3633-1 (2014). *Simulation of systems in materials handling, logistics and production – Fundamentals*. Verein Deutscher Ingenieure.

- VEIGA, F., DEL VAL, A. G., SUÁREZ, A., and ALONSO, U., (2020). “Analysis of the machining process of titanium Ti6Al-4V parts manufactured by wire arc additive manufacturing (WAAM)”. In: *Materials* vol. 13.3. DOI: 10.3390/ma13030766.
- VENKATESH, T. A., CONNER, B. P., SURESH, S., GIANNAKOPOULOS, A. E., LINDLEY, T. C., and LEE, C. S., (2001). “An experimental investigation of fretting fatigue in Ti-6Al-4V: the role of contact conditions and microstructure”. In: *Metallurgical and Materials Transactions A* vol. 32.5, pp. 1131–1146. ISSN: 1073-5623. DOI: 10.1007/s11661-001-0124-8.
- WANG, F., WILLIAMS, S., COLEGROVE, P., and ANTONYSAMY, A. A., (2013). “Microstructure and Mechanical Properties of Wire and Arc Additive Manufactured Ti-6Al-4V”. In: *Metallurgical and Materials Transactions A* vol. 44.2, pp. 968–977. ISSN: 1073-5623. DOI: 10.1007/s11661-012-1444-6.
- WILLIAMS, S. W., MARTINA, F., ADDISON, A. C., DING, J., PARDAL, G., and COLEGROVE, P., (2016). “Wire + Arc Additive Manufacturing”. In: *Materials Science and Technology* vol. 32.7, pp. 641–647. ISSN: 0267-0836. DOI: 10.1179/1743284715Y.0000000073.
- WIMMER, S. S., (2020). *Prognose und Kompensation von Formabweichungen bei der Fräsbearbeitung dünnwandiger Strukturen. [Prognosis and compensation of deflections during the milling of thin-walled structures]*. Vol. 357. Forschungsberichte IWB. ISBN: 9783831648764.
- XU, X., (2009). *Integrating advanced computer-aided design, manufacturing, and numerical control. Principles and implementations*. Hershey, Pa.: Information Science Reference. ISBN: 978-1-59904-716-4.
- XU, X., WANG, L., and NEWMAN, S. T., (2011). “Computer-aided process planning – A critical review of recent developments and future trends”. In: *International Journal of Computer Integrated Manufacturing* vol. 24.1, pp. 1–31. ISSN: 0951-192X. DOI: 10.1080/0951192X.2010.518632.
- YA, W. and HAMILTON, K., (2018). “On-Demand Spare Parts for the Marine Industry with Directed Energy Deposition: Propeller Use Case”. In: *Industrializing Additive Manufacturing - proceedings of Additive Manufacturing in Products and Applications - AMPA2017*. Ed. by KLAHN, C. and MEBOLDT, M. Cham, Switzerland: Springer, pp. 70–81. ISBN: 978-3-319-66865-9. DOI: 10.1007/978-3-319-66866-6_7.
- YI, H.-J., KIM, J.-W., KIM, Y.-L., and SHIN, S., (2020). “Effects of Cooling Rate on the Microstructure and Tensile Properties of Wire-Arc Additive Manufactured Ti-6Al-4V Alloy”. In: *Metals and Materials International* vol. 26.8, pp. 1235–1246. ISSN: 1598-9623. DOI: 10.1007/s12540-019-00563-1.
- ZHANG, P.-l., JIA, Z.-y., YAN, H., YU, Z.-s., DI WU, SHI, H.-c., WANG, F.-x., TIAN, Y.-t., MA, S.-y., and LEI, W.-s., (2021). “Effect of deposition rate on microstructure and mechanical properties of wire arc additive manufacturing of Ti-6Al-4V components”. In: *Journal of Central South University* vol. 28.4, pp. 1100–1110. ISSN: 2095-2899. DOI: 10.1007/s11771-021-4683-0.

- ZHANG, Y. M., (2011). "Arc Physics of Gas Tungsten and Gas Metal Arc Welding". In: *Welding fundamentals and processes*. Ed. by LIENERT, T. J., BABU, S. S., STEWERT, T. A., and ACOFF, V. L. ASM Handbook. Ohio: ASM International. ISBN: 978-1-61344-660-7.
- ZHOU, Y., QIN, G., LI, L., LU, X., JING, R., XING, X., and YANG, Q., (2020). "Formability, microstructure and mechanical properties of Ti-6Al-4V deposited by wire and arc additive manufacturing with different deposition paths". In: *Materials Science and Engineering: A* vol. 772. ISSN: 09215093. DOI: 10.1016/j.msea.2019.138654.

Glossary

Term	Description
acicular	“shaped like a needle” (MERRIAM-WEBSTER DICTIONARY 2022a)
epitaxial	epitaxy: “the growth of a thin layer on the surface of a crystal so that the layer has the same structure as the underlying crystal” (COLLINS ENGLISH DICTIONARY 2022)
equiaxed	“having approximately equal dimensions in all directions – used especially of [sic] a crystal grain in a metal” (MERRIAM-WEBSTER DICTIONARY 2022b)
feature	“a physical constituent of a part which is mappable to a generic shape; has engineering significance, and has predictable properties” (SHAH and MÄNTYLÄ 1995)
interlayer temperature	the temperature the weld bead is cooled down to, before the next layer is deposited
machining allowance	the material deposited additionally during the WAAM process to ensure a stable surface quality after the milling process
operations planning	the detailed planning of how to perform each operation, for example the selection of machining centers (D’ADDONA and TETI 2014)
process chain design	identification and arrangement of processes to achieve specific product characteristics and efficient production (DENKENA and TÖNSHOFF 2011)
process chain	“a sequence of process elements with the objective of transforming certain items from an input state into a conformable [desired] output state” (HENJES 2014)
process planning	locating and determining the sequence of processes to transform an input into an end product (SCALLAN 2010)
process	the most minor and impartible part of a process chain (DENKENA and TÖNSHOFF 2011); defined by its input and output parameters (HENJES 2014)

Term	Description
strain rate hardening	“the faster the deformation, the more stress needs to be applied” (ATZEMA 2017)
stress-strain diagram	Stress-strain diagrams are the result of tension tests. In Figure G.1, a typical stress-strain diagram is depicted, along with mechanical properties that can be determined.

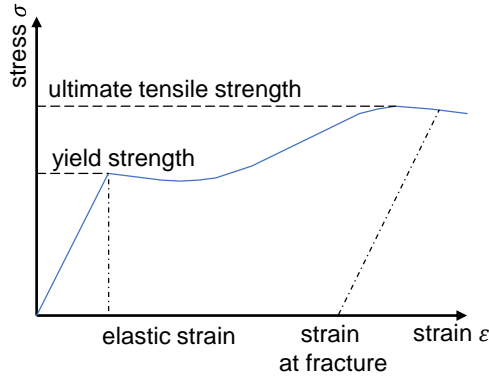


Figure G.1: Schematic stress-strain diagram

In tension tests, continually increasing, uniaxial tensile force is applied to a standard specimen. The resulting elongation is measured as well as the applied force F . The stress σ is defined as

$$\sigma = \frac{F}{A_0} , \quad (7.1)$$

where A_0 denotes the initial cross-section of the standard specimen. The strain ϵ is calculated as

$$\epsilon = \frac{L - L_0}{L_0} . \quad (7.2)$$

Here, L denotes the current specimen length and L_0 the initial specimen length. (DAVIM 2018)

Appendix A

Appendix

A.1 Descriptions of process and planning steps

Table A.1 indicates the process steps and planning steps as found in literature along with a description by the author of this thesis. If there is no explanation given, the phrasing of the publication's description is assumed to be clearly comprehensible.

Table A.1: Description of authors' designations of process and planning steps

Publication authors' designation	Description by the author of this thesis
	BUSACHI et al. 2015
WAAM system	WAAM process including the setup and online rolling
Heat treatment	heat treatment process including the setup
Machining	machining process
Wire electrical discharge machining	process, probably for the removal of the substrate plate, no detailed explanation by the publication's authors
Argon recovery	process to recover the inert argon atmosphere
	DING, PAN, CUIURI, LI, et al. 2016
CAD modeling	designing a 3D model of the desired part
3D slicing	slicing of the 3D models into 2D layers
2D path planning	torch trajectory planning in the 2D layers
Bead modeling	modeling or simulation of the desired bead geometry based on the welding parameters
Weld setting	determining the welding parameters corresponding to the desired bead geometry

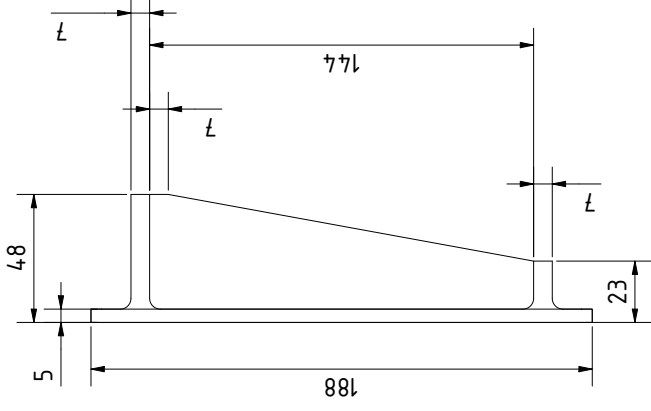
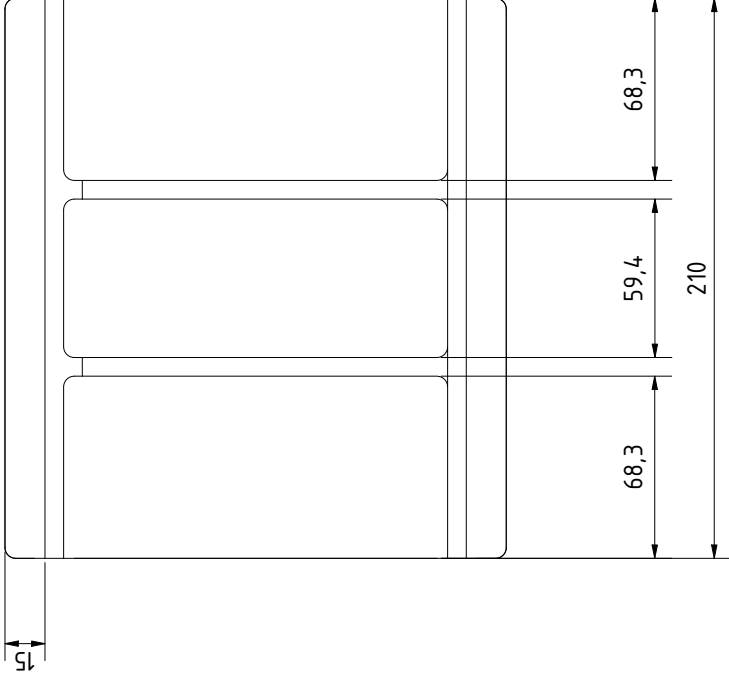
Publication authors' designation	Description by the author of this thesis
Robot code generation	translating the torch path into robot executable code
URBANIC et al. 2017	
Project setup	defining the WAAM machine, the process type, the substrate material, the wire, and the torch path strategy in the 3D component
Travel path strategy [selection]	no detailed explanation by the publication's authors
Definition of process-specific parameters	defining the parameters such as torch speed, feed speed, overlaps between path, corner radius, and voltage, essentially all parameters of the WAAM process
Travel path simulation and verification	likely refers to a collision check, no detailed explanation by the publication's authors
Generation of the numerical control code	translating the torch path into executable code
DAI et al. 2020	
Modeling	designing of a 3D model of the desired part
Slicing	slicing of the 3D models into 2D contours
Path filling	employing path planning algorithms to fill the 2D contours with lines
Tool-path generation	expanding the path lines with torch information
Weld setting	determining the welding parameters
Weld code generation	translating of the torch path into executable code
Welding	WAAM process
Machining	machining process
XU 2009	
Specification and requirement[s] analysis	analyzing the component design and identifying features, defining part requirements
Operation selection and sequencing	identifying and sequencing manufacturing operations
Resource selection	selecting machine tools, cutting tools, fixtures and clamps

Publication authors' designation	Description by the author of this thesis
Determination of operational parameters	choosing of process parameters and tool engagements
HALEVI and WEILL 1995	
Input specifications and interpretation	analyzing the technical drawing of the desired part regarding tolerances, surface roughness, dimensions, material etc.
Selection of primary processes	picking of suitable primary processes according to the analysis results
Determination of production tolerances	determining the production tolerances with regard to the technical drawing's tolerances
Selection of holding devices and datums	ensuring the adherence to the tolerances by selection of suitable holding devices (i.e., clamps) and datum axes for reference
Selection and grouping of operations	improving the economic feasibility by grouping similar operations on the same machine
Selection of [the] machine and [the] sequence of operations	–
Selection of cutting tools	–
Selection of quality assurance methods	–
Time and cost module	determining the process parameters for all operations, and calculation of the machining time and costs
Editing of [the] process sheet	assembling detailed documentation of the machining operations used for production
PRADO-CERQUEIRA et al. 2017	
3D-modeling	designing a 3D model of the desired part
Slicing in layers	slicing of the 3D models into 2D layers
Programming the path in each layer	–
CNC code generation	translating the torch path into executable code
Adjustment of welding parameters	likely an experimental definition of the welding parameters, no detailed explanation by the publication's authors

A.2 Test parts for the potential analysis

This section shows the technical drawings specifying the dimensions of the test parts, which are a structural component and a bracket.

Unspecified radii R4
Deburr and break sharp edges 0.1 ... 0.3 mm



Scale: 1:3

Design: Christina Fuchs

Part 1:
Structural Component

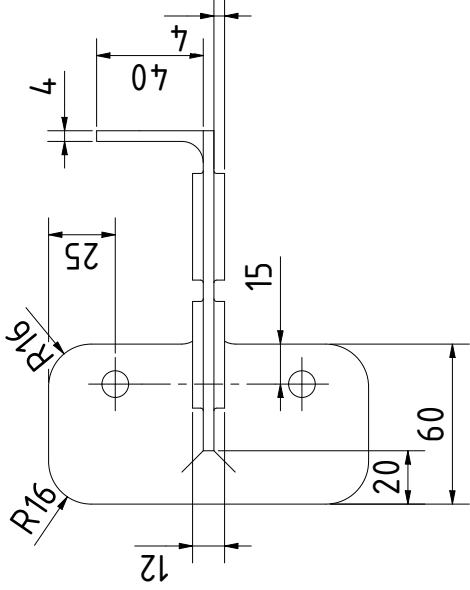
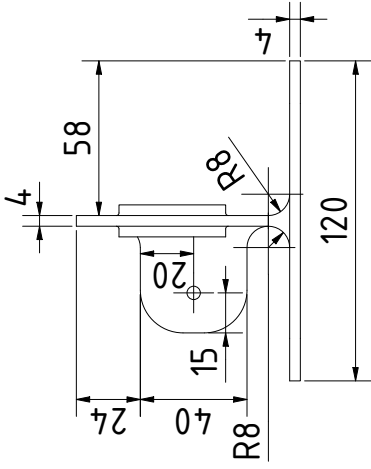
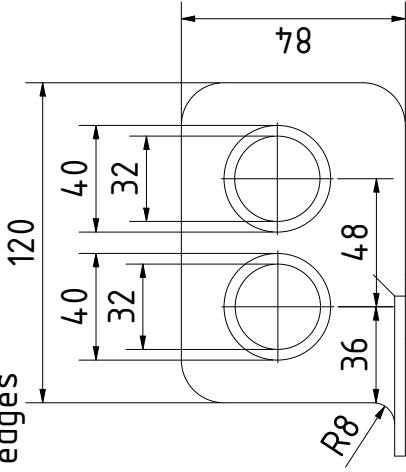
Date: 06-Jul-2022

1

A5

Unspecified radii R1

Deburr and break edges



Scale: 1:3

Design: Christina Fuchs

Part 2: Bracket

Date: 14-Jun-2022

1

A5

A.3 Data for the potential analysis

Table A.2: Initial dimensions and parameters for Test parts no. 1 and no. 2 (Chapter 6)

Parameter	Unit	Structural component	Bracket
ρ	g/cm ³	4.43	4.43
M_f	kg	1.57	0.33
bounding box dimensions	mm x mm x mm	214 x 192 x 52	88 x 124 x 144
M_b	kg	9.47	7.05
a	mm	2.00	2.00
DR_{mass}	kg/h	0.50	0.50
MRR_{mass}	kg/h	2.50	2.50
initial BTF ratio	-	6.01	21.13
initial T_m	h	3.16	2.69

Table A.3: Constants of the cost model used for the potential analysis (Section 6.1.2)

Parameter	Unit	Initial value
C_{MA}	€/m ³	270 000.00
$C_{ME,WA}$	€/h	40.00
$C_{LA,WA}$	€/h	60.00
x_{WA}	-	1.00
x_{MI}	-	1.00
$C_{ME,MI}$	€/h	40.00
$C_{LA,MI}$	€/h	60.00
T_{WA}	h	8.00
T_{MI}	h	1.00
$t_{w,WA}$	h	0.16
$t_{w,MI}$	h	$7.50 \cdot 10^{-4}$
l	-	100.00
$C_{W,WA}$	€	5.00
$C_{W,MI,X}$	€	100.00
$C_{W,MI,Y}$	€	100.00

Appendix B

Supervised Student Theses

The author supervised multiple student theses (see Table B.1). A number of them contributed to the results presented in this document. The author highly appreciates the students' work and acknowledges their contributions to this thesis.

Table B.1: Student theses supervised by this document's author

Author	Title
Robert Hoefler	Entwicklung eines Moduls zur automatisierten Roboterbahnplanung für die additive Fertigung mittels Auftragsschweißen <i>iwb</i> -Nr. 44594 (2018)
Sebastian Pohlmann	Modellierung der Systemarchitektur einer hybriden Prozesskette in der Luftfahrt <i>iwb</i> -Nr. 45673 (2018)
Ignacio Rodríguez	Design for Hybrid Manufacturing of Structural Components <i>iwb</i> -Nr. 47328 (2019)
Linge Ai	Automated Pre-Processing of CAD-Data for Hybrid Manufacturing of Structural Components <i>iwb</i> -Nr. 47613 (2019)
Carina Schmitt	Entwicklung der Softwarearchitektur eines Datenmanagementsystems für eine hybride Prozesskette in der Luftfahrt <i>iwb</i> -Nr. 50515 (2019)
Michael Launer	Untersuchung der Oberflächeneigenschaften additiv gefertigter und fräsend nachbearbeiteter Körper aus einer Titanlegierung <i>iwb</i> -Nr. 50778 (2019)
Leonhard Salcher	Prozessplanung für eine Prozesskette aus WAAM und Fräsen <i>iwb</i> -Nr. 52066 (2019)

Author	Title
Mahmoud Sakli	Characterization of the challenges in milling components manufactured by WAAM <i>iwb</i> -Nr. 52986 (2020)
Fabian Winkler	Charakterisierung der Ratterneigung bei der fräsenden Nachbearbeitung additiv gefertigter Stege aus Ti 6Al 4V <i>iwb</i> -Nr. 53892 (2020)
Anna Brack	Entwicklungen von Bearbeitungsstrategien für das Fräsen dünnwandiger Stege aus Ti 6Al 4V <i>iwb</i> -Nr. 53930 (2020)
Aaron Dietz	Datenmanagement in der Luftfahrt <i>iwb</i> -Nr. 54444 (2020)
Ophélie Leprévost	Untersuchung von Prozessparametern beim Gleitschleifen für additiv gefertigte Bauteile <i>iwb</i> -Nr. 56843 (2020)
Shichen Guo	Untersuchung der Prozesskette zur Feinbearbeitung von LBM-Bauteilen <i>iwb</i> -Nr. 56949 (2020)
Mahmoud Sakli	Determining the influence of WAAM component characteristics on the milling process <i>iwb</i> -Nr. 56951 (2020)
Ophélie Leprévost	Entwicklung einer Frässtrategie für WAAM-gefertigte Komponenten aus Ti 6Al 4V <i>iwb</i> -Nr. 59680 (2021)
Ignacio Rodríguez	Process planning and post-processing of a wire and arc manufactured model turbine <i>iwb</i> -Nr. 59796 (2021)
Tobias Fischer	Entwicklung einer Strategie zur ressourceneffizienten spanenden Nachbearbeitung von lichtbogenbasiert additiv gefertigten Luftfahrt-Strukturkomponenten <i>iwb</i> -Nr. 60386 (2021)

Appendix C

Publications and presentations

The author contributed to a number of publications and presentations. They are listed in Table C.1.

Table C.1: Presentations and publications by this thesis' author

Year	Authors and title
Presentations and conferences	
2019	Fuchs, C: Projekt Regulus (Deburring Expo 2019)
2020	Fuchs, C.; Haeussinger, C.: Prozesskettengestaltung in der Hybriden Fertigung (Vortragsreihe "Neues aus der AM-Szene")
Publications	
2019	FUCHS, C. et al., (2019). "Additive Fertigung für Flugzeug-Strukturkomponenten. [Additive Manufacturing for Structural Components in Aerospace Engineering]". In: <i>ZWF Zeitschrift für wirtschaftlichen Fabrikbetrieb</i> vol. 114.7-8, pp. 431–434. ISSN: 0947-0085. DOI: 10.3139/104.112124
2020	FUCHS, C. et al., (2020). "Determining the machining allowance for WAAM parts". In: <i>Production Engineering</i> vol. 14.5–6, pp. 629–637. ISSN: 0944-6524. DOI: 10.1007/s11740-020-00982-9
2021	FUCHS, C., SEMM, T., et al., (2021). "Decision-based process planning for wire and arc additively manufactured and machined parts". In: <i>Journal of Manufacturing Systems</i> vol. 59, pp. 180–189. ISSN: 02786125. DOI: 10.1016/j.jmsy.2021.01.016

Year	Authors and title
2021	FUCHS, C., RODRÍGUEZ, I., et al., (2021). “Process Planning for the Machining of Ti-6Al-4V Near-net Shaped Components”. In: <i>Procedia CIRP</i> vol. 101, pp. 58–61. ISSN: 22128271. DOI: 10.1016/j.procir.2020.03.155
2021	FUCHS, C., KICK, L., et al., (2021). “ASSESSMENT OF FINISH MACHINING AND MASS FINISHING AS POST-PROCESSING METHODS FOR PBF-LB/M-MANUFACTURED 316L”. in: <i>MM Science Journal</i> vol. 2021.5, pp. 5187–5194. ISSN: 18031269. DOI: 10.17973/MMSJ.2021_11_2021137
2022	FUCHS, C. et al., (2022). “Impact of wire and arc additively manufactured workpiece geometry on the milling process”. In: <i>Production Engineering</i> vol. 17.3–4, pp. 415–424. ISSN: 0944-6524. DOI: 10.1007/s11740-022-01153-8
2023	FUCHS, C. et al., (2023). “Investigation into the influence of the interlayer temperature on machinability and microstructure of additively manufactured Ti-6Al-4V”. in: <i>Production Engineering</i> vol. 17.5, pp. 703–714. ISSN: 0944-6524. DOI: 10.1007/s11740-023-01192-9
